



**GEOLOGICAL SURVEY OF CANADA
OPEN FILE 7116**

**The Volcanological and Structural Evolution of the
Paleoproterozoic Flin Flon and Snow Lake Mining Districts**

**Field Trip 3B: Joint Annual Meeting,
Geological Association of Canada–Mineralogical Association of Canada–
Society of Economic Geologists–Society for Geology Applied to Mineral
Deposits, Ottawa 2011**

**H. Gibson, S. Pehrsson, B. Lafrance, M. DeWolfe, R. Syme, A. Bailes, K.
Gilmore, C. Devine, R-L. Simard, K. MacLachlan, and B. Pearson**

2014



Natural Resources
Canada

Ressources naturelles
Canada

Canada



**GEOLOGICAL SURVEY OF CANADA
OPEN FILE 7116**

**The Volcanological and Structural Evolution of the
Paleoproterozoic Flin Flon and Snow Lake Mining Districts
Field Trip 3B: Joint Annual Meeting, Geological Association of Canada–Mineralogical
Association of Canada–Society of Economic Geologists–Society for Geology Applied to
Mineral Deposits, Ottawa 2011**

**H. Gibson¹, S. Pehrsson², B. Lafrance¹, M. DeWolfe³, R. Syme⁴, A. Bailes⁵, K.
Gilmore⁶, C. Devine⁷, R-L. Simard⁴, K. MacLachlan⁸, and B. Pearson⁶**

¹ Mineral Exploration Research Centre, Laurentian University Sudbury, Ontario

² Geological Survey of Canada, 601 Booth Street, Ottawa, Ontario

³ Mount Royal University, Calgary, Alberta

⁴ Manitoba Geological Survey, 1394 Ellice Avenue, Winnipeg, Manitoba

⁵ Bailes Geoscience Ltd., 6 Park Grove Drive Winnipeg, Manitoba

⁶ HudBay Minerals, Flin Flon, Manitoba

⁷ Paragon Minerals, 605-140 Water Street, St. John's, Newfoundland and Labrador

⁸ Association of Professional Engineers and Geoscientists of Saskatchewan,
13th Street, Regina, Saskatchewan

2014

©Her Majesty the Queen in Right of Canada 2014

doi:10.4095/292551

This publication is available for free download through GEOSCAN (<http://geoscan.ess.nrcan.gc.ca/>).

Recommended citation

Gibson, H., Pehrsson, S., Lafrance, B., DeWolfe, M., Syme, R., Bailes, A., Gilmore, K., Devine, C., Simard, R-L., MacLachlan, K., and Pearson, B., 2014. The volcanological and structural evolution of the Paleoproterozoic Flin Flon and Snow Lake mining districts: Field Trip 3B: Joint Annual Meeting, Geological Association of Canada–Mineralogical Association of Canada–Society of Economic Geologists–Society for Geology Applied to Mineral Deposits, Ottawa 2011; Geological Survey of Canada, Open File 7116, 88 p. doi:10.4095/292551



Ottawa 2011

GAC®/AGC® - MAC/AMC - SEG - SGA

Joint Annual Meeting - Congrès annuel conjoint

The Volcanological and Structural Evolution of the Paleoproterozoic Flin Flon and Snow Lake Mining Districts

H. Gibson, S. Pehrsson, B. Lafrance, M. DeWolfe, R. Syme, A. Bailes, K. Gilmore, C. Devine, R-L. Simard, K. MacLachlan, and B. Pearson



Judi Pennanen, water colour / aquarelle, 56 cm x 75 cm

May 28 - June 2, 2011



SEG
www.segweb.org



Field Trip - Excursion 3B

FIELD TRIP 3B

THE VOLCANOLOGICAL AND STRUCTURAL EVOLUTION OF THE PALEOPROTEROZOIC FLIN FLON AND SNOW LAKE MINING DISTRICTS

Harold Gibson¹, Sally Pehrsson², Bruno Lafrance¹, Michelle DeWolfe^{3,1}, Ric Syme⁴, Al Bailes^{5,1},
Kelly Gilmore⁶, Christine Devine^{6,8}, Renee-Luce Simard⁴, Kate MacLachlan¹, and Brett Pearson⁶

1. Mineral Exploration Research Centre, Laurentian University Sudbury, ON, P3E 2C6
2. Geological Survey of Canada, 601 Booth Street, Ottawa, Ontario K1A 0E8
3. Mount Royal University, Calgary, Alberta T3E 6K6
4. Manitoba Geological Survey, 1394 Ellice Avenue, Winnipeg, Manitoba R3G 2P2
5. Bailes Geoscience Ltd., 6 Park Grove Drive Winnipeg, Manitoba R2J 3L6
6. HudBay Minerals, Flin Flon, Manitoba R8A 1N9
7. Association of Professional Engineers and Geoscientists of Saskatchewan,
13th Street, Regina, Saskatchewan S4P 0V6
8. Paragon Minerals, 605-140 Water Street, St. John's, Newfoundland A1C 6H6

Field Trip Guidebook Prepared for Ottawa 2011
Joint Annual Meeting of GAC[®]/AGC[®] - MAC/AMC - SEG - SGA

May 28 - June 2, 2011

ACKNOWLEDGEMENTS

We gratefully acknowledge permission of HudBay Minerals to conduct the tour on company property and thank Hudson Bay Exploration and Development and HudBay Minerals 777 Mine in particular for their generous logistical, organizational, and research support. The SGA (Society for Geology Applied to Mineral Deposits) and Andrew Conly are thanked for support for student attendees. New data and interpretations discussed in this guide result from the joint Targeted Geoscience Initiative Program of the Geological Survey of Canada and the Manitoba and Saskatchewan Geological Surveys, with the support of industry and academia and contributions from numerous industry, academia and government colleagues. The TGI-3 Flin Flon team, particularly Ernst Schetselaar, Don White, Maggie Currie, and Doreen Ames, are thanked for discussions and support. David Price is thanked for many discussions and field tours that helped shape ideas presented here. Harold Gibson additionally acknowledges funding from an NSERC-Hudbay Minerals Laurentian University CRD grant, NSERC Discovery Grants, and the Manitoba and Saskatchewan Geological Surveys that funded and provided logistical support for 10 years of research at Flin Flon and supported six M.Sc. (Christine Devine, Dianne Mitchinson, Nicole Tardif, Kim Bailey, Eilidh Cole, and David Lewis), one Ph.D. (Michelle DeWolfe) and twelve undergraduate students. Alan Galley is thanked for many Flin Flon discussions and editorial guidance.

RECOMMENDED CITATION

Gibson, H., Pehrsson, S., Lafrance, B., DeWolfe, M., Syme, R., Bailes, A., Gilmore, K., Devine, C., Simard, R-L., MacLachlan, K., and Pearson, B., 2014. The volcanological and structural evolution of the Paleoproterozoic Flin Flon and Snow Lake mining districts: Field Trip 3B: Joint Annual Meeting, Geological Association of Canada–Mineralogical Association of Canada–Society of Economic Geologists–Society for Geology Applied to Mineral Deposits, Ottawa 2011; Geological Survey of Canada, Open File 7116, 88 p. doi:10.4095/292551

To reference parts of the report, the following is recommended:

Gibson, H., Pehrsson, S., Lafrance, B., DeWolfe, M., Syme, R., Bailes, A., Gilmore, K., Devine, C., Simard, R-L., MacLachlan, K., and Pearson, B., 2014. Day 2: Flin Flon District, *in* The volcanological and structural evolution of the Paleoproterozoic Flin Flon and Snow Lake mining districts: Field Trip 3B: Joint Annual Meeting, Geological Association of Canada–Mineralogical Association of Canada–Society of Economic Geologists–Society for Geology Applied to Mineral Deposits, Ottawa 2011; Geological Survey of Canada, Open File 7116, p. 29–34.

TABLE OF CONTENTS

| | |
|---|----|
| ACKNOWLEDGEMENTS | ii |
| INTRODUCTION | 1 |
| FIELD TRIP PROGRAM | 1 |
| REGIONAL GEOLOGY AND BACKGROUND | 1 |
| Trans Hudson Orogen | 1 |
| <i>The Flin Flon - Glennie Complex</i> | 2 |
| <i>The Amisk collage</i> | 3 |
| <i>The Snow Lake arc assemblage</i> | 4 |
| History of Exploration | 4 |
| Geology, Structure and VMS Deposits of the Flin Flon District | 5 |
| Terminology | 7 |
| Flin Flon Formation | 9 |
| <i>Club member</i> | 9 |
| <i>Blue Lagoon member</i> | 9 |
| <i>Millrock member</i> | 10 |
| <i>Mill Rock Hill section</i> | 11 |
| <i>South Main section</i> | 11 |
| <i>Smeltor section</i> | 12 |
| <i>Callinan section</i> | 12 |
| <i>Millrock Member west of the Flin Flon Lake Fault</i> | 13 |
| <i>Reconstruction</i> | 14 |
| Hidden Formation | 14 |
| <i>1920 member</i> | 14 |
| <i>Reservpor member</i> | 15 |
| <i>Stockwell member</i> | 15 |
| <i>Carlisle Lake member</i> | 15 |
| Louis Formation | 16 |
| <i>Tower member</i> | 16 |
| <i>Icehouse member</i> | 16 |
| <i>Undivided Louis formation rocks</i> | 16 |
| Structure and Metamorphism | 16 |
| 3-D Architecture of the Flin Flon district | 17 |
| DAY 1: REGIONAL CONTEXT REGIONAL CONTEXT OF THE FLIN FLON VMS DISTRICT | 19 |
| STOP 1.1: Meridian – West Arm Shear Zone | 19 |
| STOP 1.2: Missi Unconformity | 20 |
| STOP 1.3: Volcanic Rocks in the Hook Lake Block | 22 |
| STOP 1.4: Vick Lake Shoshonitic Tuff | 25 |
| STOP 1.5: Athapapuskow Basalt | 27 |
| DAY 2: FLIN FLON DISTRICT | 29 |
| STOPS 2.1 to 2.3 | 29 |
| STOPS 2.4 to 2.7 | 32 |
| STOPS 3.1 to 3.7: South Main Section | 32 |

| | |
|---|----|
| DAY 3: FLIN FLON DISTRICT | 34 |
| STOP 4. Smelter Section | 34 |
| <i>STOPS 4.1. to 4.8: Blue Lagoon member</i> | 34 |
| STOP 5. Lower Callinan Section | 36 |
| <i>Stops 5.1 and 5.2</i> | 36 |
| <i>Stop 5.3 to 5.5</i> | 37 |
| STOP 6: Beaver Road Anticline | 38 |
| DAY 4: FLIN FLON DISTRICT | 42 |
| STOP 7: Upper Callinan Section | 42 |
| <i>STOP 7.1: Columnar jointed vent facies of the 1920 member cryptoflow</i> | 42 |
| <i>STOP 7.2: Facies transitions within the 1920 member: Field evidence for emplacement as a cryptoflow</i> | 43 |
| <i>STOP 7.3: Sheared rhyolitic Tuff breccias of the Millrock member along the Upper Railway fault</i> | 44 |
| <i>STOP 7.4: Sheared 1840 Ma Phantom Lake dykes and 1872 Ma gabbroic dykes along the Upper Railway fault</i> | 45 |
| <i>STOP 7.5: Missi wedge</i> | 45 |
| DAY 5 A: FLIN FLON VMS | 48 |
| STOP 8: 777 Underground Tour | 48 |
| <i>Mine Geology</i> | 48 |
| <i>The Massive Sulphide</i> | 50 |
| <i>Underground Tour</i> | 50 |
| STOP 9: Hanging wall to the Schist Lake and Mandy Ore Bodies | 52 |
| <i>STOP 9.1: Lava tubes and megabreccias within the Hidden formation: Evidence for vent proximity</i> | 52 |
| <i>STOP 9.2: Spatter rampart and synvolcanic dykes within the Hidden formation: Evidence for vent proximity</i> | 52 |
| STOP 10: Cliff Lake Pluton | 54 |
| <i>Stop 10.1 and 10.2: Contact between the Cliff Lake Pluton and the Hooke Lake Block</i> | 54 |
| STOP 11: Icehouse Member, Louis Formation, near Louis Lake | 55 |
| <i>STOP 11.1: Massive and pillows lava flows of the Icehouse member</i> | 55 |
| <i>STOP 11.2: Pillow lavas, pillow breccia and overlying volcanoclastic rocks of the Icehouse member</i> | 56 |
| VOLCANOLOGICAL AND STRUCTURAL SETTING OF PALEOPROTEROZOIC VMS DEPOSITS IN THE CHISEL-LALOR LAKES AREA AT SNOW LAKE | 57 |
| Introduction | 57 |
| Structural History | 57 |
| VMS Mineralization in the Snow Lake Camp | 57 |
| Regional-Scale Synvolcanic Alteration Zones associated with the Snow Lake VMS Deposits .. | 58 |
| Geology and Alteration Features in the Chisel–Lalor Lakes Area, Snow Lake Arc Assemblage .. | 60 |
| DAY 5 B: SNOW LAKE AREA | 61 |
| STOP 12: Welch Lake Boninite, Anderson Sequence | 61 |
| <i>STOP 12.1: High-Ca boninite, contact between flows 1 and 3, Contact between flows 3 and 4</i> | 62 |
| <i>STOP 12. 2: Silicified/feldspathized Welch Lake basaltic andesite and Foot-Mud Sulphide</i> .. | 62 |
| <i>STOP 12.3: Stroud Lake Felsic Breccia</i> | 65 |

| | |
|--|----|
| <i>STOP 12.4: Silicification/feldspathization associated with dacite dykes in the Edwards Lake formation</i> | 65 |
| <i>STOP 12.5: Highly altered Moore Lake mafic breccia</i> | 68 |
| <i>STOP 12.6: Surface expression of the Chisel "mine horizon" (at the Ghost mine vent raise)</i> . | 68 |
| <i>STOP 12.7: Threehouse mafic volcanoclastic rocks</i> | 69 |
| REFERENCES | 71 |

INTRODUCTION

The Paleoproterozoic Flin Flon greenstone belt is a world-class Volcanic-hosted Massive Sulphide (VMS) district, host to 27 present and past-producing mines and hosting over 400 MT sulphide in its VMS deposits alone. HudBay Mineral's smelter at Flin Flon, and production from its 777, Trout Lake and Chisel North mines, sustains the communities of Creighton, Saskatchewan and Flin Flon, Manitoba and a host of other smaller regional communities. Over the past decades the Manitoba and Saskatchewan Geological Surveys, Natural Resources Canada (Targeted Geoscience Initiative 1 and 3 programs), Natural Sciences, Engineering Research Council (NSERC) and HudBay Minerals itself, have supported a variety of projects aimed at understanding the volcanologic and structural setting of the Cu-Zn deposits in this unique well exposed area.

This field trip is an outgrowth of these collective efforts and presents a significant new interpretation of the volcanic and structural control of the deposits that will be useful to researchers and explorationists in VMS terranes of any era.

The principal objectives of the field trip are to

1. Place the Flin Flon District in the context of the tectonic and magmatic evolution of the Flin Flon Belt and Trans Hudson Orogen
2. Introduce the stratigraphy, lithofacies and structural elements of the Flin Flon District
3. Reconstruct the volcanic and structural architecture and history of the district. In particular demonstrate the evidence for a large, synvolcanic subsidence structure referred to as the Flin Flon cauldron that hosts the VMS deposits and demonstrate how subsequent deformation events have modified this primary volcanic feature and its contained ore deposits.
4. Illustrate the role of volcanism and subsidence in the formation and location of VMS deposits and the role of deformation in their modification.

FIELD TRIP PROGRAM

Participants will assemble in the Victoria Inn, Flin Flon on the evening of May 28 for orientation. The first 4 days of the field trip focus on the Flin Flon Belt regional context (Day 1) and the Flin Flon Mine District (Days 2, 3, and 4). On the evening of Day 1 an evening talk will cover the district geology and exploration history of the Flin Flon belt and on the evening of Day 3, an evening talk will present the new 2D and 3D architecture of the Flin Flon district. The last day of the field trip (Day 5) comprises either an underground tour at the 777 VMS deposit or a surface tour of the geology and structure of the Snow Lake District, host to the Lalor and Chisel VMS deposits.

Parts of the field trip surface tour take place on the HudBay Minerals Plant property. This area is restricted to the public and entrance to the property requires the permission of HudBay Minerals, an appropriate safety/orientation course provided by HudBay, registration at the Main Gate House, and a daily Travel Pass obtained from the Gate House. Field trip participants will take the orientation on Saturday evening. Participants going underground at 777 mine require an additional safety briefing and fit testing for a respirator. They must be clean shaven to pass the respirator fit test. No one will be allowed underground unless they are clean shaven for a respirator. Where access to outcrops is on town roads or near private homes we ask that you respect private property.

A note on hazards: Outcrops and logs may be slippery, especially if wet and lichen covered. Outcrops are commonly steep and care is advised. Participants are asked to remain alert while on company property and obey all directives. A working railway is part of the property and vehicle activity is high.

REGIONAL GEOLOGY AND BACKGROUND

Trans Hudson orogen

The Flin Flon VMS district is situated within the southwestern Trans-Hudson Orogen (Fig. 1,2; THO), the largest Paleoproterozoic orogenic belt of Laurentia (Hoffman, 1988). THO is the site of closure of the Manikewan Ocean (Stauffer, 1984) and one of a series of orogenic belts that formed during the interval 2.00 to 1.78 Ga during amalgamation of the supercontinent Nuna. The Flin Flon belt is situated in the orogen internides of Saskatchewan and Manitoba, which are also referred to as the "Reindeer zone" by Lewry and Collerson (1990). This region preserves accreted oceanic crust and subjacent microcontinent fragments (Sask craton and East Kiseynew domain) caught during convergence of the larger Hearne and Superior cratons. Due to space limitations this guidebook cannot give a complete overview. The interested reader is referred to Corrigan et al. (1997) and references therein for a more complete overview. Additional material can be found in the numerous reports published by the Saskatchewan and Manitoba Geological Surveys.

The southwestern Trans-Hudson Orogen is a tectonic collage consisting of at least five main entities: 1) the reactivated Archean Hearne and Superior Craton margins and associated Paleoproterozoic cover sequences (Cree Lake zone and Superior boundary zone); 2) the Flin Flon – Glennie Complex (Ashton, 1999), an intra-oceanic assemblage composed of ca. 1.91-1.88 Ga primitive to evolved island arc, ocean floor, ocean plateau and associated sedimentary and plutonic rocks that developed during closure of the Manikewan Ocean (e.g. Stauffer, 1984; Syme and Bailes, 1993; Lucas et

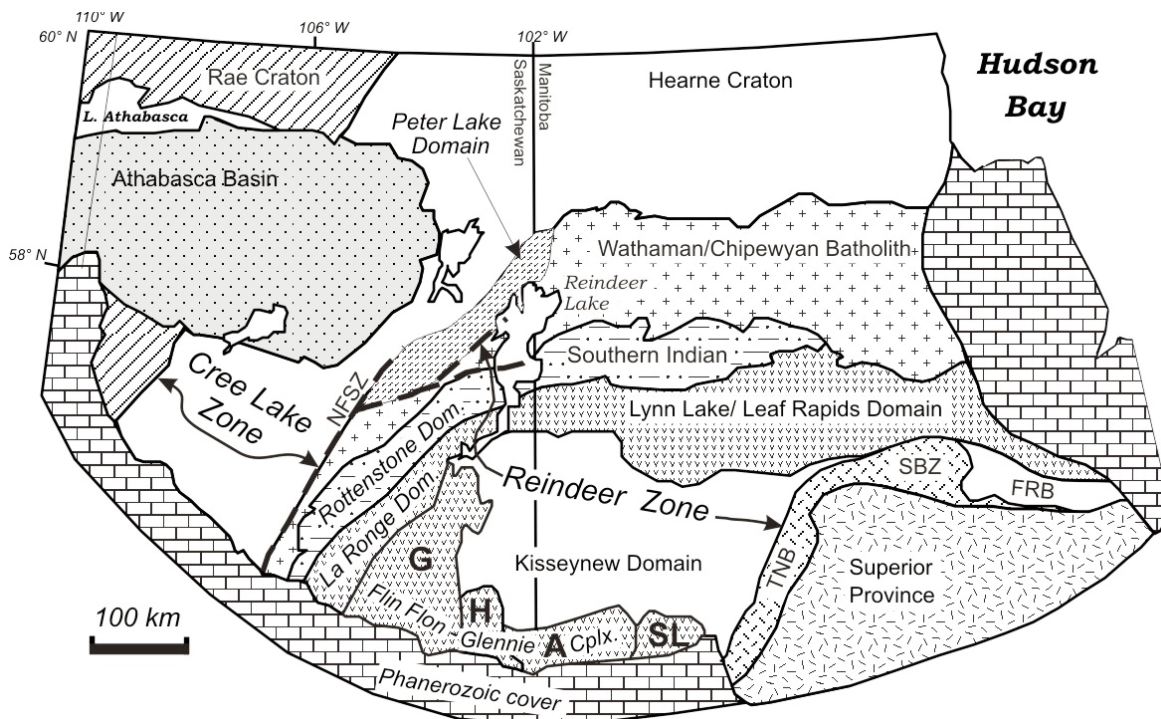


Figure 1. Simplified map of the Trans-Hudson Orogen showing main lithotectonic domains of the Reindeer Zone and bounding domains, after Corrigan et al., 2010. Cree Lake zone is the reactivated portion of the Hearne Craton. Abbreviations are: A, Amisk Lake block; FRB, Fox River belt; G, Glennie domain; H, Hanson Lake block; NFSZ, Needle Falls shear zone; SBZ, Superior Boundary Zone; SL, Snow Lake belt; TNB, Thompson Nickel Belt.

al., 1996; Ansdell, 2005); 3) the northwestern Reindeer zone, an accretionary orogen comprising ocean arc, back-arc, ocean crust and associated sediments, and sub-arc plutonic rocks of the 1.92-1.88 Ga La Ronge-Lynn Lake-Partridge Breast belts, pericratonic arcs that amalgamated before accretion to the southeastern Hearne Craton margin (Zwanzig, 2000; Maxeiner et al., 2004; Corrigan et al., 2005; Kremer, 2009), 4) the ca. 1.86 to 1.84 Ga Wathaman-Chipewyan batholith, an Andean-type continental magmatic arc emplaced along the northwestern Reindeer zone; and 5) marginal, successor and molasse basins developed during the interval 1.85 to 1.84 Ga. (Hoffman, 1988; Lewry and Collerson, 1990; Lewry et al., 1994; Lucas et al., 1994, 1996; Ansdell, 2005). All were penetratively deformed and metamorphosed during the late syn-collisional stage of the Trans-Hudson Orogeny, ca. 1.82 to 1.80 Ga (Lewry and Sibbald, 1980; Ansdell, 2005).

The Trans-Hudson Orogen preserves a relatively complete tectonostratigraphic record from early ca. 2.45 to 1.95 Ga rift to drift sedimentary assemblages deposited along Archean cratonic margins; formation and accretion of ca. 2.0 to 1.88 Ga juvenile crust, to finally 1.88-1.83 Ga post-accretion foredeep and collisional basins and successor arcs (Ansdell, 2005). The resulting wide range of preserved tectonic and magmatic settings host a variety of mineral deposit types. A combination of moderate overthickening, microcontinent accretion, and promontory-reentrant geometry

along Superior craton (e.g. Bleeker, 1990) has fostered wide areas of greenschist to lower amphibolite metamorphic conditions and upper to mid-crustal levels favourable to VMS preservation.

The Flin Flon – Glennie Complex

From east to west the Flin Flon – Glennie Complex comprises the Snow Lake arc assemblage, the Amisk collage, Hanson Lake block and the Glennie Domain (Fig. 2) all amalgamated at ca. 1.87-1.85 Ga as a result of intraoceanic accretion (Lewry and Collerson 1990; Lucas et al. 1996). The complex is host to 27 present and past-producing VMS deposits (Table 1) now preserved in fold-repeated and thrust-stacked tectonostratigraphic assemblages, that structurally overlie the Archean to earliest-Paleoproterozoic Sask Craton (Ashton et al. 2005). The Flin Flon – Glennie complex developed through five main stages (Lucas et al. 1996; Stern et al. 1999), consisting of i) 1.91-1.88 Ga formation of juvenile or pericratonic arcs, back-arc basins, ocean plateaus, ii) 1.88-1.87 Ga intraoceanic accretion, iii) 1.87-1.84 Ga post-accretion development of successor arc intrusions and inter-arc basins, and iv) 1.84-1.83 Ga terminal collision stage, first with the Sask Craton at ca. 1.84-1.83 Ga and later, at 1.83-1.80 Ga, with the Superior Craton (Bleeker 1990; Ellis and Beaumont 1999; Ashton et al. 2005). Only those parts of the complex visited on this trip will be discussed here.

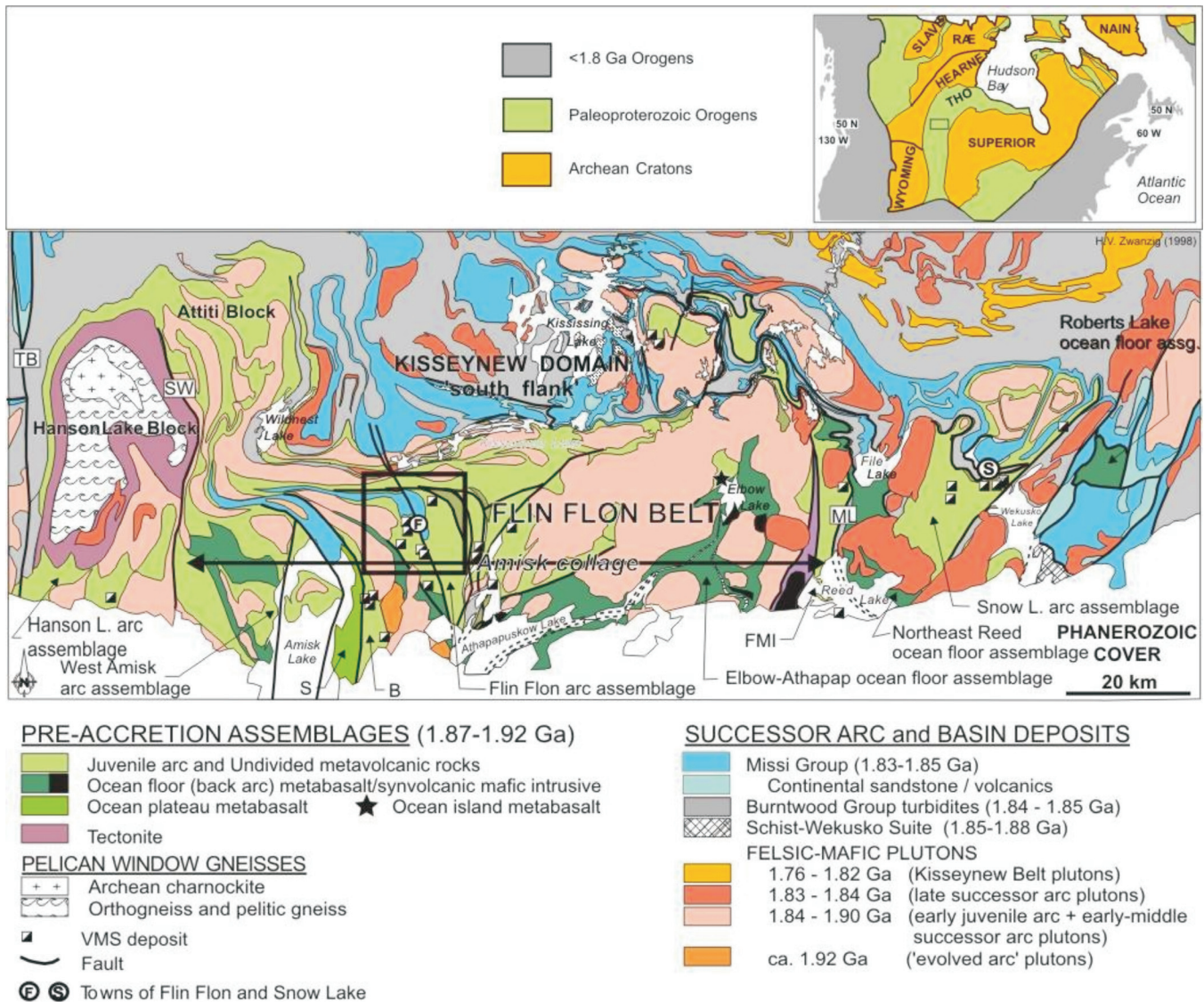


Figure 2. Map of the Flin Flon Belt after Galley et al., 2007 and references therein, illustrating the tectonostratigraphic assemblages, the location of the various accretionary assemblages, and major mineral deposits. B=Birch Lake assemblage; FMI=Fourmile Island assemblage; ML=Morton Lake fault zone; S=Sandy Bay assemblage; TB=Tabernor fault zone.

The Amisk collage

The Amisk collage is subdivided into a number of distinct juvenile arc and ocean floor, island or plateau assemblages (Fig. 2), all separated by faults and shear zones. From west to east these comprise the West Amisk arc assemblage, Sandy Bay ocean-plateau assemblage, Birch nascent arc assemblage, Mystic evolved arc assemblage, the Flin Flon arc assemblage, Elbow-Athapap ocean floor assemblage, and Fourmile Island arc assemblage. Within the Flin Flon arc assemblage distinct juvenile arc, arc-rift and mature-arc sequences host 16 VMS deposits mined to date, including the world-class Flin Flon mine and present producing 777 and Trout lake Cu-Zn mines (Galley et al., 2007). In general, there is an evolution from primitive arc tholeiites to evolved calc-alkaline arc rocks (Stern et al., 1995a) between 1.91-1.88 Ga and a < 10 Ma between VMS formation and accretion (Fig. 3).

Although the arcs are broadly juvenile, Nd isotopic and zircon inheritance data suggest variable input from Archean crust, either via sediment recycling offboard of a cratonic margin or direct formation on rifted microcontinental fragments (Stern et al. 1995; Pehrsson et al. 2009). Archean crust is preserved as thrust-imblicated slices interleaved with juvenile arc and back-arc, ocean floor crust (David & Syme 1994; Lucas et al. 1996, Syme et al. 1999).

Following the early stage of intraoceanic accretion (ca. 1.88-1.87 Ga) continental and pericratonic successor arcs and their related basins formed on the accreted collage (Fumerton et al. 1984; Whalen et al. 1999). The Missi group, a ca. 1.85 Ga alluvial-fluvial molasse sequence of sandstone and conglomerate was deposited on uplifted and eroded rocks of the Amisk collage, belts. Various mafic through felsic intrusive rocks of

Table 1. Major mines of the Flin Flon-Glennie complex. *production plus remaining resource, historical estimates not NI 43-101 compliant.

| Mine | Tonnes | Au g/t | Ag g/t | Cu % | Zn % | Discovered | Method |
|--------------|------------|--------|--------|------|-------|------------|-------------|
| Mandy | 125,000 | 3.02 | 60.15 | 8.22 | 11.38 | 1915 | Prospecting |
| Flin Flon | 62,485,362 | 2.72 | 41.28 | 2.21 | 4.11 | 1915 | Prospecting |
| Sherridon | 7,739,471 | 0.63 | 18.96 | 2.37 | 2.28 | 1922 | Prospecting |
| Dickstone | 1,077,462 | 1.56 | 9.49 | 3.91 | 2.15 | 1935 | Prospecting |
| Cuprus | 462,094 | 1.3 | 28.8 | 3.25 | 6.4 | 1941 | Prospecting |
| Birch Lake | 272,898 | 0.1 | 4.11 | 6.21 | 0 | 1950 | Prospecting |
| Schist Lake | 1,846,656 | 1.3 | 37.03 | 4.3 | 7.27 | 1947 | Geological |
| Don Jon | 79,329 | 0.96 | 15.09 | 3.09 | 0.01 | 1950 | Geophysics |
| North Star | 241,691 | 0.34 | 0.57 | 6.11 | 0 | 1950 | Geophysics |
| Flexar | 305,937 | 1.3 | 6.51 | 3.76 | 0.5 | 1952 | Geophysics |
| Coronation | 1,281,719 | 2.06 | 5.14 | 4.25 | 0.24 | 1953 | Geophysics |
| Osborne | 2,807,471 | 0.27 | 4.11 | 3.14 | 1.5 | 1953 | Prospecting |
| Chisel | 7,153,532 | 1.76 | 44.76 | 0.54 | 10.6 | 1956 | Geophysics |
| Stall | 6,381,129 | 1.41 | 12.34 | 4.41 | 0.5 | 1956 | Geophysics |
| Ghost & Lost | 581,438 | 1.2 | 39.09 | 1.34 | 8.6 | 1956 | Geophysics |
| Anderson | 2,510,000 | 0.62 | 7.54 | 3.4 | 0.1 | 1963 | Geophysics |
| White Lake | 849,784 | 0.72 | 27.1 | 1.98 | 4.64 | 1963 | Geophysics |
| Centennial | 2,366,000 | 1.51 | 26.4 | 1.56 | 2.2 | 1969 | Geophysics |
| Rod | 735,219 | 1.71 | 16.11 | 6.63 | 2.9 | 1970 | Geological |
| Westarm | 1,394,149 | 1.56 | 17.49 | 3.21 | 1.48 | 1973 | Geophysics |
| Spruce Point | 1,865,095 | 1.68 | 19.54 | 2.06 | 2.4 | 1973 | Geophysics |
| Trout Lake | 21,612,296 | 1.56 | 16.02 | 1.74 | 4.97 | 1976 | Geophysics |
| Hanson Lake | 147,332 | 1.09 | 137.14 | 0.51 | 9.99 | 1984 | Geophysics |
| Callinan | 7,773,725 | 2.06 | 24.63 | 1.36 | 4 | 1984 | Geological |
| Chisel North | 2,606,212 | 0.58 | 21.43 | 0.21 | 9.49 | 1985 | Geological |
| 777 | 21,903,539 | 2.12 | 26.94 | 2.59 | 4.39 | 1993 | Geological |
| Konuto | 1,645,691 | 1.99 | 8.91 | 4.2 | 1.63 | 1994 | Geophysics |

two distinct suites of successor arc magmatism intrude the imbricated volcano-sedimentary stack (Stern et al., 1995a).

The Snow Lake arc assemblage

The Snow Lake arc assemblage, situated between the east end of the Amisk collage and the Superior Craton (Figs. 1, 2), comprises remnants of a ca. 1.89 Ga oceanic arc volcano-plutonic complex (e.g. Galley et al., 1986; Lucas et al., 1994; Bailes and Galley, 1999), that may have evolved as a pericratonic arc outboard of the Superior Craton. It likely followed an independent evolution from the remainder of the Flin Flon – Glennie Complex prior to terminal collision (Percival et al., 2006; Corrigan et al., 2007). The Snow Lake area includes a diverse sequence of deformed and metamorphosed volcanic, sedimentary and intrusive rocks, and contains 8 of the Flin Flon belt's 27 base metal mines. These include the Chisel North Zn-Cu mine and 7 past-producers and the newly discovered Lalor deposit.

An introduction to the geology, alteration and deposits of the Snow Lake arc assemblage is contained below in the section discussing stops for Day 5

History of Exploration

Prospecting in the Flin Flon belt coincided with the beginning of the 20th century, likely following on the work of J.B. Tyrrell of the Geological Survey of Canada in the 1890's and E.L Bruce also of the GSC from 1914 to 1918. Exploration quickly gained momentum with the construction of the rail line to Churchill that shortened the length of travel time to get into the belt (Coombe Consultants 1984). The earliest prospecting appears to have been in 1896 by a Mr. Loucks who made an expedition to Reed Lake where he staked a claim (R.C. Wallace). Prospectors travelled along the major river systems from Prince Albert and subsequently from The Pas mainly looking for gold and in 1913 gold was discovered on the shore of Beaver (Amisk Lake) by the prospecting party of Thomas Creighton, Jack Mosher and Leon Dion (Coombe Consultants 1984). Gold showings and generally small deposits occur throughout the belt and there were several gold mines in production in the Wekusko Lake area prior to 1920 (Wallace) and later in the Amisk, Elbow, Douglas and Tartan Lake areas. The belt is also host to the New Britannia mine, which had total production of over 1.6 million ounces of gold from two periods of production 1949 – 1958 and 1995-2005.

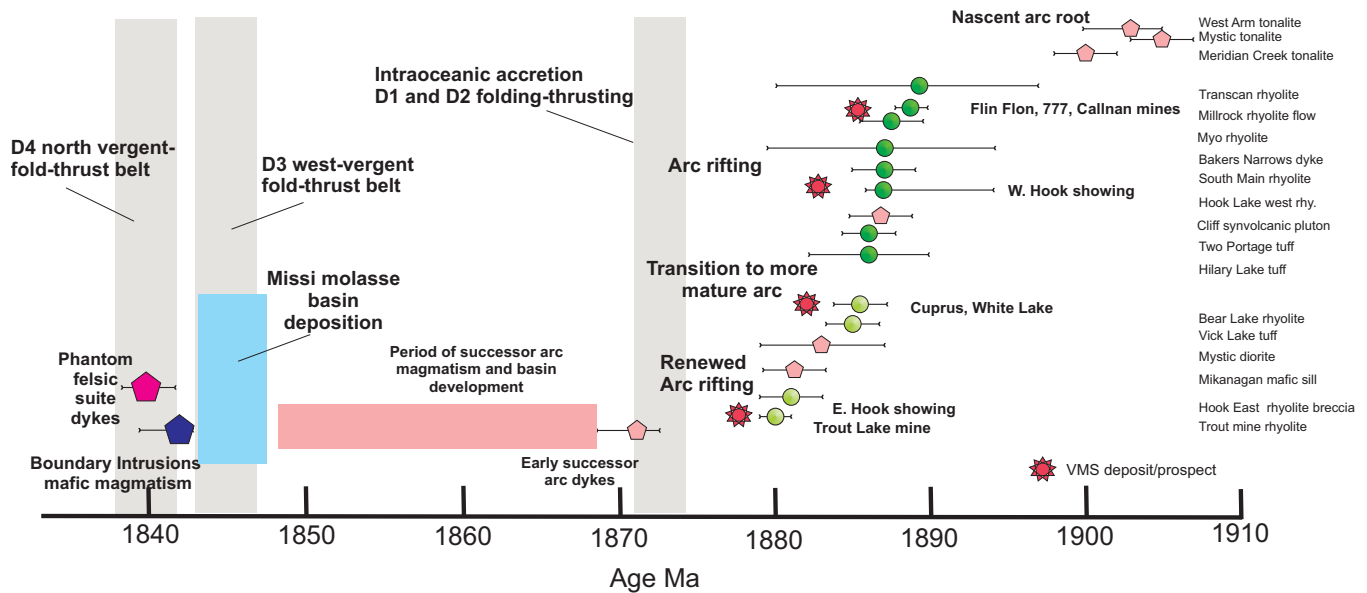


Figure 3. Temporal evolution in the Flin Flon district. Ages from Lafrance et al., submitted; Rayner, 2010; and Stern et al., 1995 (and references therein). Note VMS forming events associated with successive phases of arc-rifting over a 10 Ma time period, and the short time frame between VMS formation and D₁ accretion, ca. 8 Ma.

The Flin Flon Belt is now of course best known for its base metal production from volcanogenic massive sulphide deposits. The first base metal mines in the belt were discovered in 1915 by the same Creighton-Mosher-Dion prospecting team who were shown what became the Flin Flon Mine by a local trapper David Collins. In 1917 the Mandy Mine, also discovered in 1915 by another party, became the first producing base metal mine in Manitoba (Fig 4.). Ore was transported by barge and wagons to the rail head at The Pas and then to Trail B.C. for processing. Although the world-class Flin Flon Mine was discovered in 1915 it was not put into production until 1930 after metallurgical problems related to the fine grained nature of the ore were solved by using flotation methods. With total production exceeding 62 million tonnes at a grade of 2.64% copper, 4.13% zinc, 2.64 grams/tonne gold and 41.49 grams/tonne silver the deposit is by far the largest in the belt.

To date there have been approximately 28 producing VMS deposits in the belt of which three, 777, Trout Lake and Chisel North are currently being mined by HudBay Minerals Inc (Fig 2). Prospectors found 7 of the deposits prior to 1953 and the advent of electromagnetic geophysical technology. Since 1950, geophysical methods have been the dominant exploration method and sixteen mines were found by drill testing geophysical targets including the Trout Lake Mine

In more recent times deposits, including 777 and Chisel North, are attributed to drill testing geological or structural targets in the vicinity of known mines. Although the Flin Flon mine is the largest deposit in the belt there has been a trend to finding deposits larger than the average of 5.8 million tonnes with the Trout

Lake (21.6m), Callinan (7.8m), 777 (21.9m) and most recently the Lalor deposit which now stands at >30 million tonnes and is in a development stage. There has also been a trend to finding the deposits at deeper depths as demonstrated by 777 and Lalor which lie at depths of 500 to 1500 metres. Much of the exploration activity has also shifted to the south, exploring under the Paleozoic cover cover of flat lying carbonate rocks (Fig 2).

Nickel and PGE occurrences are also common throughout the belt and one nickel mine, Namew Lake operated from 1988 to 1993, producing 2.3 million tonnes at a grade of 0.63% copper and 1.79% nickel from a deposit under the Paleozoic cover. Exceptionally high PGE concentrations occur at the McBratney Lake occurrence where a drill hole intersected 7.3 metres that assayed 15.4 g/t Pd, 3.2 g/t Pt, 1.6% Cu, 1.2% Ni, and 21.5 g/t Au.

Lithium-bearing pegmatites are known and actively explored east of Wekusko Lake.

Geology, Structure, and VMS deposits of the Flin Flon District

The Flin Flon District is divisible into a >1.88 Ga juvenile, oceanic arc assemblage comprising basalt, basaltic andesite, rhyolite, and synvolcanic intrusions (formerly Amisk Group; Syme and Bailes, 1993), and a <1.88 Ga assemblage consisting of calc-alkaline “early successor arc” plutons (pre-Missi intrusive rocks), fluvial sedimentary rocks of the Missi Group, and “late successor arc” intrusions such as the Boundary intrusions (Bailes and Syme, 1989; Stauffer, 1990; Stern et al., 1999). A major outcome of research

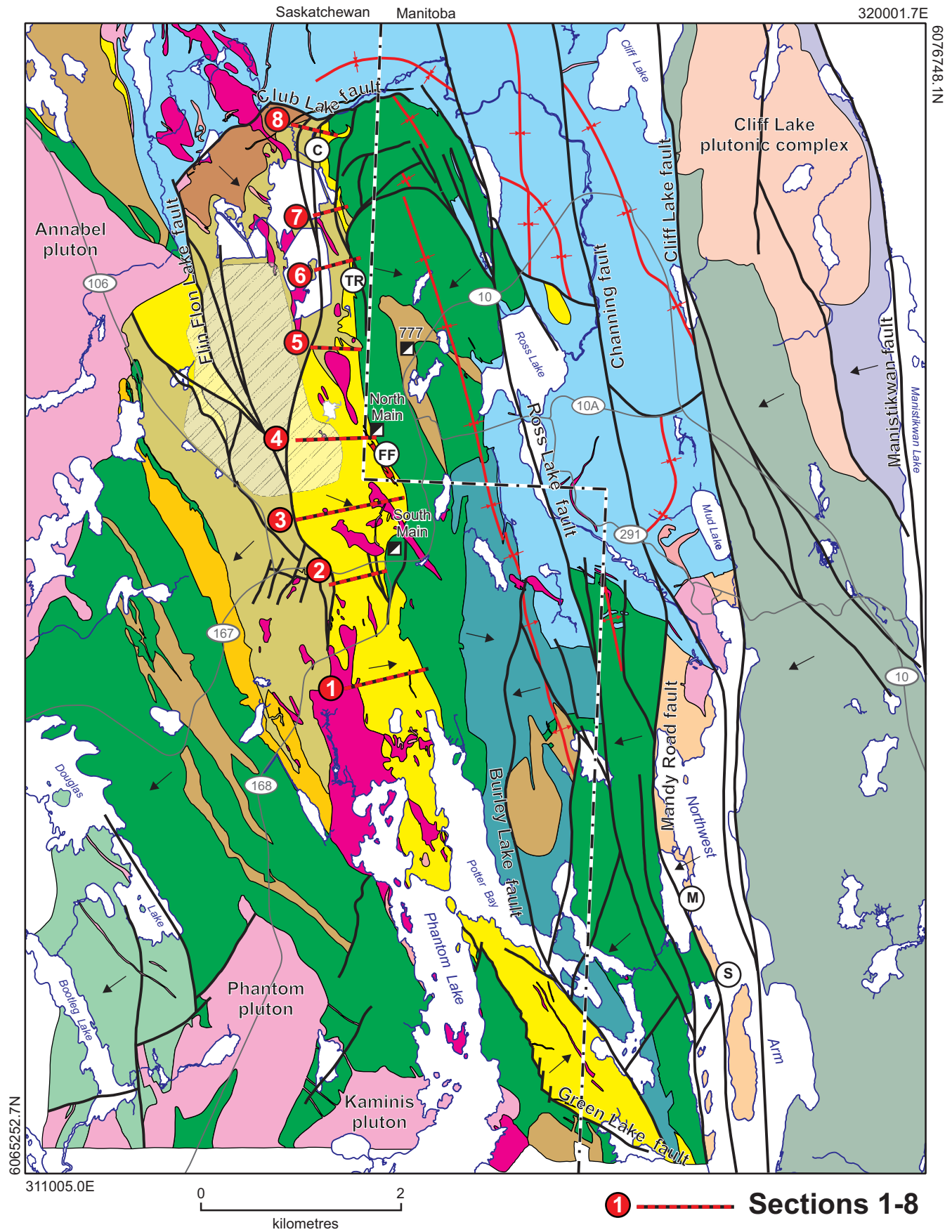


Figure 4. Geology and structure of the Flin Flon District showing the location of stops and transects (modified after Simard et al., 2010).

conducted under TGI 1, an NSERC-Hudbay Minerals-Laurentian University CRD Grant (supported by the Manitoba and Saskatchewan Geological Surveys) and TGI 3 was the development of an informal stratigraphy for strata of the Flin Flon District. This informal stratigraphy has, for the first time, allowed stratigraphic correlation within the district, and this has resulted in a new geologic map for the Flin Flon District (Fig. 4; Simard et al., 2010), which provided the basis for the new volcanic and structural reconstructions presented herein (Gibson et al., submitted). Strata within the Flin Flon block were subdivided into 4 informal and conformable formations which, from oldest to youngest, include the Flin Flon, Hidden, Louis and Douglas formations as illustrated in Figure 4 (Devine et al. 2002; 2003; Gibson et al., 2003ab; 2005; 2009ab; MacLachlan and Devine, 2007; DeWolfe, 2008; DeWolfe et al. 2009ab; Simard et al., 2010). However, as the structural architecture of the Flin Flon District and the geometry of mapped formations have been shaped by multiple generations of folding, thrusting and strike-slip faulting it is prudent to recognize that within the Flin Flon Block, major north-north-west striking early thrust faults and late strike-slip faults have dissected the block into structural panels as illustrated in Figure 5 (Simard et al., 2010). Lithofacies within each formation can differ somewhat between panels and the correlation of units between panels is not always with certainty. Thus, the description of each formation and lithofacies that follows is generalized, but details regarding lithofacies are provided, and uncertainties in stratigraphic correlation discussed, within the Stop descriptions. An idealized stratigraphic column for the Flin Flon, Hidden and Louis formations, and their members, is illustrated in Figure 6.

Terminology

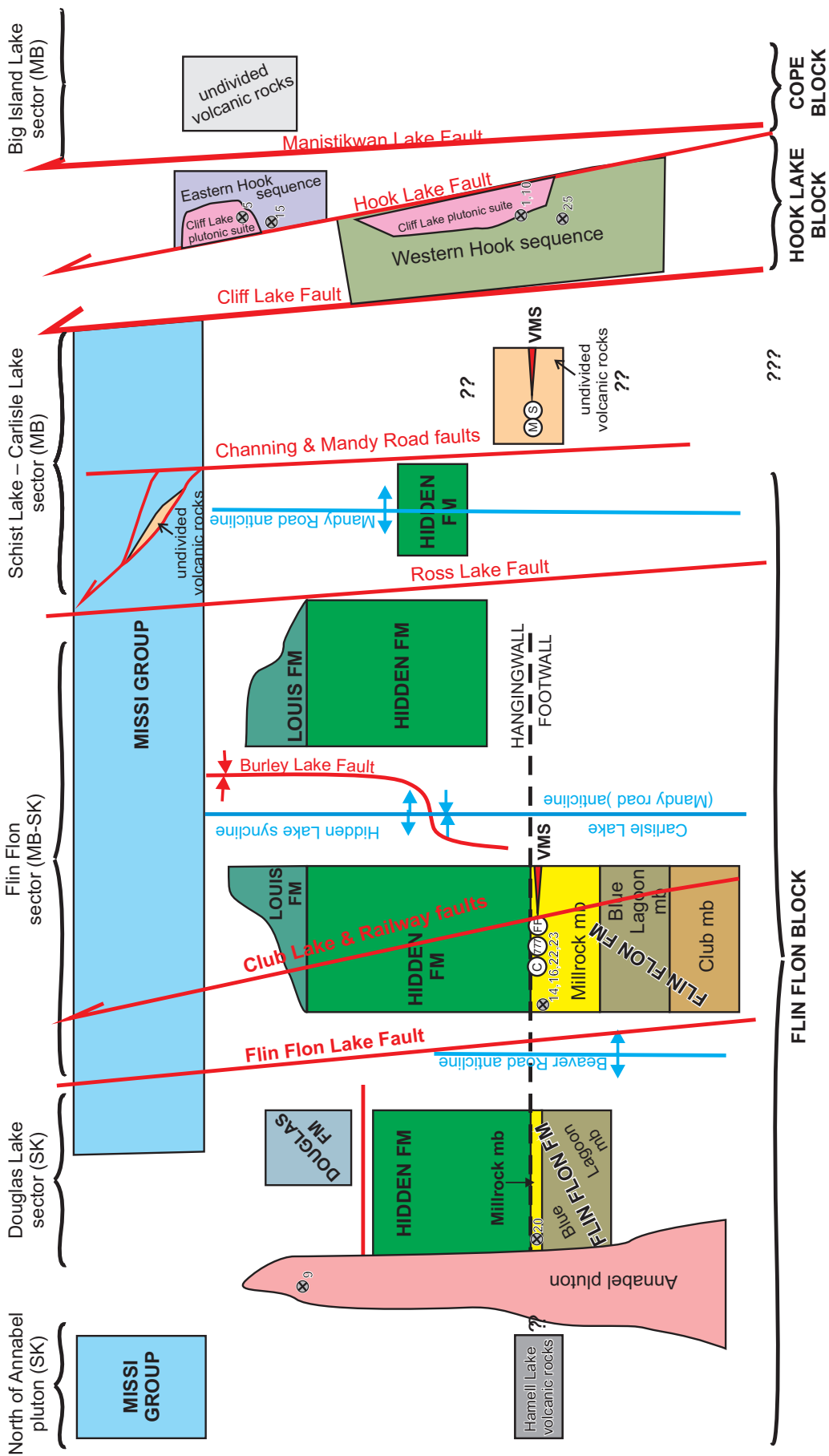
The terminology for clastic volcanic rocks is controversial, so it is important to define the terms that are being used in order to avoid confusion. Herein, the term volcaniclastic is used to describe a clastic rock composed entirely or dominantly of volcanic material and may include primary autoclastic (including hyaloclastite), pyroclastic, and peperite deposits, and their redeposited, syneruptive equivalents (White and Houghton, 2006). As many primary and resedimented volcaniclastic lithofacies are difficult to distinguish, these lithofacies are classified using the same, non-genetic, granulometric nomenclature as proposed by Fisher (1966), Fisher and Schmincke, (1984), Gibson et al., (1999) and White and Houghton (2006), which is based on the size and percentage of clasts (material >2 mm in size) relative to matrix (material <2 mm) into tuff, lapilli tuff, lapillistone, and tuff breccia.

The term “*peperite*” is used with a genetic meaning according to the definition of White et al. (2000): “peperite (n): a genetic term applied to a rock formed essentially in situ by disintegration of magma intruding and mingling with unconsolidated or poorly consolidated, typically wet sediments”.

The term “*cryptoflow*” is used to describe high level intrusive sills that possess many of the features typical of flows, including aspect ratio, but were emplaced into unconsolidated volcaniclastic deposits just below the seafloor (Gibson et al., 2003a; DeWolfe et al., 2011). It includes both massive and pillowed lithofacies that are characterized by peperite along the upper (and lower) contacts. The term megabreccia is used to describe coarse, block-rich, mafic volcaniclastic lithofacies in which the predominant clasts are angular to subangular blocks of massive and pillowed basalt, with lesser amoeboid-shaped and scoriaceous lapilli in a matrix comprising fine, cusped, shard-like lapilli and tuff. The coarse block of massive and pillowed basalt attain sizes of up to 50 m and can be difficult to distinguish from coherent flows. Megabreccias occupy and define fault bounded basins, and were transported primarily as high concentration mass flows (debris flows) that were triggered by the collapse of fault scarps during or immediately following subsidence (Gibson et al., 2009a and b; submitted).

The term “*included tuff*” is used to describe inclusions of tuff observed within massive coherent flows, or between pillows (but not within individual pillows; DeWolfe et al., 2009a). In pillowed flows, if the bedding within the tuff inclusions is well-developed and parallel to the flow contacts then the tuff is interpreted to have settled out of the water column as a suspension deposit during and after emplacement of the pillowed flow (DeWolfe et al., 2009a). If the bedding within the tuff inclusions is irregular, contorted, or absent the included tuff is interpreted to have been squeezed or injected between pillows as the flow moved over or was emplaced within unconsolidated volcaniclastic deposits (DeWolfe et al., 2009a). In the latter case the pillows may be brecciated, in situ brecciated, or veined by tuff and/or have margins composed of peperite.

The term *sedimentary* is used to describe epiclastic terrigenous and chemical sedimentary rocks; the former refers to rocks composed of material derived through chemical or mechanical weathering. Epiclastic sedimentary lithofacies are classified according to the percentages of gravel, sand, silt, and clay-sized particles, as defined by Wentworth (1922). The term “*epidote-quartz alteration*” refers to round or amoeboid patches consisting of a granular mosaic of epidote and quartz with minor actinolite in mafic volcanic rocks. Epidote-quartz alteration is attributed to relatively high-temperature (>300°C, <400°C) evolved seawater-



Note: All fold structures shown on this schematic stratigraphic figure, including the Burley Lake Fault (a faulted syncline), are pre-Missi in age. Red lines represent faults, blue lines represent folds, blue arrows represent facing directions of a given structure. Grey circles with subscripted number(s) refers to geochronology samples listed on the geochronology table to the left. (VMS: volcanicogenic massive sulphide deposits, C: Callinan, M: Mandy, S: Schist Lake)

Figure 5. Schematic stratigraphic sections of the Flin Flon area. For simplicity only pre-Missi folds are shown. Red lines represent faults, blue line folds and arrows represent facing directions on either side of a given structure. Circles denote VMS deposits where C=Callinan, FF = Flin Flon, M = Mandy and S = Schist Lake (MB = Manitoba and SK = Saskatchewan). Modified after Simard et al., 2010.

rock interaction within semi-conformable hydrothermal alteration zones associated with some VMS districts (Galley, 1993; Gibson and Kerr, 1993; Alt, 1999; Harper, 1999; Banerjee et al., 2000; Banerjee and Gillis, 2001)

The term *cauldron*, as used herein follows the definition proposed by Smith and Bailey (1968) to include “all volcanic subsidence structures regardless of shape, size, depth of erosion or connection with surface volcanism”. Cauldron is preferred over caldera as the deformation and erosion precludes reconstructing the original geometry and size of the Flin Flon subsidence structure, and the mechanisms proposed for subsidence are not unequivocally understood.

Flin Flon formation

The Flin Flon formation is exposed on both sides of the Flin Flon Lake Fault (Fig. 4) and it is subdivided in three mappable members, which from oldest to youngest, include the Club, Blue Lagoon and Millrock members (Fig. 6; Devine et al., 2002; Devine 2003; Gibson et al., 2003; Gibson et al., 2009a).

Club member

The Club member is only exposed north and west of the tailing ponds where it occurs as a shallowly dipping, south-southeast facing succession ~500m thick (apparent thickness; Fig. 4). The Club member is truncated at its base by the Club Lake Fault to the north and it is conformably overlain by the Blue Lagoon member to the south and east (Fig. 4).

The Club member consists of massive, aphyric coherent rhyolite, monolithic rhyolite breccia, and rhyolite-clast-bearing mafic volcanoclastic and bedded tuff lithofacies intercalated with lesser aphyric mafic flows. The coherent rhyolite associated volcanoclastic lithofacies are interpreted as part of rhyolite flow or dome complexes with their in-situ and transported flank breccias (Devine, 2003; Gibson et al., 2005). The associated heterolithic mafic volcanoclastic rocks are interpreted to have been derived from the proximal resedimentation of pre-existing mafic and to a lesser extent felsic volcanoclastic lithofacies and their localized accumulation within basin(s) suggests that strata of the Club member were erupted and deposited during or after subsidence. The fine, well bedded tuff is interpreted to be a product of suspension sedimentation and low-concentration density currents resulting from concomitant mafic pyroclastic eruptions that accompanied effusive mafic and felsic volcanism (Gibson et al., submitted).

Blue Lagoon member

The Blue Lagoon member (Fig. 4) is characterized by distinctly plagioclase phyric flow lithofacies (15 to 20 % plagioclase up to 1.2cm) and plagioclase crystal-rich

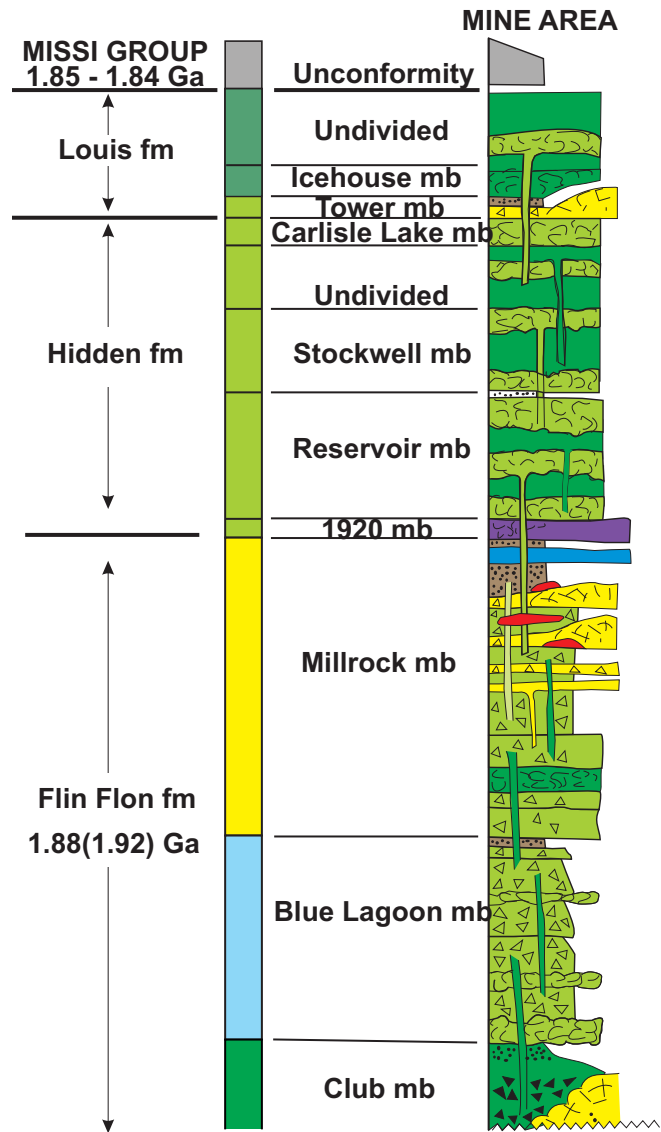


Figure 6. Idealized stratigraphic column showing generalized lithofacies through the Flin Flon, Hidden and Louis formations east of the Flin Flon Lake Fault and on the west limb of the Hidden Lake Syncline modified after Gibson, et al., (2007; 2009a). (lithofacies color – yellow = rhyolitic lithofacies where triangles denote breccia; lighter and darker green, uniform = massive flow/sill/dyke, pillow symbol = pillowed lithofacies; lighter green with triangles = volcanoclastic lithofacies, primarily megabreccias, brown + bedded tuff lithofacies and red = massive sulphide).

volcanoclastic lithofacies. East of the Flin Flon Lake Fault, the Blue Lagoon member lies conformably on the Club member and is conformably overlain by rocks of the Millrock member (Fig. 4, and sections 5 to 8 in Fig. 7). The base of the Blue Lagoon member is characterized by the intercalation of plagioclase-phyric pillowed lithofacies with the plagioclase-crystal-rich volcanoclastic lithofacies which suggests the latter, in part, may be transported autoclastic deposits of the former (Devine, 2003). Where the volcanoclastic units contain clasts of aphyric basalt and/or rhyolite the volcanoclastic units are interpreted to be syneruptive, redeposited deposits generat-

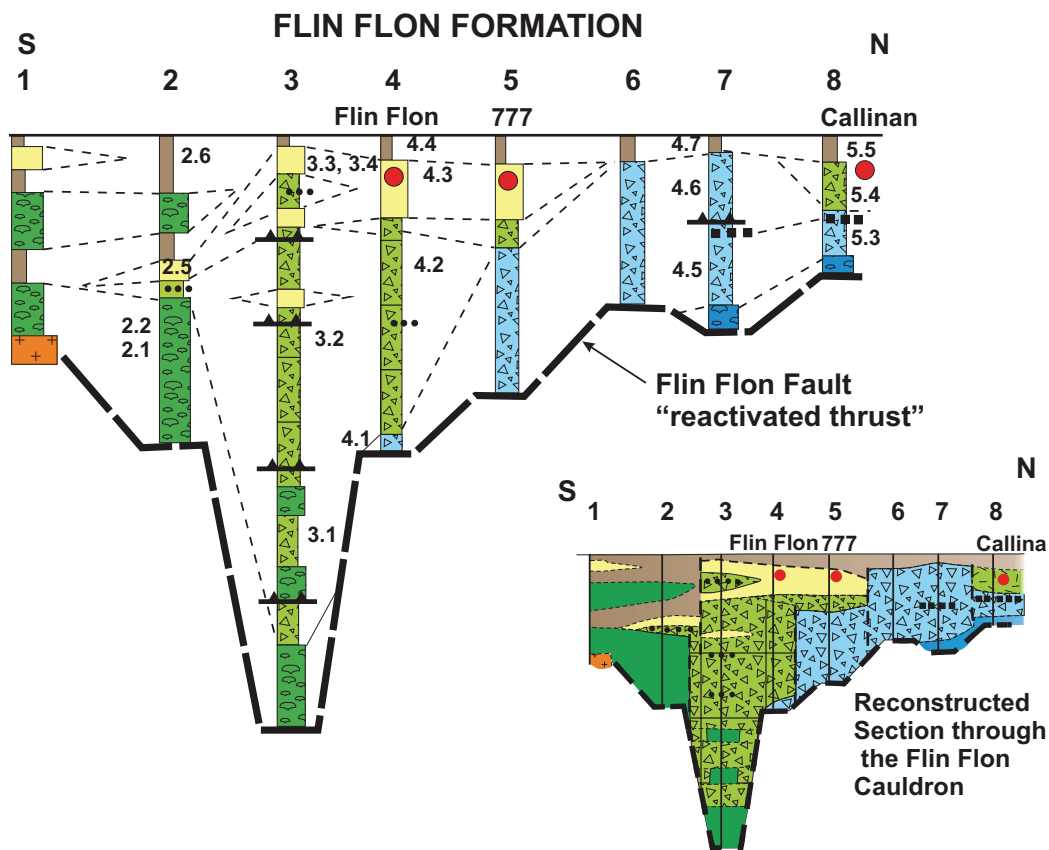


Figure 7. Stratigraphic sections through the Flin Flon Formation on the west limb of the Hidden Lake Syncline (excluding the Club member) showing generalized lithofacies, thrust faults and Stop locations (dark blue and light blue with triangles = coherent flow and volcanoclastic (megabreccia) lithofacies of the Blue Lagoon member; dark green and lighter green with triangles = coherent flow/sill and volcanoclastic (megabreccia) lithofacies, yellow = coherent and breccia lithofacies and brown = bedded tuff lithofacies of the Millrock member; red circle = massive sulphide deposit; and orange = Boundary intrusion; modified after Gibson et al., 2009; submitted). Sections represent a south to north cross section through the Flin Flon cauldron and illustrate its facies architecture.

ed through subsidence and collapse of faults scarp walls (Devine, 2003; Gibson, et al., 2006; 2009a) The upper portion of the Blue Lagoon member is characterized by thick, heterolithic, plagioclase-crystal-rich volcanoclastic and flow lithofacies. The volcanoclastic lithofacies are interpreted as primary pyroclastic deposits, their syneruptive redeposited equivalents and/or subsidence induced megabreccias, deposited by mass flows into rapidly subsiding, fault-controlled basins (Devine, 2003; Gibson et al., 2005; 2006; 2009a and b). The Blue Lagoon member is characterized by abrupt changes in the thickness and limited lateral continuity of units indicate the presence of several distinct synvolcanic fault blocks (Fig. 7). The dominance of coarse volcanoclastic versus flow lithofacies within the Blue Lagoon member east of the Flin Flon Lake Fault is interpreted to a product of extensive and long-lived, subsidence-triggered, mass-flow sedimentation (Gibson et al., 2006; 2007; 2009a; submitted).

West of the Flin Flon Lake Fault, the Blue Lagoon member is characterized by a localized thick accumulation of coarse, plagioclase-crystal-rich heterolithic mafic volcanoclastic, mega-breccia, and tuff lithofacies

interbedded with aphyric and plagioclase-phyric mafic flow lithofacies. The volcanoclastic lithofacies occur within synvolcanic “sub-basins” in the dominantly mafic flow lithofacies and collectively define a larger subsidence structure (Gibson et al., 2003; 2006; 2007; MacLachlan and Devine, 2007).

Millrock member

The Millrock member is host to over 80 million tonnes of massive sulphide ore with average grades of 4.4% Zn, 2.2% Cu, 2.2g/t Au and 32g/t Ag within the Flin Flon, Callinan, and 777 VMS deposits (Bamburak, 1990; Thomas, 1990). The Millrock member is exposed east and west of the Flin Flon Lake Fault (Fig 4). East of the Flin Flon Lake Fault, the Millrock member is traceable along strike for >5 km where it ranges in apparent thickness from <10m in the north to >500m in the south. Its lithofacies are discontinuous and define syn-volcanic basins that range from tens to several hundreds of metres in width (Gibson et al., 2006; 2009 a). Because of this lateral variability in lithofacies thickness and extent, the Millrock member will be described for the four sections examined during the

field trip: the Millrock Hill (and south), South Main, Smelter and Callinan sections (sections 2, 3, 5 and 8 : Figs. 4 and 7).

Mill Rock Hill Section

The Millrock member has an apparent maximum thickness of 600 metres, dips moderately and faces to the east and consists, from oldest to youngest, of an aphyric to sparsely plagioclase porphyritic basaltic pillowed flow lithofacies (section 2: Figs 4 and 7). Intercalated with the pillowed lithofacies is an amoeboid breccia lithofacies that increases in abundance upwards. The amoeboid breccia facies consists of irregular to bomb-like, fluidal, amygdaloidal (up to 20% quartz amygdules) basaltic fragments with distinctly chilled margins in a finer-grained matrix composed of millimetre-sized, cusped, chloritized lapilli. The amoeboid clasts are intact and broken, and the breccia is crudely bedded, where beds are defined by an abrupt change in the size and abundance of amoeboid fragments; the beds are discontinuous. The amoeboid breccia lithofacies is conformably overlain and gradational into a basaltic scoria lithofacies that consists of rounded to irregular, fluidal, bomb-like clasts within a matrix composed of millimetre-sized, cusped chloritic shards and finer tuff. The principal difference between the amoeboid breccia and basaltic scoria lithofacies is that the former is clast to matrix supported and intercalated with pillowed flow lithofacies, whereas the latter is dominantly matrix supported and the scoria clasts are smaller and many have a more fluidal form. The amoeboid breccia facies is interpreted to be a product of mild fire-fountain eruptions, and essentially represent submarine spatter deposits (Fig 8.1), that along with intercalated pillowed flows constructed small, low relief pillow volcanoes (Gibson et al., 2009; submitted). The basalt scoria lithofacies is a product of more vigorous fire-fountain eruptions, which blanketed the pillow volcano with fine tephra and fluidal bombs (Fig. 8.1 and 8.2; Gibson, et al., 2009a; submitted).

The basaltic scoria lithofacies is conformably overlain by coherent, quartz-feldspar phyric rhyolite and heterolithic and monomictic rhyolite breccia lithofacies. The coherent quartz-phyric rhyolite facies grades outwards and upwards into in situ brecciated, then clast rotated breccia and into monomictic, transported rhyolite breccias comprised of angular blocks of rhyolite up to 1 m in size. This transition from coherent rhyolite to rhyolite breccia is interpreted to define a coherent rhyolite dome, its carapace breccia and flank breccias produced by mass wasting (over steepening) of the dome (Fig 8.3 and 8.4; Gibson et al., 2006; 2009a; submitted; e.g. McPhie et al., 1993). The coherent and monomictic rhyolite breccia yielded a U-Pb zircon age of 1888.9 Ma +/- 1.6 Ma (Rayner, et al., 2010). More sparsely

quartz-porphritic rhyolite sills or cryptodomes occur throughout the Millrock member (Fig 8.5) and along with the coherent rhyolite flow define a rhyolitic vent area that is coincident with the older basaltic vent area that constructed the underlying pillow volcano (Gibson et al., 2009 a). This was followed by faulting and emplacement of basalt dykes that are feeders for the overlying Hidden Formation basaltic flows (Fig 8.5).

South Main Section

At South Main, the Millrock member is a moderately-dipping, east- to northeast-facing succession with a total apparent thickness, including thrust repetitions, of approximately 1000m (sections 3 and 4 of Figs. 4 and 7). The base and bulk of the Millrock member consists of a thick megabreccia lithofacies and lesser coarse mafic volcanoclastic lithofacies that are locally intercalated with aphyric to sparsely plagioclase-phyric and lesser plagioclase-phyric (15-20% plagioclase) basaltic flow lithofacies (Gibson et al, 2006; submitted). The mafic volcanoclastic lithofacies, mainly tuff breccia and breccia are characteristically monolithic, and composed of aphyric, scoriaceous, amoeboid- to fluidal-shaped basalt fragments, and more rounded, equant basalt fragments. The megabreccia lithofacies consists mainly of angular to subangular blocks, up to 10's of metres in size, of aphanitic, amygdaloidal, massive and pillowed basalt, with minor amoeboid and scoriaceous clasts in a finer-grained, tuff to lapilli tuff matrix (Gibson et al., 2006; 2009a). Volcanoclastic lithofacies composed entirely, or dominated by fluidal, amoeboid ("spatter") and scoriaceous clasts have been interpreted as products of fire-fountain and/or strombolian eruptions (Gibson et al., 2006; 2009a; submitted). The thick, poorly sorted and crudely bedded megabreccia lithofacies, previously referred to as the Creighton member of the Flin Flon formation (Devine, 2003), is interpreted to represent subsidence-triggered, debris-avalanche deposits derived from the collapse of fault scarp walls composed of pillowed flows, and mafic volcanoclastic deposits (Gibson et al., 2006; 2009a). Lateral variations in the thickness of megabreccia units are consistent with their emplacement by high-concentration mass flows into localized, fault-controlled depositional basins within a larger subsidence structure (Fig 9) (Devine, 2003; Gibson et al., 2006; submitted).

The mega breccia lithofacies fines upward, is intercalated with aphyric pillowed basalt flows, and is conformably overlain by coherent quartz(feldspar) phyric rhyolite and breccia lithofacies interpreted to represent rhyolite domes and cryptodomes (Bailes, et al. 2001). The rhyolite domes, cryptodomes and bedded tuff lithofacies are interpreted to define the Flin Flon mine stratigraphic interval. A coherent, quartz-feldspar phyric rhyolite dome at South Main yielded a U-Pb

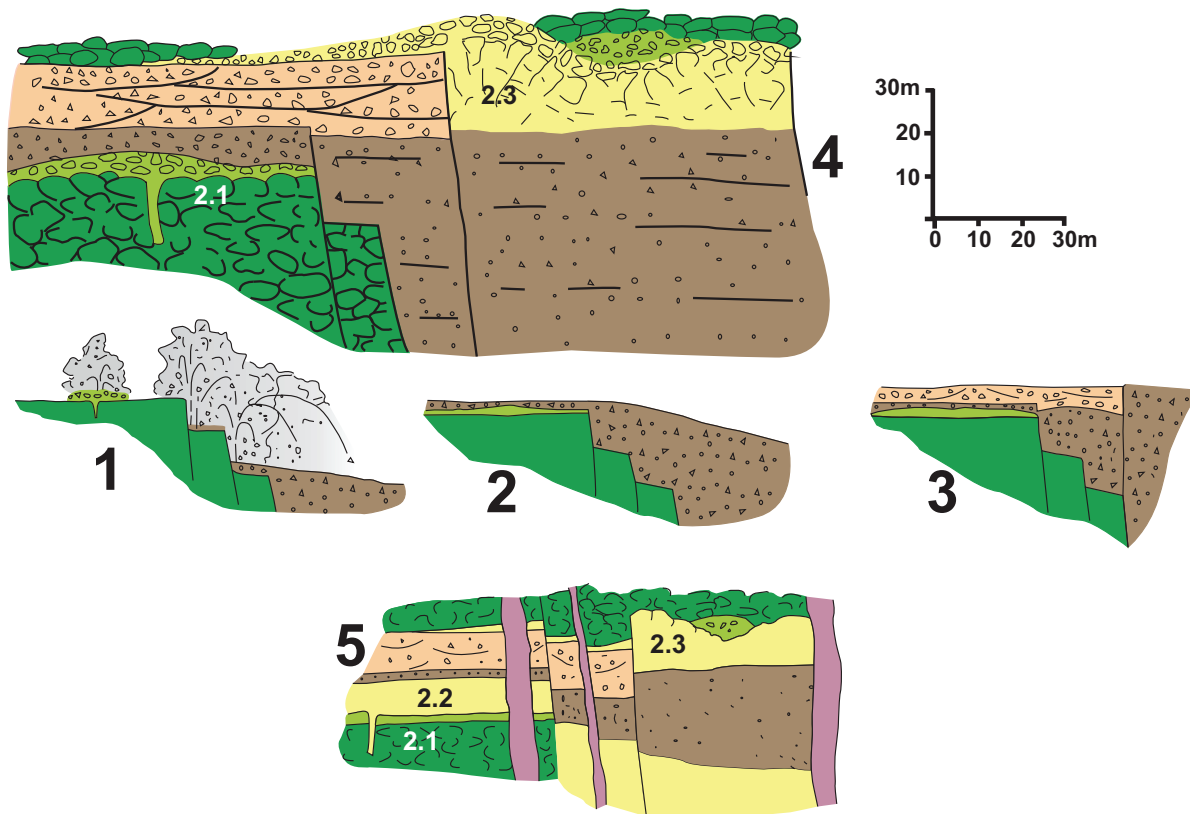


Figure 8. Possible reconstruction of the sequence of volcanic events that produced the facies architecture of the Millrock member at Millrock Hill (after Gibson et al., 2009a).)dark green = pillow and lesser amoeboid breccia lithofacies; light green = amoeboid breccia lithofacies; darker brown = scoria lithofacies, lighter brown = heterolithic rhyolite-basalt lithofacies, yellow = coherent and monolithic rhyolite breccia lithofacies; dark green and light green pillowed and amoeboid breccia lithofacies above the rhyolite belong to the Hidden formation.

zircon age of 1887.1 Ma \pm 2.2Ma (sample PQB-1707-08; Rayner, 2010).

Smelter Section

The Millrock member in the Smelter section consists, from oldest to youngest, of a monolithic basalt breccia lithofacies, a quartz-phyric coherent rhyolite and breccia lithofacies, a heterolithic breccia and tuff lithofacies, and a bedded tuff lithofacies (section 5 in Figs 4 and 7). The monolithic basalt breccia facies is framework supported, crudely bedded and is interpreted to be a finer, more distal facies of the megabreccia lithofacies in the South Main section. The coherent rhyolite and breccia lithofacies is interpreted to represent rhyolite domes whereas the heterolithic breccia and tuff lithofacies are interpreted to represent carapace and flank breccias to the rhyolite flows or domes (Devine, 2003; Gibson, 2006; Gibson et al., 2009a; e.g. McPhie et al., 1993). The bedded tuff lithofacies is interpreted to represent the same bedded tuff as at South Main and along with the quartz-phyric coherent rhyolite and breccia, are interpreted to define the Flin Flon-777-Callinan stratigraphic interval. However, the massive base of a quartz-phyric rhyolite dome located at the Smelter section and interpreted to represent the immediate footwall to the Flin Flon VMS deposit was dated

at 1903 \pm 5 Ma, in marked contrast to the 1888 Ma age obtained from interpreted stratigraphic equivalent rhyolite domes at South Main and at Millrock Hill (sample FF92-1; Stern et al., 1999). More geochronological work is required to clarify this \sim 10 Ma age discrepancy.

Within the Millrock member the coherent and volcanoclastic rhyolite units define localized “felsic volcanic centres”. Massive sulphide lenses at the Flin Flon, 777 and Callinan deposits occur principally at or near the top, but also within, below, and lateral to rhyolite flow dome complexes indicating a long-lived hydrothermal event where felsic volcanism was accompanied by ore deposition (Figure 9). The bedded tuff lithofacies occurs above the massive sulphide deposits and defines the top of the Millrock member (Figs 7 and 9; Gibson et al., 2007, 2008; 2009; submitted).

Callinan Section

North of the mine site, the Millrock member constitutes a steeply-dipping, northeast-facing succession that is 10-150m thick (apparent thickness). Its uppermost unit, the bedded tuff lithofacies, is the same as that described at the previous sections and in this section it thickness ranges from 5 to 40 m. It is underlain either

VMS Ore Environment - Flin Flon Cauldron

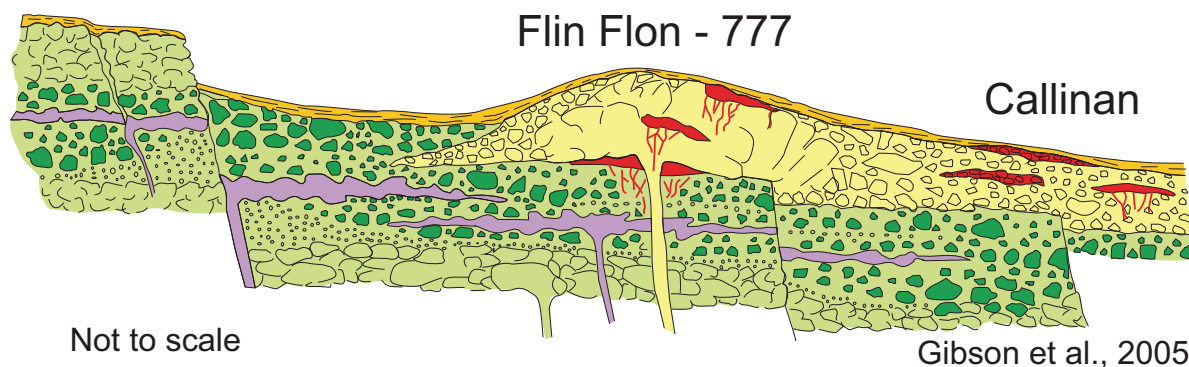


Figure 9. Reconstruction showing the facies architecture and volcanic environment post formation of the Flin Flon, Callinan and 777 VMS deposits (pre-Hidden formation volcanism, modified after Gibson, et al., 2005). Millrock member lithofacies as follows; light green with symbols = pillowed flows, light green with darker green clasts = coarse volcaniclastic and megabreccia lithofacies; lighter green with circles = scoria-rich lithofacies, purple = basalt sills (peperite on margins); yellow = coherent and monomictic rhyolite breccia lithofacies; darker yellow = bedded tuff lithofacies and red = massive sulphide.

by Blue Lagoon volcanoclastic lithofacies (sections 6 and 7 of Figs 8 and 9) or by a massive to crudely-bedded, heterolithic mafic breccia lithofacies of the Millrock member that ranges up to 150m in thickness and is restricted to the Callinan section (section 8 of Fig. 9). The base of the heterolithic mafic breccia lithofacies occupies scour channels within the underlying crystal-rich lithofacies of the Blue Lagoon member. The localized lateral extent of the heterolithic mafic breccia lithofacies is consistent with emplacement into a distinct fault-bounded basin (Devine, 2003) and the crude layering has been interpreted to suggest emplacement by mass flows into a rapidly subsiding structurally controlled basin (Devine, 2003).

The mafic bedded tuff lithofacies is dominantly ash-sized with minor lapilli-sized scoria clasts, plagioclase crystals, and beds containing accretionary lapilli (Gibson et al., 2006). The lateral continuity of bedded tuff lithofacies (along the entire strike length of the Millrock member; Fig 9), dominance of plane-parallel beds, and occurrence of accretionary lapilli support deposition by suspension sedimentation and, to a lesser extent, by low concentration density currents where the eruption column(s) at times broke the water-air interface to form the accretionary lapilli that occur within the waterlain bedded tuffs (e.g., Cas and Wright, 1987; Fisher and Schmincke, 1984; McPhie et al., 1993; Gibson et al., 1999; 2006). Local cross-bedding and scour structures are interpreted to result from bottom current reworking (Gibson, 2006). The bedded tuff unit represents a significant hiatus in effusive volcanism that followed emplacement of rhyolite domes and cryptodomes, and formation of the VMS deposits (Fig. 9; Devine, 2003; Gibson et al., 2003b; Gibson et al., 2009a).

Millrock member west of the Flin Flon Lake Fault

West of the Flin Flon Lake Fault (Fig. 4), the Millrock member occurs in three thrust panels. The first is located immediately west of the Flin Flon Lake Fault near the Creighton landfill site, where the Millrock member occurs as screens of monolithic and heterolithic mafic breccia, felsic tuff and lapilli tuff, and coherent to brecciated quartz-phyric and quartz-plagioclase-phyric coherent rhyolite within a “fault-bounded” mafic dyke and sill complex (Bailey, 2006; MacLachlan, 2006a, b, and c; MacLachlan and Devine, 2007; Bailey et al., submitted). A sample of the quartz-phyric lapilli to block breccia lithofacies (that may either represent a cryptodome or a dome) yielded an U-Pb zircon age 1889 ± 9 Ma (sample PQB07-KM157-01-01; Rayner, 2010). This age is interpreted to represent the maximum age of the breccia and is consistent with the other dated Millrock member rhyolite dome rocks except for the rhyolite dome in the Smelter section.

Stockwell (1960) and HudBay Exploration and Development Inc. recognized a monolithic felsic breccia lithofacies, interpreted to be Millrock member, under what is now the southeast corner of the tailings pond. Millrock member also occurs at Hilary Lake, where it consists of a thin-bedded to laminated mafic and felsic tuff lithofacies, a felsic volcanoclastic lithofacies, and remnants of an extrusive coherent rhyolite lithofacies at Myo Lake to the south (Bailey, 2006; MacLachlan and Devine, 2007; Bailey et al., submitted). A sample of the finely bedded felsic tuff lithofacies southeast of Hilary Lake yielded a U-Pb zircon age of 1886 ± 4 Ma (sample PQB07-KM156-01-01; Rayner, 2010). A sample of a quartz-plagioclase phyric, synvolcanic felsic sill collected approximately 2 km southeast, near Myo Lake where it transgresses the southern extension of the felsic tuff lithofacies,

yielded an age of 1888.9 +/- 1.7 Ma (sample 05MYO-01; Bailey, 2006)

Reconstruction

The cross-section through the Millrock member in Figure 7 was constructed using the four sections described above, plus four other sections as shown in Figure 4 (Gibson et al., 2009 a). In order to minimize non-stratigraphic variations in thickness, the reconstruction is restricted to the west limb of the Hidden Lake syncline, and sections were located to minimize structural thickening due to thrust fault duplication (Gibson et al., 2009 a; submitted). As illustrated in Figure 7, the abrupt lateral change from coherent basaltic flow lithofacies south of Millrock Hill to the thick discontinuous basaltic volcanoclastic and megabreccia lithofacies between Millrock Hill and the Smelter section is interpreted to define one structural margin of a larger subsidence structure or cauldron that hosts the FlinFlon-Callinan-777 VMS deposits (Syme and Bailes, 1993; Gibson et al., 2006; 2007; 2009; MacLachlan and Devine, 2007). Abrupt lateral changes in thickness in the volcanoclastic and megabreccia lithofacies are interpreted to reflect their deposition within smaller fault bounded basins within the larger cauldron (Devine, 2003; Gibson et al., 2003b; 2009). The package of coherent mafic flow lithofacies and the overlying intercalated volcanoclastic rocks and mafic flows observed south of Millrock Hill are interpreted to lie outside or inwards, along the structural margin of the cauldron (Gibson et al., 2009). The Flin Flon, Callinan, and 777 deposits formed within this large, subaqueous cauldron, where they are spatially and temporally associated with the construction of rhyolite flow and dome complexes that were emplaced during the waning stage of Flin Flon formation volcanism (Devine, 2003; Gibson, et al., 2006; 2009). Millrock rhyolitic volcanism and VMS ore-formation was followed by a period of explosive basaltic volcanism from vents located primarily at, and south of Millrock Hill (Gibson et al., 2009). The bedded tuff lithofacies that extends across the cauldron and south of Millrock Hill is a product of these eruptions. A simplified, diagrammatic illustration of the sequence of volcanic, tectonic (subsidence) and VMS ore-forming events are illustrated in Figure 10 (Gibson et al., 2007).

Hidden formation

The Hidden formation is composed of mafic flows, sills and volcanoclastic rocks, with subordinate basaltic-andesite flows, rhyolite flows and felsic volcanoclastic rocks (Stockwell, 1960; Bailes and Syme, 1989; DeWolfe et al. 2004; 2005; 2006; DeWolfe, 2008). It is divisible into four mappable members: the 1920 member, the Reservoir member, the Stockwell

member, and the Carlisle Lake member (DeWolfe et al., 2009a; Figs 4 and 7). The base of the Hidden formation is placed at the last occurrence of tuff and/or rhyolite of the underlying Millrock member of the Flin Flon formation, and is marked by: 1) aphyric to sparsely plagioclase porphyritic basalt flows and/or sills of the Reservoir member; or 2) amphibole-porphyroblastic basaltic andesite rocks of the 1920 member; (DeWolfe, 2008; 2009a). Although localized, alteration associated with the Flin Flon-Callinan-777 ore system has been traced into the Hidden formation (Ames et al., 2002; 2003; Tardif; 2003).

1920 member

The 1920 member occurs on the west limb of the Hidden Lake syncline (Fig. 4) where it comprises aphyric Fe-Ti-P basaltic andesite cryptoflows (DeWolfe et al., 2009a and b), and aphyric to sparsely plagioclase-phyric Fe-Ti-P basalt flows and sills.

North of the Railway fault, the 1920 member is easily recognisable by its abundant randomly oriented acicular amphibole porphyroblasts (25-50%) and by its light metallic blue colour on fresh surface. It forms a thick massive to pillowed aphyric basaltic-andesite cryptoflow (DeWolfe, 2008) with an approximate strike length of 1.1 km. East of the Flin Flon open-pit and south toward Phantom Beach the flows and sills of the 1920 member form a thin east-facing succession with a total apparent thickness of 50-200m. Here the flows and sills lack the amphibole porphyroblasts so characteristic in the north; the regional "amphibole-in" metamorphic isograd runs east-west around Hidden Lake, between the two 1920 member occurrences.

The 1920 member, although more correctly identified as Fe-Ti basalt or Fe-Ti basaltic-andesite, has been referred to as "icelandite" in the immediate Flin Flon surrounding because of its more andesitic composition relative to surrounding basalts, and its Fe-Ti-enrichment, which resembles true mid-ocean-ridge-derived icelandite as first described by Carmichael (1967) (DeWolfe et al., 2009b). Fe-Ti basalt or Fe-Ti basaltic-andesite in arc environments have been recognized before where they were interpreted to have been derived through the assimilation of hydrated mafic crust (older lavas) by mafic magma emplaced into shallow-level (<2 km) magma chambers in a rift environment (DeWolfe et al., 2009b; Barrie and Pattison, 1999; Perfit et al., 1999 Embly et al., 1988;). Such shallow-level magma chambers are a manifestation of high-temperature rift environments that could have generated and sustained the high-temperature convective hydrothermal systems necessary for the formation of massive sulphide mineralization, like at Flin Flon (DeWolfe et al., 2009b), which make the recognition of "icelandite-like" unit a potential VMS exploration tool.

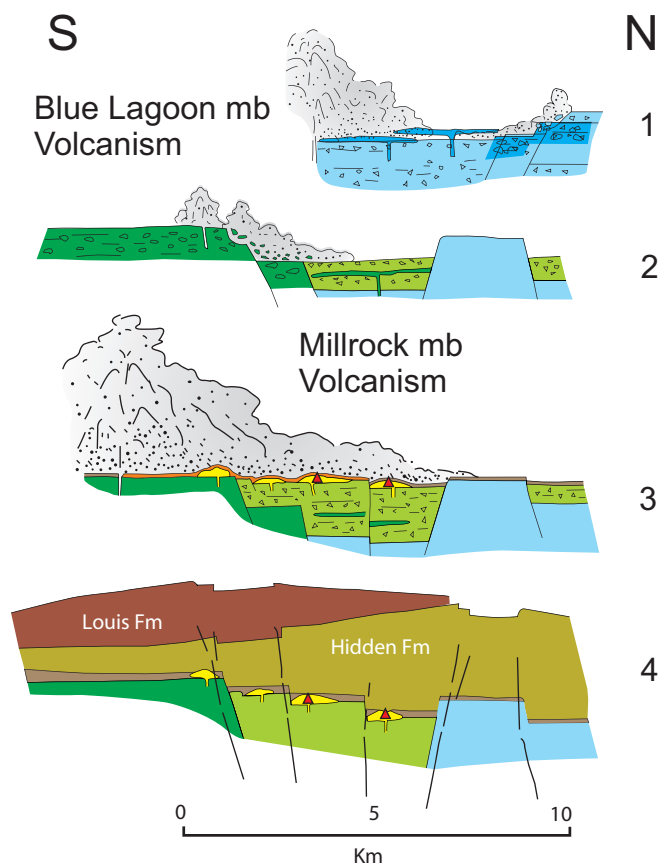


Figure 10. Sequence of interpreted volcanic, subsidence and VMS ore-forming events (modified after Gibson, et al., 2009a; submitted; legend colour scheme as in Figure 9). **1)** Localized subsidence accompanied Blue Lagoon effusive and pyroclastic eruptions. Piece-meal collapse into nested basins, re-deposition of volcanoclastic lithofacies (megabreccias). Subsidence centred in the north. **2)** Initial effusive eruptions of the Millrock member constructed small basaltic lava shield on the “then” south margin of the cauldron. Piece-meal collapse in the north and along south margin triggered collapse of the lava shield to produce thick mega-breccia deposits. Collapse was accompanied by pyroclastic and effusive eruptions, within the Flin Flon cauldron. **3)** Eruption rhyolite localized to nested faults basins within the cauldron led to the construction of rhyolite flow-dome complexes. High-temperature hydrothermal discharge was localized in time and space to rhyolite dome construction to form the Flin Flon, Callinan and 777 deposits. Ore formation was followed by voluminous basaltic pyroclastic eruptions that were centred along the south margin but tephra blanketed the entire cauldron and south margin. **4)** Dominantly effusive eruption of basalt (lesser andesite) constructed the Hidden and Louis formation lava shields that buried the Flin Flon cauldron and VMS deposits (DeWolfe et al., 2009). Lava shield construction was accompanied by localized and minor subsidence.

Reservoir member

The Reservoir member forms a steeply- to moderately-dipping succession with an apparent thickness of 400-800m which is folded around the Hidden Lake syncline and the Burley Lake fault. It can be traced along strike for >6 km from the Club Lake fault to the north to Phantom Lake in the south. The Reservoir, Stockwell, and 1920 members, are thrust-repeated by a set of two north-east trending thrust faults, and the Upper and Lower Railway, and Catherine thrusts faults. East of the Flin Flon open-pit, portions of the Reservoir mem-

ber are repeated along with the top of the Millrock member of the Flin Flon formation by a west-verging north-trending thrust fault. West of the Flin Flon Lake fault, the Reservoir member forms a homoclinal steeply-dipping southwest-facing sequence with an apparent thickness of >1000 m.

The Reservoir member comprises aphyric, plagioclase-phyric and pyroxene-plagioclase-phyric basalt flows, with minor of volcanoclastic rocks (DeWolfe et al., 2009a). The flows are mainly massive (>70% in volume) and pillowed (>30% in volume) and contain some large lava tubes. Aphyric massive flows are usually 5-15 m thick and pillowed flows usually 10-50 m thick. The majority of flows are variably peperitic, or contain included tuff. Both massive and pillowed flows commonly show light green quartz-epidote alteration patches, usually elongated and parallel to flow contact in the massive flows, and ovoid to amoeboid in shape in the pillowed flows. Volcanoclastic rocks occur as thin, discontinuous units between flows and pillows, or included in flows (peperitic).

Stockwell member

The Stockwell member occurs north of the Lower Railway fault where it forms a generally south facing moderately-dipping sequence with an apparent thickness up to 300 m that is thrust-repeated with portions of the Reservoir and 1920 members (Fig. 4). The Stockwell member comprises massive, pillowed and breccia facies of strongly plagioclase (15-50%) and pyroxene (>5%) porphyritic basalt flows and is locally overlain by a mafic volcanoclastic unit (DeWolfe et al., 2009a).

Carlisle Lake member

The Carlisle Lake member occurs between the Burley Lake fault and the Channing-Mandy Road fault (Fig. 4). South of Carlisle Lake, the Carlisle Lake member forms a homoclinal steeply-dipping west-facing sequence with an apparent thickness >800 m including potential structural thickening by the Ross Lake fault. North of Carlisle Lake, on the east side of the Ross Lake fault, the Carlisle Lake member rocks are folded/faulted around the Mandy Road anticline and form an east-facing sequence >400 m thick truncated to the east by the Channing-Mandy Road fault. The base of the Carlisle Lake member is truncated to the east by the West Mandy Road Fault, but the top is exposed on the peninsula between Burley Lake and Potter Bay of Phantom Lake.

The Carlisle Lake member comprises aphyric to sparsely plagioclase-phyric, plagioclase-phyric basalt flows, mafic volcanoclastic rocks, and minor amount of felsic volcanic rocks and is interpreted to represent a lateral equivalent to the Reservoir member (DeWolfe, 2008; Simard, 2006a). Where the Reservoir member is

interpreted to record the onset of mafic magmatism forming the Hidden shield volcano above the Flin Flon subsidence structure, the Carlisle Lake member most likely occupies a subsidence structure on the side of the main volcanic edifice (DeWolfe, 2008; Simard, 2006a).

Louis formation

The Louis formation is composed of basalt flows and mafic volcanoclastic rocks, with subordinate amount of rhyolitic flows and felsic volcanoclastic rocks (Figs 4 and 7). It represents a second episode of mafic volcanism following that of the Hidden formation (DeWolfe et al., 2009a).

The Louis formation is subdivided in two members, the Tower and Icehouse members, as well as a package of undivided basalt flows (Fig. 7; DeWolfe et al., 2009a). The base of the Louis formation is placed at the first occurrence of rhyolite and associated volcanoclastic rocks of the Tower member. Where the Tower member is not present, the base of the Louis formation is defined by the first occurrence of plagioclase-pyroxene porphyritic basalt flows. The top of the Louis formation is not exposed and is represented by the present-day erosion surface.

Tower member

The Tower member occurs at the base of the Louis formation and consists of massive to in situ-brecciated, aphyric or sparsely plagioclase- and quartz-phyric rhyolite overlain by, and locally underlain, by mafic tuff (DeWolfe et al., 2009a). Where the coherent rhyolite portion of the Tower member is not present, the member is defined by a laterally extensive mafic tuff which includes lapilli-tuff beds containing rhyolite fragments derived from the coherent rhyolite portions (DeWolfe et al., 2009a).

The coherent portion of the Tower member rhyolite occurs near the northern extent of Louis and Burley lakes. The rhyolite is interpreted to have been emplaced as a flow or dome with associated autoclastic breccias, and marked the onset of a new magmatic episode in the hangingwall of the Flin Flon-Callinan-Triple 7 VMS deposits (DeWolfe et al., 2009a).

Icehouse member

The Icehouse member occurs on the east side of the Burley Lake fault where it forms a steeply-dipping, east-facing sequence (25-100 m thick) of strongly plagioclase-pyroxene-phyric basaltic, pillowed to massive flows and mafic volcanoclastic rocks near the base of the Louis formation. From north to south the Icehouse member changes from a thick (~100 m) single facies massive flow to a thin (~25 m) multifacies flow with a massive bottom and a pillowed top (DeWolfe et al., 2009a). There is a gradational contact along strike

where the massive facies grades into pillowed facies over a distance of 1–2 m. Finely laminated epidote-quartz-altered mafic tuff commonly occurs between the pillows. The upper margin of the pillowed facies of the Icehouse member is irregular and broken, with a gradation over a distance of 1 m from intact pillows to pillow breccia to an overlying volcanoclastic facies.

North of Louis lake, the massive facies is overlain by a plane-bedded mafic tuff or a mafic lapillistone. The mafic tuff is ≤ 2 m thick and is strongly silicified. West of Louis Lake, overlying the pillowed facies, is a 20 m thick, normally graded, crudely bedded, heterolithic volcanoclastic unit.

The massive Icehouse member flow is interpreted to have formed from the ponding of lava within an inner fault-bounded graben parallel to the feeding fissure (DeWolfe et al., 2009a). Where it grades laterally and vertically from massive facies into pillowed facies as the flow becomes thinner is likely the result of the flow overriding the wall of an inner graben that ponded the Icehouse member flows to the north (DeWolfe et al., 2009a).

Undivided Louis formation rocks

The undivided rocks of the Louis formation account for >90% of the formation, and are present on both sides of the Burley Lake fault. They consist of aphyric to sparsely plagioclase-phyric, plagioclase-phyric, and plagioclase-pyroxene-phyric massive and pillowed basalt flows intercalated with subordinate amount of mafic volcanoclastic rocks (DeWolfe, 2008). West of the Burley Lake fault, the undivided Louis formation rocks sit conformably over either mafic volcanoclastic unit of the Icehouse member, mafic tuff of the Tower member, or aphyric flows of the Reservoir member, Hidden formation. On the east side of the Burley Lake fault, they rest directly on aphyric flows of the Carlisle Lake member, Hidden formation. The top of the undivided Louis formation rocks occurs at the present-day erosion surface.

Structure and Metamorphism

Six ductile deformation events D_1 to D_6 are recorded in rocks of the Flin Flon mining district (Lafrance et al., submitted). D_1 and D_2 occurred during intraoceanic accretion of the Flin Flon arc to other volcanic terranes prior to the emplacement of a suite of ca. 1872 Ma gabbroic dykes (Fig. 3; Rayner, 2010) and deposition of the Missi Group as a cover sedimentary sequence unconformably on volcanic basement. The basement volcanic rocks were folded and possibly faulted during the development of the D_1/F_1 Burley Lake syncline, and were refolded by the NNW-striking D_2/F_2 Hidden Lake fold system, comprising the prominent Beaver Road anticline, Hidden Lake syncline, and Mandy

Road anticline. The F_1 Burley Lake syncline is a faulted syncline that lacks the weak axial plane cleavage that is associated with the F_2 Hidden Lake fold system.

During D_3 , the development of a fold-thrust system, possibly in response to the final accretion of the Flin Flon terrane to the Glennie terrane, produced west-verging, map-scale folds (Pipeline, Mud Lake and Grant Lake synclines) within stacked, east-dipping, thrust sheets of basement and cover rocks bounded by NNW-striking thrust faults (e.g. 1920 fault). Because D_3 and Missi deposition are both bracketed between ca. 1847 Ma, the age of the youngest Missi detrital zircon, and ca. 1842 Ma, the age of crosscutting Boundary intrusions (Fig. 3), uplift and erosion of the basement, and deposition of Missi sediments must have occurred early during D_3 , with the Missi basins quickly thereafter deformed during migration of the D_3 orogenic front.

Collision of the amalgamated Flin Flon-Glennie complex with the Sask craton began as the intervening stretch of oceanic crust between the two microcontinents disappeared through subduction beneath the Flin Flon-Glennie complex. This D_4 collisional event produced N-directed thrust faults (Club Lake, Railway, Catherine faults) and east-trending folds (Flin Flon Creek syncline) that truncate the early west-directed fold-thrust system. D_4 was broadly coeval with but outlasted the emplacement of ca. 1840 Ma Phantom Lake dykes. A strong, SE-plunging, stretching lineation formed during thrusting, and the axis of pre-existing regional folds were rotated into near-parallelism with the lineation, deforming the F_3 Pipeline syncline into a km-scale sheath fold.

The first penetrative regional cleavage (S_5) formed during D_5 . S_5 is a continuous chloritic foliation that wraps around flattened pillows and volcanic fragments in basement volcanic rocks, is defined by the flattening of pebbles and cobbles in conglomerate, and occurs as a disjunctive to continuous cleavage defined by insoluble opaque material, white mica, and chlorite cleavage planes in sandstone and conglomerate matrix. S_5 strikes NW to NNW (320° to 350°) and dips moderately to steeply (50° - 80°) to the NE. It transects the axial plane of regional F_3 and F_4 folds in the Missi cover rocks and is associated with dextral reactivation and shearing of D_3 thrust faults and lithological contacts near the hinge and along the NW-striking limbs of the Hidden Lake syncline. A strong SE-plunging, stretching lineation is associated with D_5 shear zones. It is interpreted as a composite lineation that represents the total finite strain during D_4 and D_5 , that is, it initially formed during D_4 and then was rotated and intensified during D_5 .

The last regional ductile structures in the Flin Flon mining district formed during D_6 during terminal closure of the Manikewan Ocean and collision of the Sask craton and Flin Flon-Glennie complex with the Superior craton at ca. 1.83 Ga to ca. 1.79 Ga. ESE-WNW compression during D_6 produced a second, regional, NNE-striking cleavage and reactivated E-striking D_4 thrust faults as dextral shear zones and NW-striking lithological contacts, D_3 thrust faults and D_5 dextral shear zones as sinistral shear zones.

3D Architecture of the Flin Flon District

A key component of the Flin Flon Targeted Geoscience Initiative-3 project was development of a '3D knowledge cube' of the Flin Flon mine camp. The 'cube' is a model built from serial lithostratigraphic and fault surfaces represented in 3D space that also contains the background drill hole and map constraints. The 3D modelling experiment was designed to test new methods of 3D data analysis and integration (Schetselaar et al., 2010), as well as testing existing structural models for extension of the mine horizon at depth.

The 3D geologic model (Fig. 11) was created from integrated analysis of drill core, mine and surface geological maps and new 2D and 3D seismic data (White et al., 2009). Evaluation of the topology of the 3D lithostratigraphic surfaces and numerous shear zones and thrust faults suggest that the Flin Flon mine camp is underlain by an E-dipping stack of thrust imbricates formed by pre- to post-Missi Group D_{1-3} deformation events. The dominantly east-dipping stack, although still controlling the overall geometry at depth, was subsequently deformed by E-trending D_4 ductile thrust faults that internally imbricated the Missi metasedimentary rocks and overthrust juvenile Flin Flon arc assemblages on top of younger Missi Group rocks with a northerly vergence.

The VMS-hosting Millrock member has been stacked on at least four structural levels due to a combination of the two phases of west-directed thrusting and the latest north-directed thrusting. This has enhanced the VMS potential in the footwall and hangingwall of the orebodies where both thrust systems intersect, by bringing Millrock member prospective units to shallower depths. Drilling in the footwall of 777 mine, underpinned by this new model, led to the recent discovery of a new Zn-rich ore lens, termed the West zone (Malinowski et al., 2008; Pehrsson et al., 2009). The Millrock member and contained ores have furthermore formed a detachment surface at the broad scale relative to the more competent Hidden and Blue Lagoon mafic volcanic sequences.

Thrusting within the Missi cover has also enhanced exploration potential as it brought discrete thrust slices of Flin Flon arc assemblage rocks up into the basin.

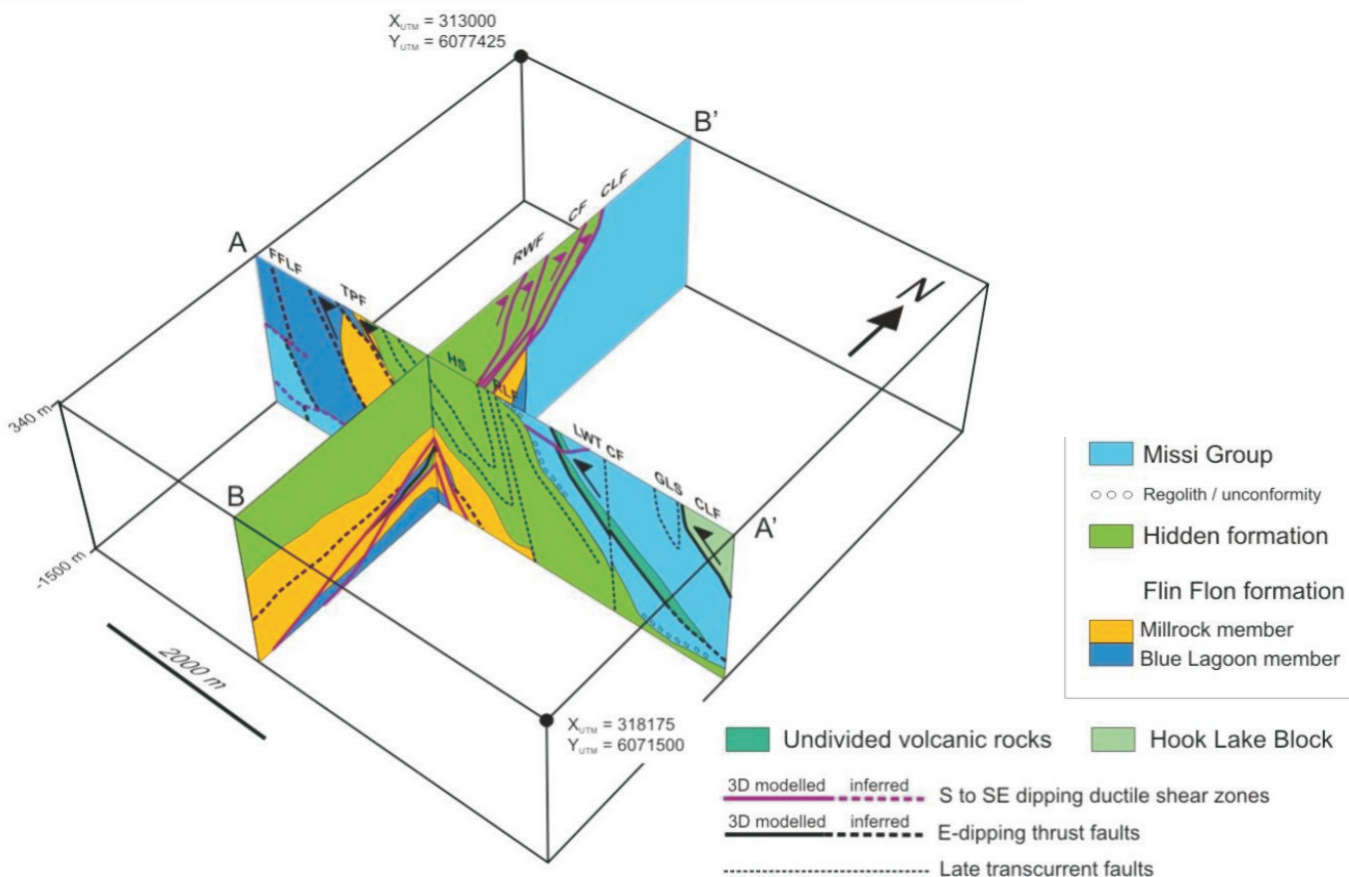


Figure 11. 3D block diagram of the Flin Flon mine camp showing modelled and inferred lithostratigraphic units and faults on EW- and NS-trending sections. CLF = Club Lake fault, CF = Catherine fault, RWF = Railway faults, FFF = Flin Flon Lake fault, TPF=Tailings pond faults, LWT=Lakeview thrust, CF=Channing fault, CLF = Cliff Lake fault, HS = Hidden syncline, GLS = Grant Lake syncline. After Schetselaar et al., 2010.

These slices host the known Lakeview Cu-Zn showing which outcrops and recently discovered mineralization contained within a wholly blind panel 100s m below the basin (Pehrsson et al., 2009). Late N-trending brittle-

ductile subvertical faulting, in part reactivating older west-vergent thrusts, has further segmented the imbricate stack, complicating the correlation of lithostratigraphic successions across them.

DAY 1: REGIONAL CONTEXT OF THE FLIN FLON VMS DISTRICT**STOP 1-1: Meridian – West Arm Shear Zone*****Coordinates***

UTM: N 6068723 E 309684

Overview

The structural relations between the Flin Flon, West Arm and Mystic Lake assemblages and ‘stitching’ intrusive rocks are well exposed in the Meridian Creek area, Saskatchewan (Fig. 12, Syme et al., 1996; Reilly, 1990, 1991, 1992; Thomas, 1989, 1990, 1991).

The West Arm ocean floor assemblage is separated from the Flin Flon arc assemblage by the Meridian-West Arm shear zone. The West Arm assemblage rocks are in tectonic contact with evolved arc plutonic rocks of the Mystic Lake assemblage along the Mystic Lake shear zone, which engulfs the entire Mystic Lake assemblage and rocks of the Birch arc assemblage to the west. West Arm assemblage units appear to be progressively eliminated from south to north between the Mystic Lake and Flin Flon assemblages. The timing of initial juxtaposition of these assemblages along the two shear corridors (D_1), as well as subsequent syn-magmatic deformation (D_2), is indicated by cross-cutting relations with various U-Pb dated intrusive rocks (Stern and Lucas, 1994; Lucas et al., 1996).

Both the Meridian-West Arm and Mystic Lake shear zones contain a SSE-striking, steeply west-dipping penetrative foliation (S_1) associated with D_1 - D_2 deformation. It is defined by the crystallographic alignment of inequidimensional minerals (biotite, amphibole), "flattened" quartz grains and/or quartz-feldspar ribbons. Within intensely deformed units, the S_1 -parallel compositional layering is defined by sheared and/or isoclinally folded (i.e., transposed) quartz veins and both mafic and felsic veins and sheets (Reilly, 1991). Boudinage of veins and compositional layers occurs in both horizontal and vertical planes, suggesting that the shear zones accommodated a component of flattening strain. Many of the felsic veins (tonalite, aplite, and pegmatite) appear to have been emplaced during the ductile deformation event responsible for S_1 and the transposed layering (Lucas et al., 1996). True mylonitic occur in narrow (cm-scale) ductile shear zones in both felsic and mafic intrusive rocks (Reilly, 1991). S_1 is associated with a shallow to moderately SSE-plunging extension lineation (L_1), generally defined by quartz-feldspar rods (polycrystalline aggregates) although locally by amphibole. Development of an L_1 amphibole lineation and growth of oriented hornblende in the necks of boudinaged pyroxenite veins indicates metamorphism synchronous with D_1 - D_2 deformation, probably related to plutonism (i.e., 'regional' contact metamorphism; cf. Lucas et al., 1996).

Stop description

The Meridian-West Arm shear zone is a relatively narrow (<250 m) high strain corridor marked by greenschist-grade, foliated and lineated tectonites derived principally from the West Arm assemblage. Detailed study of the shear zone suggests a dextral component of shear along the contact between the tectonostratigraphic assemblages (Syme et al., 1996). In contrast, the West Arm assemblage transposed into a 100-250 m wide band of laminated mafic-felsic tectonite and mylonite adjacent to the Flin Flon assemblage. The felsic layers in the tectonite are derived from intrusive sheets, a feature it shares in common with in the Mystic Lake shear zone. Kinematic indicators are infrequently observed but include dextrally-extended veins, asymmetrically-extended and back-rotated boudins, and dextral C/S fabrics developed in protomylonite (Reilly, 1992, Lucas et al., 1996).

The Anabel pluton (1886 Ma; Stern and Lucas, 1994), which cross-cuts the Flin Flon arc assemblage, the Meridian-West Arm shear zone and the tectonized West Arm assemblage of the easternmost part of the Mystic Lake shear zone (Lucas et al., 1996) provides a minimum age for the Meridian-West Arm shear zone (Thomas, 1993 and references therein). The Anabel pluton is well foliated to mylonitic within about 25-50 m of its margin; the foliation is parallel to the Meridian-West Arm shear zone foliation and probably formed during continued, post-emplacement deformation along the shear zone. Cessation of deformation along the Meridian-West Arm shear zone is bracketed by the ages of two feldspar porphyry dykes: an 1847 Ma plagioclase-phyric dyke cuts across the shear zone at a low angle but contains the S_1 foliation whereas an 1839 Ma K-feldspar-phyric dyke cuts across the shear zone at a high angle. This result is consistent with the 1838 Ma age of the Boot-Phantom pluton (Heaman et al., 1992), which also cross-cuts the shear zone at a high-angle and does not contain the S_1 foliation (Thomas, 1989).

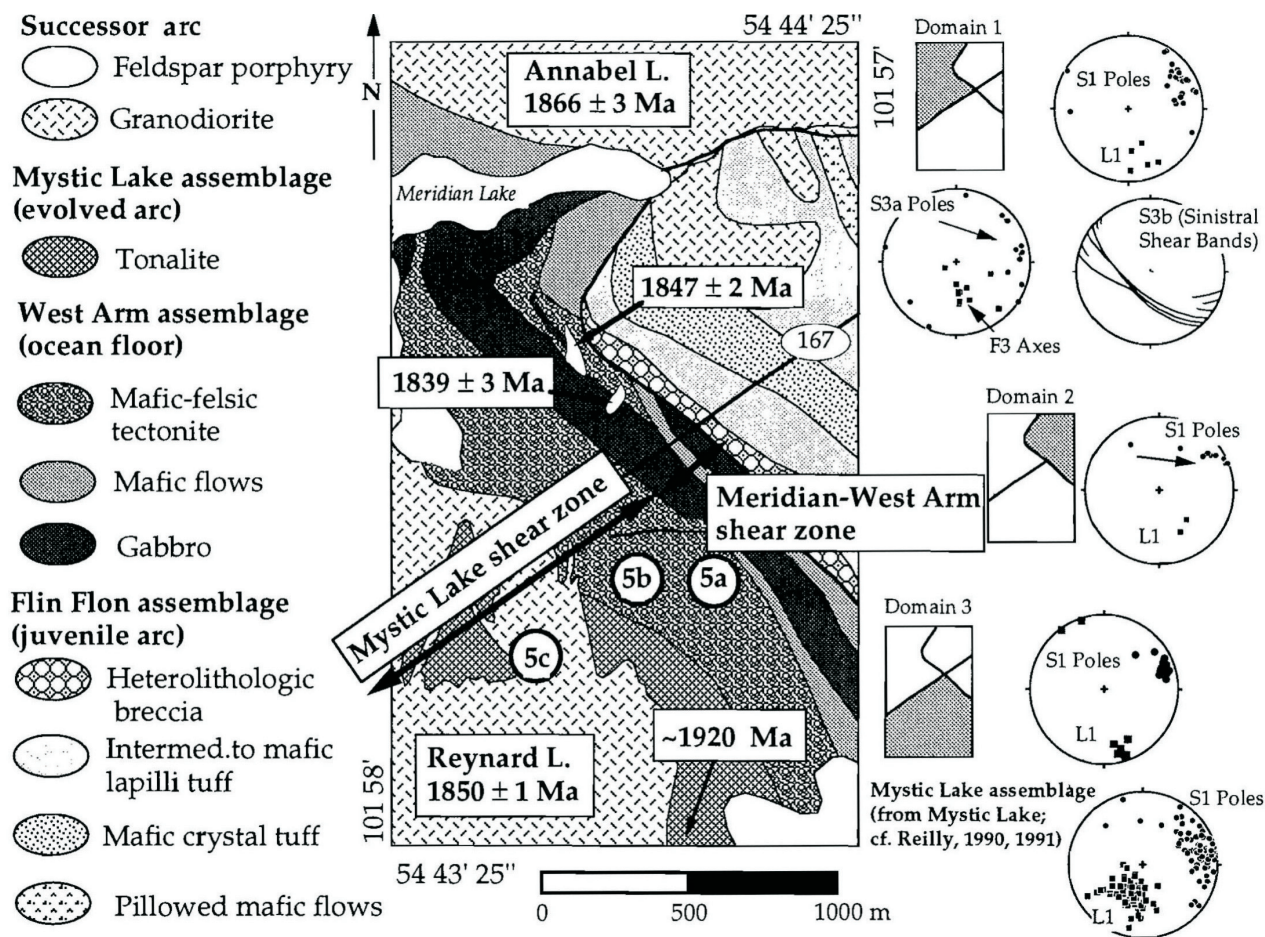


Figure 12: Geological map of the Meridian Creek-Hutton Bay (Meridian Lake) area, after Thomas (1990, 1992; in Syme et al., 1996). The Meridian-West Arm shear zone includes the westernmost 50 m of the Flin Flon arc assemblage and all of the West Arm assemblage units in the map area. The Meridian-West Arm shear zone merges with the Mystic Lake shear zone in the Mystic Lake assemblage units. U-Pb age determinations from Stern et al. (1993) and Stern and Lucas (1994). Equal area stereonet display structural data from Reilly (1990, 1991) and Lucas (pers. comm. 1996). Fabrics correlate with deformation events as follows: $S_1/L_1 = D_1-D_2$. Location maps for stereonet data show structural domains relative to Highway 167 and the boundary between the Flin Flon and West Arm assemblages south of Meridian Lake.

Features to note:

- Laminated, felsic-mafic tectonites derived from the West Arm ocean floor assemblage and syn-tectonic intrusive sheets.
- Evidence for dextral kinematics (west-side-up and to the north relative to the Flin Flon assemblage): asymmetrically-extended pyroxenite veinlets with back-rotated boudins; note also that amphibole is replacing clinopyroxene.

STOP 1-2: Missi Unconformity

Coordinates

UTM N 6070730 E 316930

Overview

The Missi Group continental sedimentary rocks form a cover sequence to the 1.92-1.88 Ga tectonostratigraphic assemblages (Bruce, 1918; Ambrose, 1936; Stockwell, 1960) similar to that of the Timiskaming sequences in the Superior Province. Key features of the Missi Group siliciclastic rocks include:

- 1) unconformable deposition on deformed rocks of the Amisk collage as well as on successor arc plutons;
- 2) development of an oxidized paleosol (regolith) at the unconformity (Holland et al., 1989);
- 3) removal of significant stratigraphic section along the (angular) unconformity (ca. 2 km; Bailes and Syme, 1989);

- 4) presence of clasts derived from the 1.92-1.88 Ga assemblages (e.g., pillowed basalt, iron formation), successor arc plutons (medium- to coarse-grained granitoid rocks) and jasper (Bailes and Syme, 1989; Syme, 1987; Stauffer, 1990);
- 5) dominated by fluvial-alluvial deposits of crossbedded and massive sandstone, with rare laminated argillite (Stockwell, 1960; Syme, 1988)
- 6) rare trachyandesite sills (Syme, 1988)

Together, these features suggest that Missi sedimentation occurred during post-accretion arc magmatism on an uplifted and deeply incised terrain (Bailes and Syme, 1989; Stauffer, 1990), where depositional environments included alluvial fans and braided river systems. D₃ structures (e.g., folds, steep belts, shear zones) and associated topography may have controlled the pattern of fluvial drainage systems and associated Missi suite sedimentation (Lucas et al., 1996). The Missi sandstone at Flin Flon were deposited at ca. 1845 Ma, bracketed by the age of the youngest detrital zircon (1847 Ma; Ansdell et al., 1992; Ansdell, 1993) and the oldest cross-cutting intrusion (1842±3 Ma Boundary Intrusion; Heaman et al., 1992). The unconformity cuts through a significant amount of basement section and is markedly angular (Stockwell, 1960; Bailes and Syme, 1989), suggesting that the basement was deformed prior to or during erosion and sedimentation, consistent with regional constraints (Lucas et al., 1996). The Flin Flon arc assemblage and Missi sedimentary cover rocks at Flin Flon were deformed and metamorphosed at greenschist to lower amphibolite grade conditions (Ambrose, 1936; Bailes and Syme, 1989; Digel and Gordon, 1995). Fedorowich et al. (1995) present biotite and hornblende Ar-Ar data that indicate peak metamorphism at 1820-1790 Ma in the Flin Flon area, coeval with regional peak metamorphism and deformation across the Trans-Hudson Orogen (e.g., Gordon et al., 1990; Ansdell and Norman, 1995; David et al., 1996).

Stop description

The outcrop, informally called the Missi outlier (Fig. 13), exposes a regolith at the unconformable contact between pillowed flows of the Carlisle Lake member of the Hidden Formation and fluvial conglomerate and sandstone of the Missi Group. The altered volcanic rocks that make up the regolith are strongly oxidized and red or maroon in color up to a depth of ~ 3 m below the contact and they become pale green due to chloritization up to a depth of ~5 m below the contact (Holland et al. 1989). The regolith contains spectacular, spheroidally weathered, pillowed volcanic rocks (corestones) with hematite liesegang rings. The corestones decrease upward in size from the weakly weathered pillowed flow at the base of the regolith to the strongly oxidized hematite layer at the top of the regolith where they completely disappear due to the intense paleo-weathering (Holland et al. 1989).

Four generations of structures overprint the Missi outlier. The Missi outlier is folded into a tight, east-trending, F₄ syncline with an axial planar, bedding-parallel S₄ foliation (Gale et al. 1999). Changes in younging direction across the axial plane of the fold are given by the polarity of trough crossbeds in thick sandstone beds. The syncline is refolded by north-striking, tight to open, F₅ folds, which

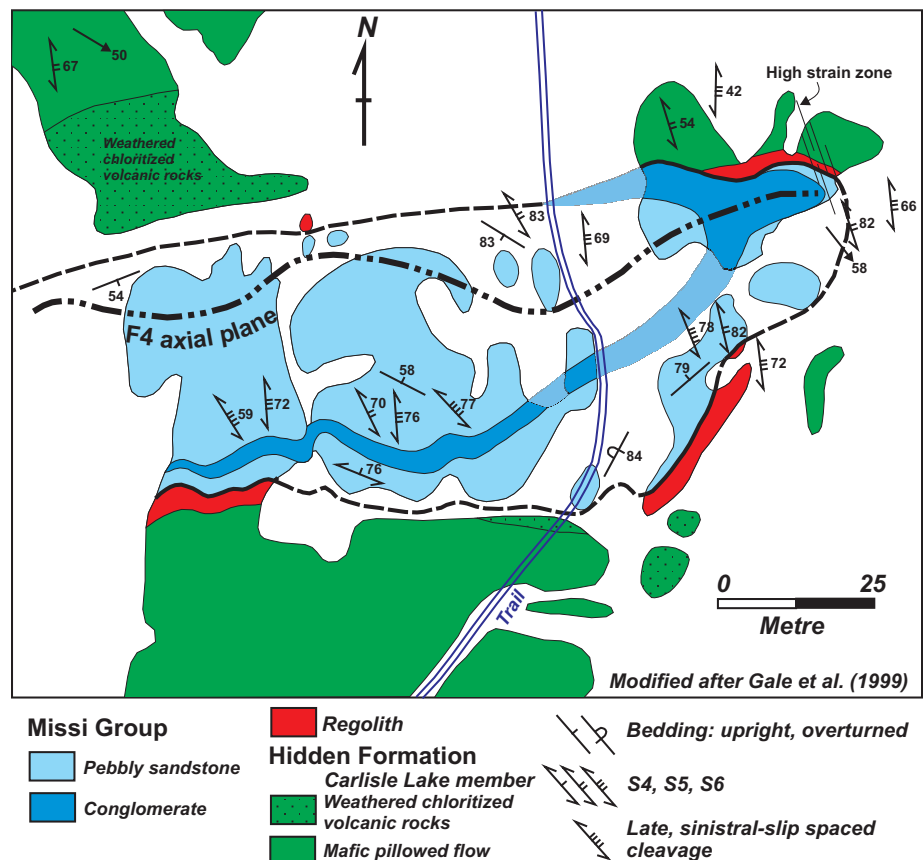


Figure 13. Structure of “Missi outlier”, an infolded exposure of the unconformity between Missi Group metasedimentary rocks and volcanic rocks of the Hidden formation. From Lafrance et al., submitted.

have an axial planar, steeply-dipping, S_5 cleavage. S_5 varies in strike from 330° to 350° and is defined by the flattening of clasts in conglomerate. A D_5 high strain with a SE-plunging stretching lineation cuts through the nose of the fold in the eastern part of the outcrop. The high strain zone and S_5 are overprinted by a steeply-dipping, closely-spaced, disjunctive S_6 cleavage, varying in strike from 350° to 010° . S_6 is pervasive through the outlier and is dragged or refracted in sinistral fashion into a local spaced cleavage, striking 310° to 330° , which is likely associated with the formation of late brittle faults.

STOP 1-3: Volcanic Rocks in the Hook Lake Block

Coordinates

UTM: N 6065220 E 321259

Overview

Flin Flon arc assemblage sequences are marked by large-scale intercalation of effusive, fragmental and intrusive rocks. Such units are on the scale of 10s to 100s of metres thick. The sequences are internally complex, in which successive units vary with respect to flow or bed morphology, phenocryst content, and composition. It is this variability that distinguishes arc assemblage rocks from the monotonous basalt (\pm diabase) successions in the Elbow-Athapuskow ocean-floor assemblage.

The outcrop-scale stratigraphy at this Stop mirrors the map-scale characteristics of the arc assemblage (Syme et al., 1996). Here we will examine the components and bedforms of a mafic pyroclastic unit typical of the upper part of the Hook Lake suite stratigraphy (Figs. 14 and 15; Syme et al., 1996). Mafic pyroclastic rocks are common in the Hook Lake and Flin Flon suites, but are less common elsewhere within the Flin Flon arc assemblage.

The flows are part of the juvenile arc tholeiitic series, characterized by HFSE depletion and generally flat REE patterns (Stern et al., 1995a). Primary augite phenocrysts have very low contents of Ni, Ti and Cr typical of arc tholeiites (Turnock and Syme, 2002), consistent with the whole-rock geochemistry (Stern et al., 1995a). Hook Lake suite rocks have 'juvenile' Nd-isotopic characteristics, plotting within the Flin Flon MORB-OIB field (i.e., overlapping with the likely mantle source), implying that the influence of significantly older (e.g., Archean) crust was minimal (Stern et al., 1995a).

The rocks to be examined (Fig. 16) are part of a 300 m thick unit comprising intercalated pillowed basalt flows, scoria-rich tuff and pillow fragment breccia. The environment of deposition is subaqueous as indicated by the presence of intercalated pillowed flows. However, the physical characteristics of juvenile components in the tuffaceous members of the sequence (discussed below) suggest that the tuff was erupted in a subaerial or very shallow water environment, and deposited in shallow water close to the source vent(s).

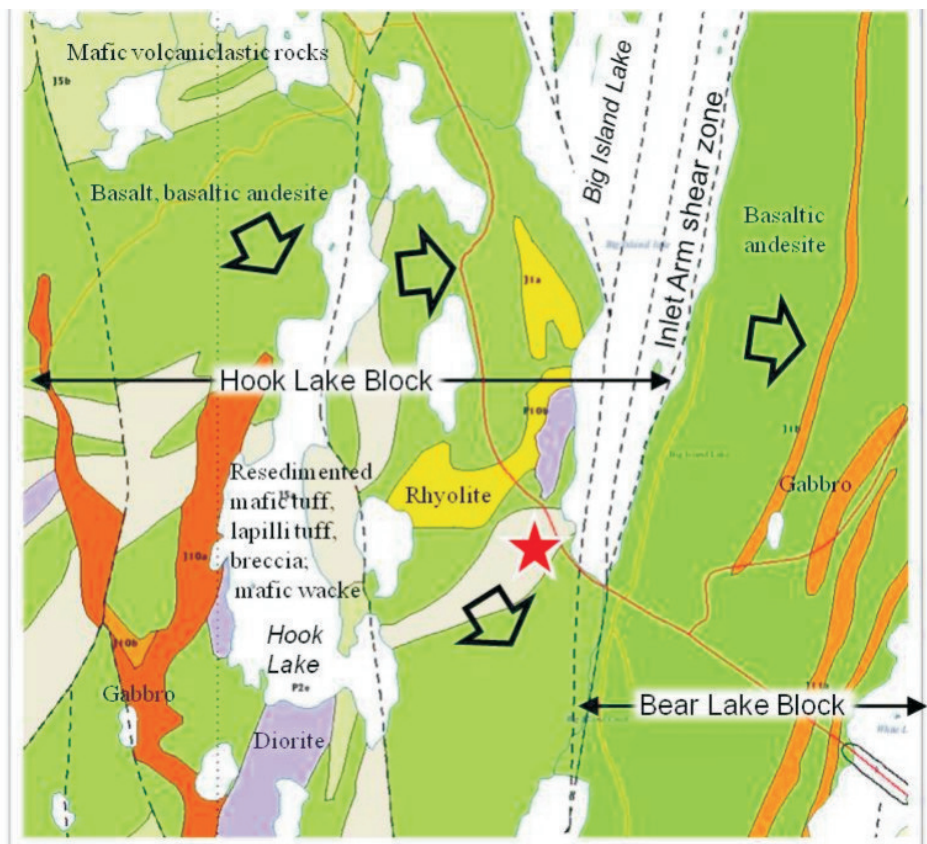


Figure 14. Simplified geological map of the Hook Lake area, southwest of Flin Flon (NATMAP Shield margin Working Group, 1998). The Hook Lake block (a tholeiitic juvenile arc suite) is juxtaposed against the Bear Lake block (a transitional tholeiitic-calc-alkaline juvenile arc suite) by the Inlet Arm shear zone. Red star: stop location in the subgreenschist portion of the Hook Lake block. Black arrows: younging direction of strata.

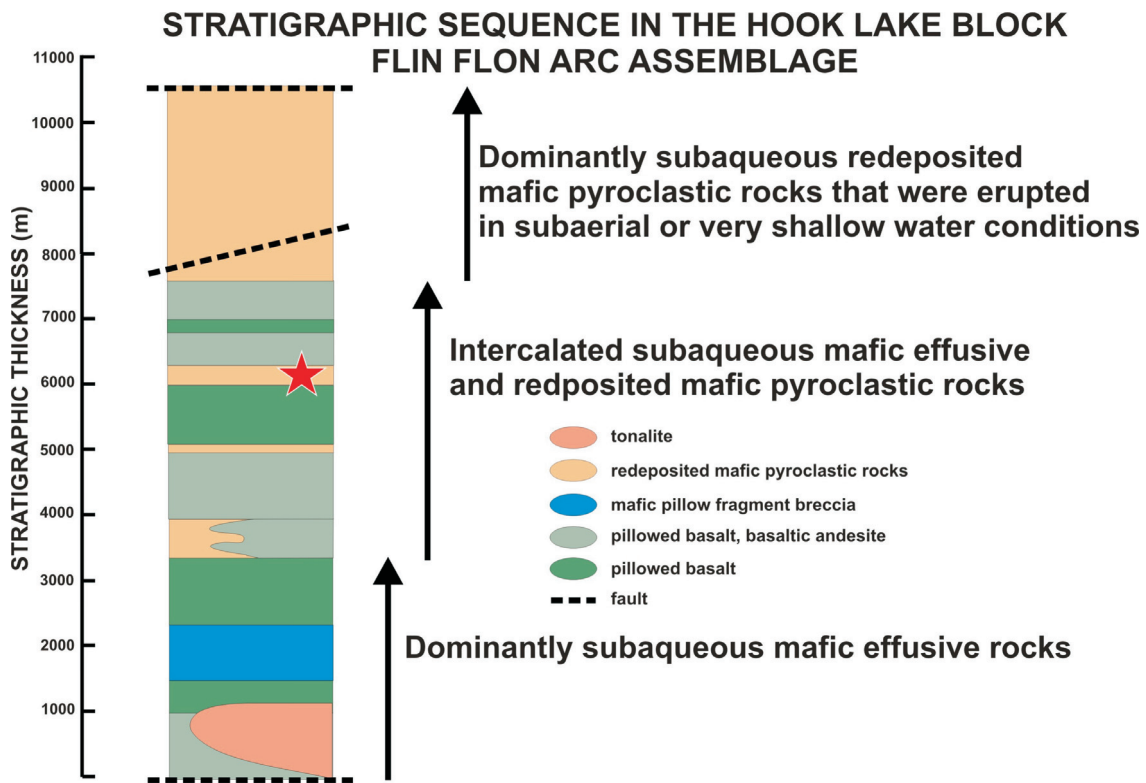
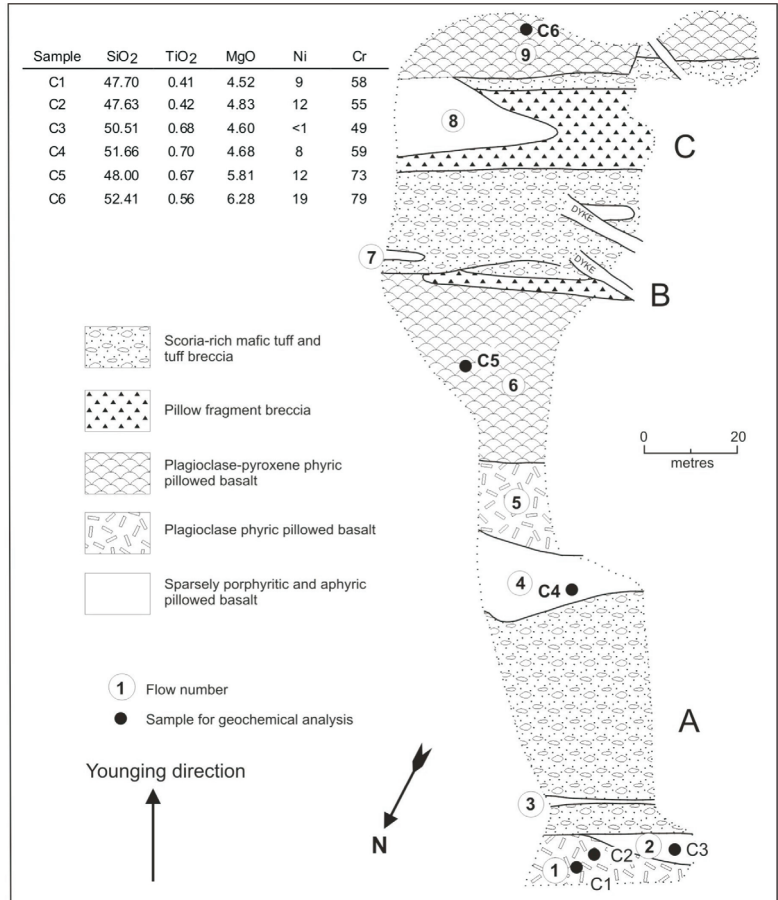


Figure 15. Stratigraphic sequence in the Hook Lake Block (based on Bailes and Syme, 1989). Red star indicates stratigraphic position of field trip stop.

Stop description

The outcrop area (Fig. 14) is located in the Hook Lake block, southeast of Flin Flon. Parking is on an abandoned road on the south side of Highway 10, just west of the south end of Manistikwan (Big Island) Lake. This area lies within the subgreenschist (prehnite-pumpellyite) zone of metamorphism: the prehnite-out, pumpellyite-out, actinolite-in isograd lies 1.5 km to the north (Digel and Gordon, 1995, Syme, 1989). On this particular outcrop both prehnite and pumpellyite are rare to absent, the rocks are virtually unfoliated, and primary textures are exceptionally

Figure 16. Stratigraphic sequence at the field trip stop. Geology modified from Corkery (pers. comm., 1983). From Bailes and Syme (1989), Syme et al. (1996). Subaqueous pillowed basalt flows are intercalated with bedded scoria-rich mafic tuff and tuff breccia. Pillowed flows vary from aphyric to coarsely porphyritic, but are all geochemically similar arc tholeiites. A: scoria-rich tuff, beds 0.8-13.4 m thick; thicker beds contain trains of accessory blocks that can be matched to flows 1 and 3. B: tuff breccia and pillow fragment breccia both contain abundant pillow fragment blocks derived from underlying flow 6. The tuff-breccia has a scoria-rich matrix, whereas the pillow fragment breccia has no scoria in the matrix. C: pillow fragment breccias are thick bedded (5-6 m) and heterolithologic.



well preserved. The Inlet Arm fault (defining the western edge of the Inlet Arm shear zone in the Bear Lake block) is approximately 500 m to the east.

Pillowed flows are 2-40 m thick, and contain 5-30% plagioclase phenocrysts and 1-5% amphibole pseudomorphs after pyroxene phenocrysts. Flows on this outcrop are basalt and basaltic andesite with 4.52-6.28 wt.% MgO (note that both SiO₂ and MgO increase up-section). Some flows abruptly terminate in the exposed section. Amygdules range in size up to 6 mm but vary in size and abundance between flows and between pillows in a single flow. Concentric bands of carbonate-filled amygdules occur in the margins of pillows in flow 6. Pillow fragment breccia is directly associated with flows 6 and 8; amoeboid pillow flow-top breccias are absent. Pillow fragment breccia beds are 3-5 m thick, contain fragments to 20 cm, and include both monolithologic and heterolithologic types. Monolithologic breccias can in some instances be shown to contain fragments identical to the directly underlying basalt flow. Breccia beds have fragment-supported bases and matrix-rich tops but do not display normal size grading (Fig. 17). Fragments are angular, and in many cases are clearly fragments of pillows that have broken along radial and concentric fractures, producing characteristic pie-shaped clasts. Proximal breccias may contain complete, unfragmented pillows. Scoria tuff and breccia beds (<1-13 m thick) are typically less than 5 m thick. Beds less than 1 m thick are normally graded with respect to plagioclase crystal size (Fig. 17). Beds

thicker than 1 m are commonly reverse graded at the base. Tuff and breccia beds include A and AB types, and in some instances contain "trains" of accessory blocks. The occurrence of scoria in Bouma-type beds intercalated with pillowed basalt indicates the pyroclastic material was transported and deposited by subaqueous density currents.

Scoria particles range in size from about 1 mm to 6 cm and are well preserved. They are framework supported with vesicles and inter-particle voids filled predominantly with carbonate. Scoria shapes are controlled by a combination of vesicle walls, fracture surfaces, and chilled droplet margins. The particles are interpreted to have been produced during explosive subaerial magmatic eruptions on a volcanic island. During eruptions, rapidly vesiculating magma droplets in the eruption column were fragmented by internal gas pressure, with subsequent fragmentation of some clasts due to thermal shock on contact with seawater.

Accessory angular blocks of amygdaloidal pillowed up to 40cm across are interpreted to be ballistic fragments that can be unambiguously matched to specific flows lower in the sequence (e.g. blocks in unit 'A' match flows 1 and 3). The blocks commonly occur in discontinuous "trains" (1 block thick) and as isolated fragments; both "trains" and isolated blocks can occur at any level within a tuff bed (Fig. 19). The blocks are much larger and denser than the matrix scoria and were clearly not in hydraulic equilibrium with the density current that deposited the scoria. The accessory blocks may have been torn from vent walls by periodic phreatic/phreatomagmatic explosions which punctuated the dominantly magmatic, scoria-producing, eruptions.

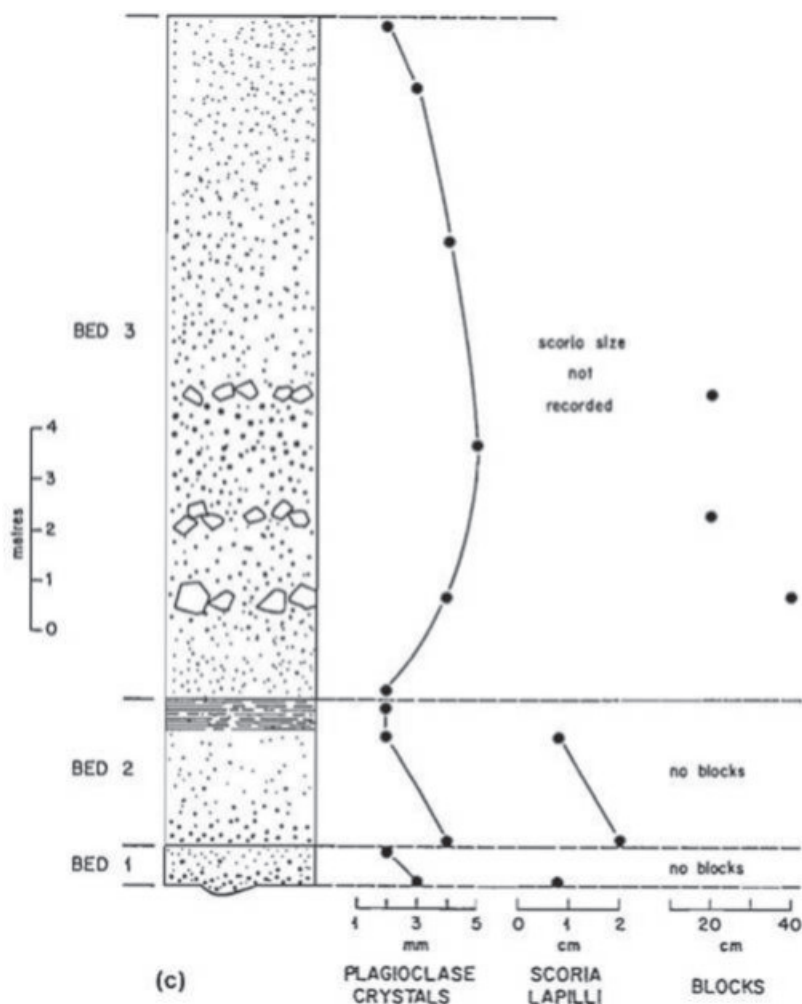


Figure 17. Bedforms with turbidite-like sequence of internal divisions (Syme et al., 1996) indicate that the pyroclastic material was deposited from subaqueous density currents. Grading displayed by these three scoria tuff beds near the base of the section is demonstrated by variation in the maximum size of plagioclase crystals and scoria lapilli. Bed 1 is normally graded (Bouma A type), bed 2 is normally graded – parallel laminated (AB type), and bed 3 is reverse- to normally graded with three crude layers of accessory blocks (size up to 40 cm). The latter are fragments derived from pillowed flows lower in the sequence.

STOP 1-3: Vick Lake Shoshonitic Tuff

Coordinates

UTM: N 6068456 E 326708

Overview

Intra-arc tectonic processes are recorded in the stratigraphic components of some of the fault-bounded successions in the Flin Flon arc assemblage (Syme et al., 1996; Syme et al., 1999). The Bear Lake block (Fig. 18; Bailes and Syme, 1989), defined as the stratigraphic package contained between the Inlet Arm fault and Northeast Arm shear zone, contains a particularly clear example of intra-arc rifting. The lithologic components of the Bear Lake block are well exposed, allowing more stratigraphic interpretation and reconstruction than is generally possible in less well-exposed areas.

The Bear Lake block contains three contrasting volcanic associations: 1) a 4 km thick, mildly calc-alkaline arc sequence; 2) 200 m of ferrobasalt; and 3) 1 km of basin-fill shoshonitic tuff with turbidite bedforms (Bailes and Syme, 1989; Syme and Bailes, 1993; Stern et al., 1995a; Syme et al., 1999).

These components are interpreted to record the construction and subsequent rifting of part of an oceanic arc. At this stop we will examine the topmost member of this succession, the shoshonitic Vick Lake tuff, to establish the deep basinal nature of these rocks. Bear Lake basaltic andesite forming the faulted base of the arc succession represents a shoaling subaqueous shield volcano >3.3 km thick (Bailes and Syme, 1989). Volcanism apparently ended with caldera collapse of the shallow-water, upper portions of the subaqueous shield. Caldera formation was abruptly succeeded by effusion of intracaldera subaqueous rhyolite flows and contemporaneous infilling of the southward-deepening basin by felsic and intermediate volcanoclastic rocks. Graphitic mudstone, chert and stratabound massive sulphides (Cuprus and White Lake mines; Bailes and Syme, 1989; Syme and Bailes, 1993) were deposited at the top of the calc-alkaline sequence, in sub-basins which may have heralded an intra-arc rifting event (Syme et al., 1999). This rift event is represented by a 150-200 m thick ferrobasalt formation (Bailes and Syme, 1989) with N-MORB characteristics (Stern et al., 1995a; Lucas et al., 1996). Deposition of the sulphides may have occurred in the earliest stages of arc extension, and are thus plausibly associated with an episode of high heat flow subsequently manifest by the extrusion of basalt derived from a MORB-like mantle. Inter-flow rhyolite crystal tuff beds in the ferrobasalt have a U-Pb zircon age of 1886 ± 2 Ma (Gordon et al., 1990), establishing the age of the rifting. The resulting arc-rift basin was subsequently filled with 900 m of fine-grained shoshonitic pyroclastic material deposited from subaqueous density currents (Vick Lake tuff). This shoshonitic material has a U-Pb age of 1885 ± 3 Ma (Stern et al., 1993), clearly indicating that the rifting and shoshonitic volcanism were virtually coeval.

Samples from the Vick Lake tuff suite plot within the basaltic trachyandesite and trachyandesite fields on a silica versus $\text{Na}_2\text{O} + \text{K}_2\text{O}$ plot, and the high-K field on the silica versus K_2O plot, distinct from all other rocks within the Flin Flon belt (Stern et al., 1995a). K_2O contents range from 2.3-6.5 wt.%, Na_2O from 1.0-5.0 wt.%, and $\text{K}_2\text{O}/\text{Na}_2\text{O}$ ratios from 0.4-7.0. The high K_2O contents are interpreted to reflect magmatic values, supported by the

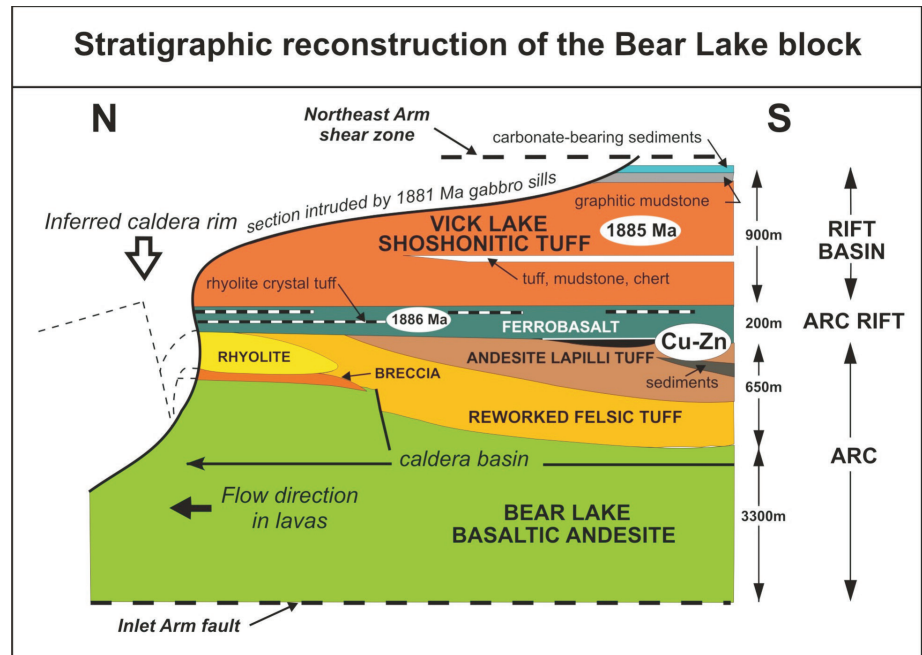


Figure 18. Stratigraphic relationships in the Bear Lake block, Flin Flon arc assemblage (Syme et al., 1996, 1999; modified from Syme and Bailes, 1993). The section contains three major groups of rocks: (1) transitional tholeiitic-calc-alkaline Bear Lake suite (comprising Bear Lake basaltic andesite, caldera-fill rhyolite, felsic volcanoclastic and intermediate volcanoclastic rocks), (2) arc-rift ferrobasalt, and (3) rift basin Vick Lake suite shoshonite tuff. The Cuprus and White Lake VMS deposits occur in a unit of graphitic mudstone at the top of the calc-alkaline sequence, overlain directly by arc-rift ferrobasalt.

strong positive correlation of K_2O with less-mobile, incompatible elements such as Th and La. The shoshonitic rocks differ from the tholeiitic and calc-alkaline rocks in having higher Al_2O_3 (16-21 wt.%), lower MgO (2.3-3.0 wt.%), and higher P_2O_5 contents (0.3-0.45 wt.%) at any given silica value. The HFSE characteristics of the Vick Lake shoshonite suite partly overlap those of the tholeiitic and calc-alkaline series at Flin Flon, but extend to more extreme values for some elements and ratios. They are characterized by greater enrichment in LREEs [$(La/Yb)_n = 3-7$; $La_n = 25-40$], and flat to slightly fractionated HREE profiles. The rocks have particularly high Ba (640-2000 ppm), Sr (450-1000 ppm), and Th (2.1-3.4 ppm), features consistent with a shoshonitic affinity (Morrison, 1980).

- Shards (0.05-0.4 mm) are aphyric, have equant to tabular shapes and grain boundaries defined by straight to conchoidal fracture surfaces and vesicle walls. Vesicles (<0.05 mm) are round, oval or tube-shaped, and are filled with very fine grained epidote, chlorite, feldspar or quartz. Shards are recrystallized and replaced by a mixture of albite, subordinate quartz, epidote, chlorite and sericite.
- Pumice granules are typically less than 3 cm long and up to 30 cm in some pumice-rich beds. They contain plagioclase phenocrysts similar in size and shape to unbroken crystals in the matrix. The shape of pumice granules and blocks ranges from oval, equant to irregular. Vesicles (50-80%; <0.4 mm) are round, oval or tube-shaped, filled by a polygranular mosaic of feldspar and quartz.
- Euhedral plagioclase crystals and angular crystal fragments (0.1-2 mm) comprise approximately 15-40% of tuff beds. Normal size and abundance grading of plagioclase is typical in most beds. Broken euhedral prisms of magmatic hornblende comprise 0-3% of tuff and are typically concentrated in the bases of beds.

Aphyric or plagioclase phyric microclasts (<2 mm) are common in the lower parts of graded beds where they comprise up to 15% of the tuff. These clasts are interpreted as juvenile glass fragments, bounded largely by conchoidal fracture surfaces, with shapes subsequently smoothed by abrasion. Subrounded microlitic lithic clasts (<0.5 mm) are interpreted as accessory components, in that they have a crystalline pilotaxitic texture of plagioclase microlites.

The Vick Lake tuff sequence is well bedded and broadly upward fining (Bailes and Syme, 1989); beds range from 0.2-18 m in thickness and average 1 m. The beds have a Bouma-type internal zonation similar to turbidites, comprising one or more of a graded "A" division, parallel laminated "B" division, ripple laminated "C" division, parallel laminated "D" division, and very fine grained, structureless "E" division top (Fig. 19). Most of the beds are AB(E) types. In the mid- to upper part of the "A" division, and rarely in the "B" division, many beds contain discrete pumice-rich layers (1 mm to 5 cm in width) composed of small (<10 mm) pumice granules. Thin pumice-rich layers are discontinuous along strike, whereas thicker layers (5 cm) are continuous along strike for at least 5 m and show only minor variations in thickness. Grading, defined by an upward decrease in the size of plagioclase crystal fragments, is continuous from base to top of beds. Note that this normal size grading is continuous across the pumice granule layers, indicating that the layers are integral parts of the beds and do not represent separate depositional events.

The basal 250 m is characterized by abundant thick beds containing large pumice fragments, but

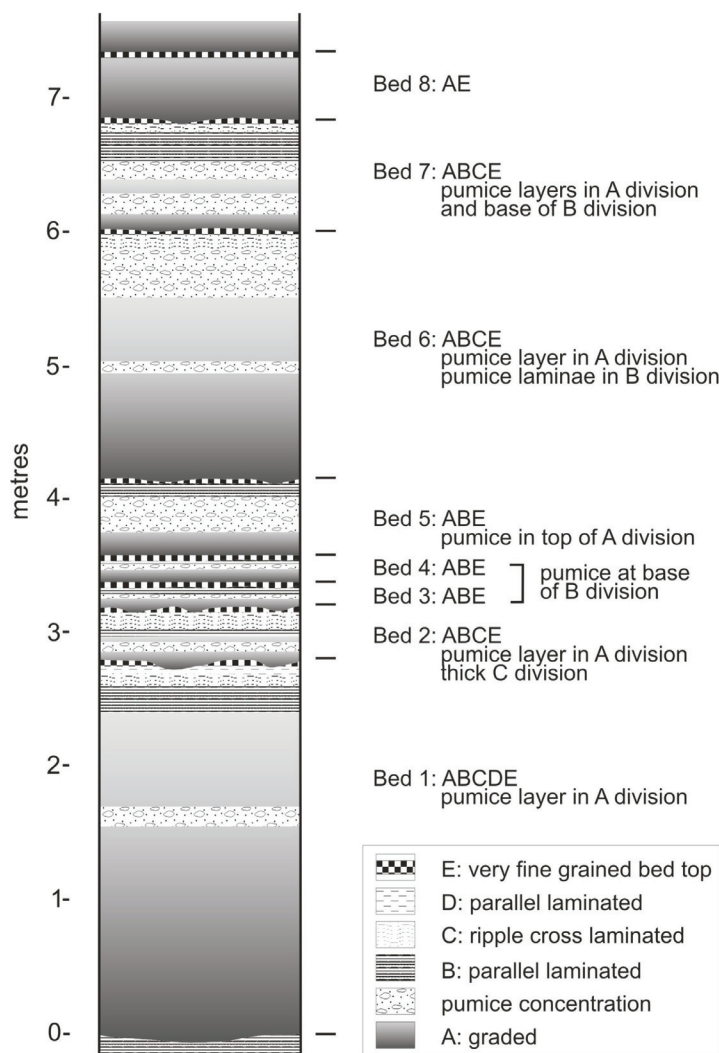


Figure 19. Sequence of 8 measured beds, Vick Lake shoshonite tuff (Syme et al., 1996). The tuff is composed of particles (glass shards, crystal fragments, pumice) produced by explosive volcanic processes in a shallow subaqueous to subaerial environment. Turbidite bedforms indicate that this pyroclastic material was deposited from turbulent subaqueous density currents, probably in a marine basinal setting.

such fragments are rare in the upper two-thirds of the unit. Bed thickness also decreases upward within the unit. Within the uppermost 100 m Vick Lake tuff is interlayered with pyritic, graphitic mudstone.

Vick Lake tuff is interpreted to have erupted in a subaerial environment, following a period of extensive calc-alkaline island arc and arc-rift volcanism (Syme et al., 1996). Ash particle morphology and the abundance of pumice suggest that the tephra was produced in shallow water or subaerial phreatomagmatic and plinian eruptions. The pyroclastic material likely entered the water column from base surges, pyroclastic flows and fallout. It was transported by turbulent subaqueous density currents from the flanks of the subaqueous portion of the cone into an adjacent back-arc basin, forming Bouma-type "turbidite" bedforms. The presence of beds up to 19 m thick suggests that the sequence is proximal to source vents. A number of individual beds may have been deposited during a single eruption event, but the 900 m thick sequence represents a large number of eruptions relatively closely spaced in time. The general upward fining of the sequence, and gradual increase and ultimate dominance of pelagic sedimentary components in the upper 180 m of the unit indicates a gradual cessation of pyroclastic volcanism, with increasing proportions of graphitic shale deposited between eruptions. Modern analogues of the Vick Lake shoshonite suite (Stern et al., 1995a) erupt late in the evolution of oceanic arcs (e.g., Morrison, 1980; Gill and Whelan, 1989).

Stop description

The outcrop is located approximately 700 m above the base of the unit. A sequence of eight beds, ranging from 0.20 to 2.80 m thick, is exposed at the top of the cliff-forming outcrop. These beds include ABCDE, ABCE, ABE and AE types, most of which have pumice layers in the A or B division (Fig. 18, Syme et al., 1996). Bases of beds are commonly scoured into the E divisions of underlying beds, in some instances removing all of the very fine grained bed tops (e.g., base of bed 1). Flame structures ornament the bases of some beds. Plagioclase crystals and crystal fragments display normal size grading (e.g., bed 1). The cream-weathering, very fine-grained E division bed tops represent settling of the finest ash through the water column between eruptions, and are particularly prominent by virtue of their colour and grain size contrasts. Delicate ripple laminae are preserved in the C divisions of beds 1, 2 and 6.

STOP 1-5: Athapapuskow Basalt

Coordinates

UTM: N 6051066 E 344980

Overview

Juvenile ocean-floor assemblages include a number of distinct basalt sequences and related mafic-ultramafic complexes (Stern et al., 1995b, Syme et al., 1999). The basalts occur in a semi-continuous belt between the Elbow Lake and Athapapuskow Lake, and are collectively termed the 'Elbow-Athapapuskow assemblage' (Stern et al., 1995b). The Elbow-Athapapuskow ocean-floor assemblage is up to 25 km wide, has a strike length of 100 km (Syme and Bailes, 1993; Syme, 1994; Stern et al., 1995b), and is everywhere either in fault contact with arc volcanic rocks, or the contact with arc rocks is stitched by younger plutons. The assemblage consists entirely of subaqueous basalt and related intrusive rocks, in which there are no known occurrences of felsic volcanic rocks, terrestrial sedimentary rocks, or older crystalline basement (Syme, 1988, 1991, 1992, 1993, 1994). Gabbro and diabase dykes and sills are common, although no sheeted dykes are known.

At this stop we will examine flows assigned to the Athapapuskow basalt exposed on the property of Athapap Lodge (Fig. 20). Athapapuskow basalt is a minimum of 1-2 km thick, and contains abundant diabase, gabbro, and rare ultramafic sills. The age of Athapapuskow basalt is constrained by the U-Pb zircon age of a contained syn-volcanic diabase sill (1904 +/-4 Ma, Stern et al. 1995b) and predates slightly the age of the Flin Flon mine horizon.

Three different flow morphologies are recognized (Syme, 1988). Thin (1.5-5 m) massive sheet flows are the dominant flow type. They have chilled bases, non-amygdaloidal basal zones, highly vesicular central zones and flow tops containing large (to 2 cm) amygdaloids. Thick massive flows (>30 m) contain only sporadic 2-8 mm amygdaloids but have strongly amygdaloidal flow tops. Pillowed flows are rare, and occur intercalated with the other flow types. The eruptive environment is subaqueous, demonstrated by the occurrence of the intercalated pillowed flows. Epidote-dominated alteration features such as ovoid epidote domains, epidote-filled amygdaloids, epidotized amygdaloidal flow tops, and epidote veins are common. These features are consistent with synvolcanic hydrother-

mal alteration in the porous portions of subaqueous flows.

Stop description

Six thin (1-1.5 m), massive basalt flows exposed this Stop are characteristic of the dominant, thin-flow facies of Athapapuskow basalt (Fig. 20, Syme et al., 1996), and lie in a sequence that locally young to the north. The flows are completely or partially exposed, ranging in thickness from 1 to 1.5 m with sharp, planar flow contacts and in some instances are recessive weathering. Flows 3 and 5 in the sequence are plagioclase phyric and the remainder are aphyric. Bases of flows are chilled against underlying flows, and pipe vesicles to 10 cm long occur at the bases of some of the thicker flows. The flows have non-amygdaloidal lower zones, highly amygdaloidal centres, and weakly amygdaloidal tops (to 1 cm). They are characterized by intense epidote alteration and the flow top surface is in some instances crenulated or ropy (e.g., top of flow 4). Epidosite domains are concentrated in the amygdaloidal (porous) parts of flows and are interpreted as synvolcanic seafloor alteration features. Aphyric basalt dykes cut across the flows at a high angle; their relationship to the flows is unknown. This outcrop lies approximately 500 m N of the margin of the Cranberry shear zone, and contains a dextral fault occupied by an epidote vein. Some flow contacts (e.g., between flows 5 and 6) are sheared. Thin massive flows such as these are typical of Athapapuskow basalt, but thick (e.g., 30 m) massive flows and pillowed flows also occur.

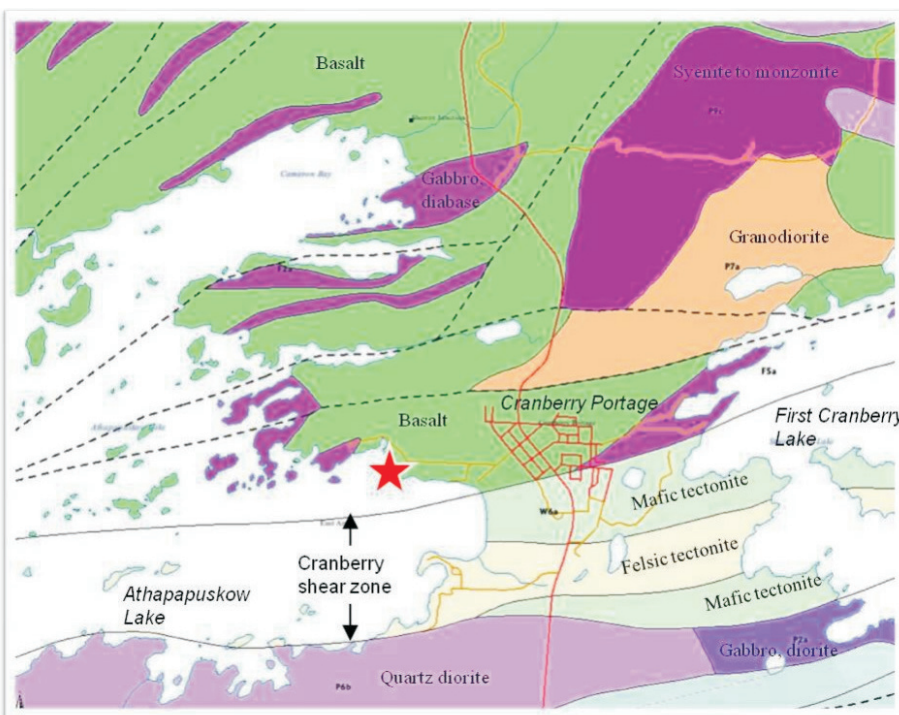


Figure 20. Simplified geological map of the Cranberry Portage area (NATMAP working group, 1998) modified from Podolsky, 1951, 1958) and Syme (1993). The area is underlain by Athapapuskow basalt, a member of the Elbow-Athapapuskow ocean-floor assemblage, which was intruded by granitoid plutons and subsequently transected by the Cranberry shear zone (Syme, 1993, 1995; Ryan and Williams, 1996). Star: outcrop of Athapapuskow basalt sheet flows, located on the property of Athapap Lodge, 145 Brydges Ave. NW, Cranberry Portage.

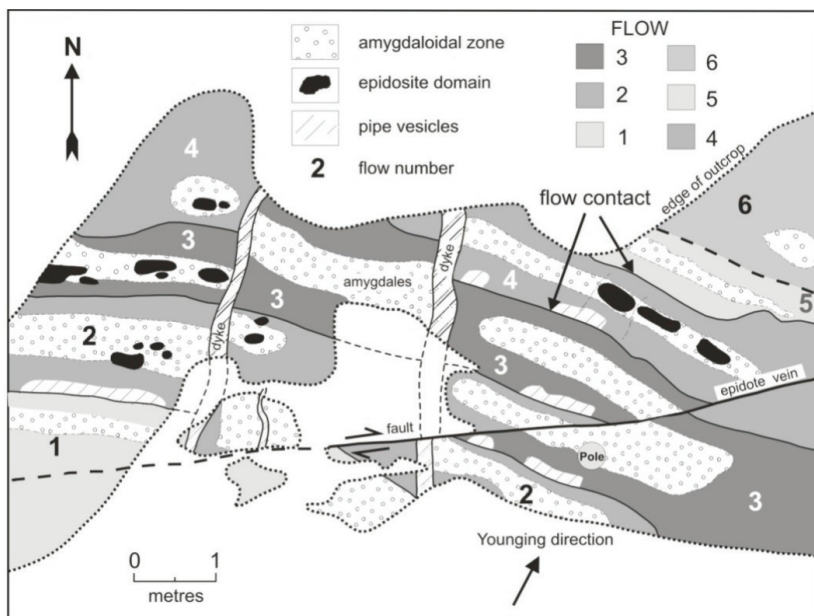


Figure 22 Outcrop map for Athapapuskow basalt (Syme et al., 1996). The local volcanic stratigraphy young to the north. Six massive flows (numbered 1 to 6) are completely or partially exposed, ranging in thickness from 1 to 1.5 m. Flows 3 and 5 are plagioclase phyric and the remainder are aphyric. Thin massive flows such as these are typical of Athapapuskow basalt, but thick (e.g., 30 m) massive flows and pillowed flows also occur. These thin flows commonly have chilled bases with pipe vesicles, non-amygdaloidal lower zones, highly amygdaloidal centres, and weakly amygdaloidal tops. The flow top surface is in some instances crenulated or ropy (e.g., top of flow 4). Epidosite domains are concentrated in the amygdaloidal (porous) parts of flows and are interpreted as synvolcanic seafloor alteration features. Aphyric basalt dykes cut across the flows at a high angle; their relationship to the flows is unknown. This outcrop lies approximately 500 m N of the margin of the Cranberry shear zone, and contains a dextral fault occupied by an epidote vein. Some flow contacts (e.g., between flows 5 and 6) are sheared.

DAYS 2-4:

During Days 2 through 4, variations in the lithofacies and volcanic architecture of the Flin Flon District, as well as key structural features and their timing, will be demonstrated by examining seven stops through the Flin Flon stratigraphy as illustrated in Figures 4 and 8. The first four stops are sections through lithofacies that comprise the Flin Flon formation and, in particular the Millrock member, which demonstrate evidence for synvolcanic subsidence and that exhibit primary volcanic and deformational features. The first Stop is the Millrock Hill section (Stop 2) followed by the South Main (Stop 3), Smelter (Stop 4), Lower Callinan sections (Stop 5), and then across the Flin Flon Lake Fault to the Beaver Road Anticline section (Stop 6). Stop 6 illustrates lithofacies that are indicative of subsidence early in the development of the Flin Flon cauldron, and the role of synvolcanic faults and subsequent deformational events in shaping the Beaver Road Anticline. The Upper Callinan section (Stop 7), provides a section through basaltic and andesitic lithofacies that comprise the Hidden formation, in particular the 1920 member, along the west limb of the Hidden Lake Syncline. Structural features, such as the Railway Thrust Faults, which offset the VMS-hosting Millrock member, will be examined at several key localities within Stop 7. Viewed from a larger perspective, Stops 2 through 7 provide a south to north cross-section through the lithofacies and architecture of the structurally modified Flin Flon cauldron, starting with its south structural margin at Millrock Hill and moving northward into the interior of the cauldron where numerous, nested “basins”, which comprise the subsidence structure, contain the Flin Flon, Callinan and 777 VMS deposits (Figs 4 and 7).

Stop 8 is an underground tour at the 777 mine and Stop 9, located on the east limb of the Hidden Lake Syncline, will illustrate volcanic and subsidence –related features of volcanic strata in the hanging wall of the Schist and Mandy VMS deposits (Hidden formation). At Stop 10, located in the Western Hooke Lake Block, the synvolcanic Cliff Lake Pluton and a high temperature alteration zone within overlying volcanic strata are examined.

STOP 2. MILLROCK HILL SECTION

Mill Rock Hill is, perhaps, the most widely known and “visited” outcrop in the Flin Flon mining district. The name was derived from the coarse rhyolitic breccias that were colloquially named “Mill Rock” after the term coined by Don Sangster (Sangster, 1972) to describe coarse, felsic breccias that are typically within earshot of a mine’s mill! Mill Rock Hill has been mapped at various scales: Stockwell (1960) at 1:12 000 scale, Thomas (1994) at 1:5000 scale, Syme (1997) at 1:400; Price (unpublished HBED map) at 1:2000 and Gibson et al. (2001) at 1:500 scale. The description and interpretations presented build upon this previous work, particularly the descriptions in Galley et al. (2002), and include results of 1:500 to 2:000 scale mapping of the on-strike extension of Millrock member lithofacies (Gibson et al., 2005; 2007; 2009a).

STOPS 2.1 to 2.3

Stratigraphy

A stratigraphic section illustrating lithofacies within the Millrock member of the Flin Flon formation and the Hidden formation, and location of substops that will be visited at Stop 2 are shown in Figures 7 and 22. The substops are described in ascending stratigraphic order and provide a complete section and description of lithofacies that comprise the Millrock member.

Coordinates

Stop 2.1: UTM 6071032, 314395

Stop 2.2: UTM 6071073, 314415

Stop 2.3: UTM 6071108, 314475

Stop Descriptions

At Stop 2.1, pillowed basaltic flow lithofacies are intercalated with amoeboid breccia lithofacies. These lithofacies are volumetrically the most significant and they extend from Millrock Hill west to the Flin Flon Lake Fault. The pillowed lithofacies consist of dark green to brownish green, aphyric and subordinate feldspar phyric flows that contain up to 25% quartz (epidote)-filled amygdules, typically <5mm in size (up to 1 cm) that are concentrated toward pillow margins and are typically pipe-like in morphology and radial in orientation. The amoeboid breccia lithofacies is framework supported, and contains amygdaloidal, amoeboid-shaped fluidal fragments, and subangular blocky clasts of amygdaloidal aphyric basalt, and lesser clasts of broken and intact pillows, in a finer lapilli- to

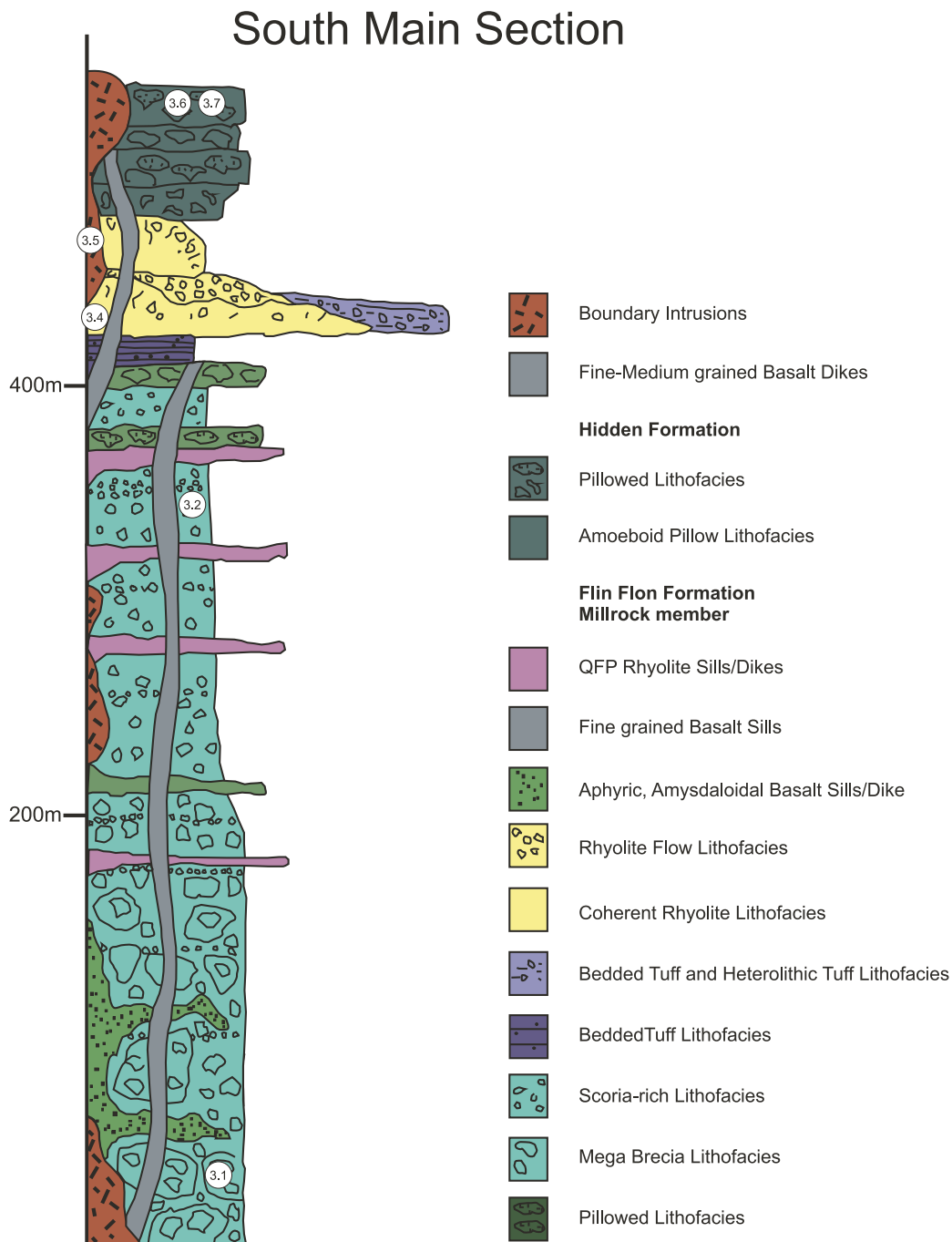


Figure 22. Idealized stratigraphic section through the Millrock member at Millrock Hill showing the lithofacies and stop locations.

tuff-sized basaltic matrix. Within an amoeboid clast, the amygdules are concentrated toward the clast margin, which is defined by a 1 -2 cm wide, rusty brown to green chilled margin that is sparsely to non amygdaloidal. The pillowed lithofacies is often discontinuous, and decreases in abundance upward. Crude bedding in the amoeboid breccia lithofacies is defined by variations in clast size, and/or by thin, pillow-thick, discontinuous flows. Irregular to lensoidal, sparsely quartz phyric coherent rhyolite occurs as sills and dykes within the pillowed and amoeboid breccia lithofacies. The rhyolite is aphanitic and/or spherulitic, locally flow banded, and has sharp contacts with adjacent basaltic lithofacies.

At Stop 2.2. a 10 – 15 m thick, sparsely quartz phyric (<5%, <2mm) rhyolite sill has a sharp, planar, and slightly sheared lower contact with the amoeboid breccia lithofacies and is slightly discordant to stratigraphy (Gibson et al., 2001). The base of the sill is massive and weakly in situ brecciated, and the interior is massive and faintly flow banded. The upper margin of the sill is in situ brecciated (alteration around fractures imparts a pseudobrec-

cia appearance) and locally appears pumaceous (up to 30% fine, 1mm quartz amygdules). The upper contact with the basaltic scoria lithofacies is chilled and sharp. The sill was emplaced into the mafic volcanoclastic unit at or near the contact between the amoeboid breccia and conformably overlying scoria lithofacies. The scoria lithofacies is 6 m thick at this locality but thickens abruptly, over a 150 m strike length, where it attains a maximum thickness of 30m. It consists of scoriaceous, aphanitic and aphyric, basaltic fragments in a fine, lapilli to tuff-sized mafic matrix. The scoriaceous basalt clasts have intact (unbroken) chilled margins, and a vesicle distribution that is typical of spatter (bombs) as described for the underlying amoeboid breccia lithofacies. The bomb-like shape of the clasts, their scoriaceous nature and amygdule distribution, intact chilled margins, tuff-to angular lapilli-sized matrix, absence of bedding and intercalated flows are characteristics consistent with their generation by subaqueous fire fountain eruptions (Fig. 8; Devine, 2003; Gibson et al., 2009a). The abrupt lateral increase in thickness of this unit from 6 to 30 m indicates that this unit was erupted and deposited within a restricted, synvolcanic fault-bounded basin. Faults which bound this basin do not appreciably offset overlying units, indicating that they are synvolcanic.

The rhyolitic sill and basaltic scoria lithofacies are overlain by a 30-35 m thick unit comprised of coarse, heterolithic basalt-rhyolite breccia and rhyolite breccia lithofacies. The basalt-rhyolite breccia lithofacies has a limited lateral extent (approximately 300 m) and contains abundant quartz-phyric (<3 mm, <10% quartz and or feldspar phenocrysts) rhyolitic clasts that ranges up to 2 m in size. The rhyolite clasts are typically white weathering, block- or slab-like in form, and are massive or flow banded. Some rhyolite blocks exhibit in situ brecciation, or have jigsaw fit fractures that are typical of blocks derived through autoclastic fragmentation (i.e., McPhie et al., 1993; Gibson et al., 1999). Subordinate, brown weathering, aphyric, mafic clasts (1-20 cm) are angular, non-amygdaloidal to scoriaceous. Clast counts indicate that the rhyolite clasts increase in size towards the top of the section (Devine, 2003). The matrix is fine-grained and mafic; the fine reddish-coloured, lapilli-sized clasts within the matrix are identical to the chilled margins of amoeboid and scoria clasts in the underlying units. Overall, the lithofacies is clast-supported, very poorly sorted, and locally displays crude bedding, graded bedding and, in one locality a large scour channel. The rhyolite breccia lithofacies conformably overlies the rhyolite-basalt breccia lithofacies and contains block to tabular clasts of quartz-phyric rhyolite (<8%, 2-8 mm quartz and feldspar phenocrysts), some of which have a jigsaw fit, or are in situ brecciated. This monomictic lithofacies fines upwards, has bed thicknesses <1.5m, and is neither vertically or laterally extensive. The dual mafic and felsic character of the basalt-rhyolite breccia lithofacies is interpreted to be a product of multiple sources (Devine, 2003; Gibson, et al., 2006). The basalt clasts and matrix components are interpreted to have been derived from an external source (i.e., the margins of the depositional basin) and/ or from the underlying mafic volcanoclastic lithofacies. The rhyolitic clasts are interpreted to have been derived from nearby syndepositional, quartz-phyric, rhyolite flows or domes and transported by high concentration mass flows generated during periods of dome collapse triggered, perhaps, by over steepening during growth, or by mild phreatomagmatic eruptions that were initiated by or accompanied, collapse (Fig. 8; Gibson et al., 2006). The occurrence of larger rhyolite clasts up section may be attributed to the increase in size and proximity of the rhyolite dome(s) over time (Devine, 2003). Rapid thickness variations of some units indicate that syn-sedimentation subsidence occurred during their deposition.

At stop 2.3, a coherent quartz phyric rhyolite flow (< 8% quartz crystal, < 3-8mm in size) weathers a distinctive yellow-white colour and is light greenish yellow on fresh surface. The coherent rhyolite ranges up to 13 m thickness and is characterized by a massive to flow-banded interior that grades outward into an inner zone of in situ breccia that grades outwards into an intact but clast rotated, chaotic, non-bedded breccia with lapilli-sized clasts that are commonly flow-banded and are interpreted to be a product of autoclastic fragmentation during dome emplacement and growth (Fig. 8; Devine, 2003). The autoclastic breccia grades into the rhyolite breccia lithofacies, the latter was derived from the margins of the coherent rhyolite during dome growth and collapse. The coherent rhyolite and associated volcanoclastic lithofacies thin rapidly away from the dome, and are replaced in the section by the rhyolite-basalt breccia lithofacies, The relationships between the lithofacies are obscured by folding and local fault offsets.

The heterolithic rhyolite-basalt, rhyolite breccia and coherent rhyolite lithofacies are overlain by a 150 m thick pillowed lithofacies comprised of plagioclase phyric pillowed basalt flows and up to 40 m of aphyric massive to pillowed basalt flows and flow breccias of the Hidden formation. These basalts differ from those of the Millrock member by their distinctive buff weathering color, sparse epidote-quartz hydrothermal alteration, and abundance of plagioclase phenocrysts.

STOPS 2.4 to 2.7

Coordinates

Stop 2.4: UTM 6071020, 314600

Stop 2.5: UTM 6071045, 314625

Stop 2.6: UTM 6071020, 314700

Stop 2.7: UTM 6071156, 314722

Structure

The geology of Mill Rock Hill has been controversial for many years due to complex lithofacies relationships and due to overprinting deformation. The structural pattern at Mill Rock Hill is dominated by the presence of Z-shaped folds that are parasitic to the F₂ Hidden Lake syncline and that are overprinted by a NW-striking, steeply dipping, S₅ foliation defined by flattened clasts in rhyolite breccias (Gibson et al., 2001; Lewis et al., 2006). S₅ becomes more pronounced in a 5 to 10 metre-wide, NW-striking, high strain zone exposed along the east side of Millrock Hill. The high strain zone has a strong SE-plunging (35°) stretching lineation and it possibly originated as an early thrust fault that was reactivated during D₅. S₅ is refolded by small outcrop-scale folds that have an axial plane, ENE-striking, S₆ slaty cleavage. S₆ becomes more intense and rotates in anticlockwise fashion within a network of northwest-striking discrete faults, suggesting that it formed during the development of this late network of D₆ sinistral faults, which dissect Millrock Hill.

Stop 2.4 is located at major fault zone within the aphyric pillowed flows and intrusions of the Hidden formation. This fault zone is the continuation of the northwest-trending thrust fault that truncates the Millrock Hill syncline to the north. Stop 2.5, located immediately east of the interpreted thrust fault exposes a rhyolite breccia lithofacies, which is interpreted to be a structural repetition of the Millrock member. Further to the east, at Stop 2.6, a bedded tuff lithofacies, typical of the uppermost Millrock member, is intruded by fine-grained and aphanitic basalt sills and a younger, fine-grained felsic intrusion of the Phantom Lake series. The bedded tuff lithofacies consist of thin-bedded to laminated, to thick-bedded basaltic tuff. Scoriaceous basaltic lapilli define crude layers within some beds or occur as isolated lapilli. Fine, <5mm, round to elliptical, light coloured accretionary lapilli occur within some beds. A pillowed lithofacies of the overlying Hidden formation (1920 member) is exposed at Stop 2.7, but is separated from the Millrock bedded tuff lithofacies by green weathering, aphanitic, and quartz-amygdaloidal aphyric basalt sills (?).

***NOTICE:** Stops 2.3 through 2.5 and Stop 2.7 are on the HudBay Minerals Plant property. This area is restricted to the public and entrance requires the permission of HudBay Minerals.*

STOP 3. SOUTH MAIN SECTION

In this cross section, we examine lithofacies that comprise the Millrock member and the lowermost units of the Hidden formation. The traverse begins within the Millrock member approximately 500m west-northwest of the South Main shaft. All lithofacies and the location of the substops are shown on Figures 7 and 23. Descriptions of Stops 3.3 to 3.7 are modified from Galley et al. (2002).

Coordinates

Stop 3.1: UTM 6071850, 314172

Stop 3.2: UTM

Stop 3.3: UTM 6071633, 314634

Stop 3.4: UTM 6071707, 314731

Stop 3.5: UTM 6071707, 314731

Stop 3.6: UTM 6071581, 314683

Stop 3.7: UTM 6071401, 314634

Stop Descriptions

At Stop 3.1, a fault occurs at the contact between a basaltic, bedded tuff lithofacies, which is typical of the uppermost Millrock member, with a megabreccia lithofacies, which is typical of the basal portion of the Millrock mem-

ber. The fault trends northwest, dips steeply to the east, and is crudely parallel to strata. It is interpreted to be a thrust fault that placed an “older” megabreccia lithofacies on a “younger” bedded tuff lithofacies within the Millrock member. The megabreccia lithofacies contains blocks of massive, aphyric to sparsely plagioclase phyric, amygdaloidal basalt that include intact pillows, broken pillows, massive basalt and blocks of pillowed flows that range up to 50m in size. The blocks have sharp contacts with the matrix. Irregular, intact to broken amygdaloidal, amoeboid clasts of aphyric basalt locally dominate the lithofacies and are often associated with subrounded scoriaeous basalt lapilli; the latter may define crude scoria-rich beds. The matrix consists of angular, plate-like lapilli and fine, mafic tuff. The breccias are poorly sorted, with local evidence of crude bedding and fine upwards to Stop 3.2, where the breccias consist of angular and lesser amoeboid clasts of aphyric amygdaloidal basalt and scoria. Local, discontinuous, scoria-rich beds and thin pillowed flows occur within the upper part of the finer, megabreccia lithofacies. Dykes and sills of fine- to medium-grained, variably feldspar and pyroxene phyric basalt, irregular aphyric amygdaloidal basalt, and quartz and quartz and feldspar phyric rhyolite cross cut the megabreccia as do younger Phantom Lake and Boundary intrusions. The coarse volcanoclastic lithofacies is interpreted to have been emplaced primarily as high concentration mass flow or debris flow, derived through the collapse of synvolcanic fault scarps during episodic subsidence. The breccias define a primary synvolcanic, fault bounded sub-basin within the interpreted larger scale Flin Flon cauldron (Fig 9 and 12). The amoeboid clasts are interpreted as spatter and along with the scoriaeous lapilli may be a product of mild fire-fountain eruptions that accompanied subsidence. The thin pillowed flows intercalated with the coarse block-rich breccias are interpreted to be a product of episodic effusive eruptions that occurred within the South Main “sub-basin”.

The bedded tuff lithofacies at Stop 3.3, is located southwest of and along strike from the coherent rhyolite and breccia lithofacies that comprise the South Main flow-dome complex. It consists of rusty weathering, pyritic, thin- to medium-bedded basaltic tuff that stratigraphically overlies an aphyric pillowed flow whose base defines the top of the megabreccia lithofacies. The bedded tuff is overlain by a heterolithic, tuff lithofacies that consists of thin-bedded, mafic and felsic tuff intercalated with lapilli tuff containing quartz phyric rhyolite lapilli and lesser basaltic lapilli. The felsic lapilli were interpreted to be locally derived from detritus that was shed from the adjacent South Main rhyolite flow-dome complex (Bailes et al., 2003). This sulphide-rich bedded volcanoclastic lithofacies is considered to represent the Flin Flon mine stratigraphic interval.

At Stop 3.4, a coherent rhyolite lithofacies, of the South Main rhyolite flow-dome complex, has a thickness of 100m and consists of three facies: a lower aphyric, a middle quartz-plagioclase phyric autoclastic pumice breccia, and an upper coarsely quartz phyric flow-banded facies. The flow-dome complex is cross cut by numerous synvolcanic mafic intrusions as well as a prominent Boundary intrusion breccia; the latter will be examined at Stop 3.5. Lower phases of the South Main flow-dome complex are well exposed in large outcrops to the northwest.

Plug and dyke-like bodies of the Boundary Intrusion suite consisting of meladorite, pyroxenite and felsic derivatives were

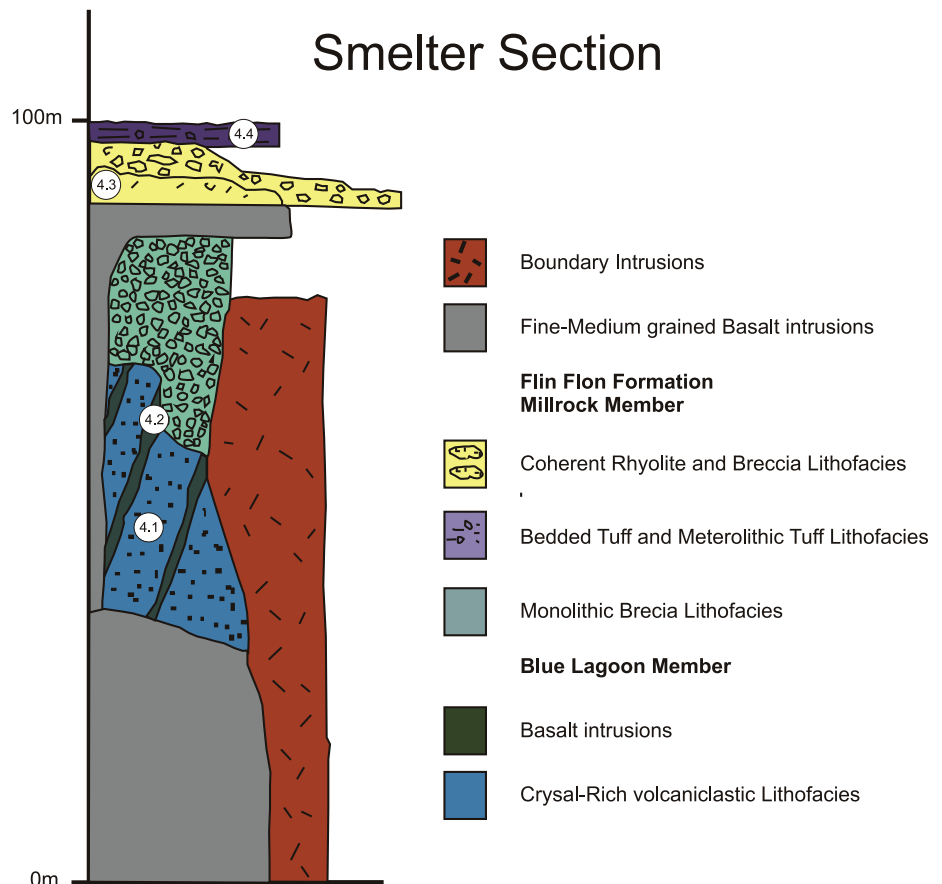


Figure 23. Idealized stratigraphic section through the Millrock member at South Main showing the lithofacies and stop locations.

emplaced into folded supracrustal rocks, including sedimentary rocks of the c.a. 1845 Ma Missi Group (Syme and Forester, 1977). Emplacement of these intrusions was locally accompanied by prominent brecciation of the country rocks and earlier crystallized phases of the intrusions themselves.

Stop 3.6 is located at the base of a 40(+) m thick, aphyric pillowed flow lithofacies. The lithofacies is characterized by pillows with prominent radial pipe amygdules and mega pillows up to 15 m in diameter that were likely feeder tubes for the pillowed flow. The pillowed lithofacies overlies another aphyric pillowed lithofacies that also contains pillows with prominent radial pipe amygdules, but with amoeboid forms and is cross-cut by highly irregular synvolcanic dykes. The contact between the two pillowed lithofacies is traceable for 350 m along strike.

DAY 3: FLIN FLON DISTRICT

STOP 4. SMELTER SECTION

In this cross-section evidence for an angular unconformity between the Blue Lagoon and Millrock members will be examined. Lithofacies exposed in this section and the locations of substops are shown in Figures 7 and 24 Stop descriptions are modified from those of Syme et al. (1996), Galley et al. (2002), as modified by Devine (2003).

STOPS 4.1 to 4.8: Blue Lagoon member

Coordinates

Stop 4.1: UTM 6073524, 314100

Stop 4.3: UTM 6073677, 314217

Stop 4.5: UTM 6074770, 314020

Stop 4.6: UTM 6074840, 314115

Stop 4.7: UTM 6074780, 314035

Stop 4.8: UTM 6075145, 314090

Stop Descriptions

The stratigraphic succession starts with a crystal-rich volcanoclastic lithofacies of the Blue Lagoon member at Stop 4.1. The lithofacies is a thickly bedded plagioclase crystal tuff and lapilli tuff. Plagioclase crystals comprise 12-40% (>0.1 to 1.5 cm) of the lithofacies and primary features are obscured by recrystallization and alteration. The angular unconformity between Blue Lagoon crystal-rich volcanoclastic lithofacies and an overlying, monolithic breccia lithofacies of the Millrock member is best exposed at Stop 4.2 The unconformity surface is sharp, unfaulted and truncates bedding in the crystal tuffs at a high angle. Thin (1 m) mafic sills in the crystal tuff and lapilli tuff are also clearly truncated at the unconformity; the dykes have chilled margins and amygdaloidal interiors. The angular unconformity is interpreted to be a product of synvolcanic faulting prior to emplacement of the Millrock member. The Millrock monolithic breccia lithofacies weathers a dark green color, is poorly sorted and clast supported. It contains angular to subangular clasts (up to 40 cm) of epidote altered, aphyric, amygdaloidal basalt (5-25 % quartz amygdules < 1cm) in a fine-grained, tuff-sized matrix. Quartz phyric rhyolite lapilli comprise <1% of the unit. The lithofacies is crudely bedded and locally displays normal grading. The aphyric amygdaloidal basalt clasts in this lithofacies are smaller but the same as those within the megabreccia at South Main; these two lithofacies are interpreted to be stratigraphically equivalent, with the monolithic basalt breccia lithofacies representing a more distal facies.

Coherent and breccia rhyolite lithofacies conformably overly the monolithic basalt breccia lithofacies at Stop 4.3 and are interpreted to define a rhyolite flow, referred to as the Mine rhyolite (Galley et al., 2002). The rhyolitic lithofacies have been traced on surface, in underground workings, and in exploration drilling for approximately 3 km. They attain a maximum thickness of 150 m northwest of the smelter complex and thin to the north and to the south. A framework supported, monomictic breccia lithofacies composed of angular to subrounded, quartz-phyric rhyolite fragments in a finer, tuff-sized matrix occurs at the base. The rhyolite clasts contain 1-2% euhedral quartz phenocrysts (0.4-1.2 mm) and 4% euhedral tabular plagioclase phenocrysts (0.4-2 mm). The basal breccia facies is overlain by a coherent lithofacies (6073677; 314217) that contains <5% euhedral quartz phenocrysts (0.2-2.5 mm), 7% euhedral plagioclase phenocrysts (0.2-1.2 mm) and attains a maximum thickness of 50m. The coherent lithofacies, which is interpreted to comprise a flow interior, grades upwards into an upper, clast supported breccia lithofacies (UTM 6073629, 314217), which contains irregular to tabular slabs of flow banded

rhyolite ranging up to 1.9 m long that have the same phenocryst population as the underlying coherent lithofacies. The flow banded slabs comprise 5-20% of the breccia and occur in a matrix composed of angular to subangular rhyolite lapilli in a dark grey rhyolite tuff-sized matrix. The Mine rhyolite is correlated with coherent rhyolite domes, cryptodomes and sills exposed at Millrock Hill and at South Main; however, the Mine rhyolite has a U-Pb zircon age of 1.9 Ga in contrast to 1.88 Ga U-Pb zircon ages obtained from the Millrock and South Main rhyolites (Stern et al., 1999). The reason for this age discrepancy is uncertain at this time.

Stop 4.4 is a virtual stop of a bedded tuff and heterolithic tuff lithofacies that comprise a 35 m thick unit, which overlies the Mine rhyolite (referred to as the 'Railway volcanics', by Bailes and Syme, 1989). The bedded tuff lithofacies is thick- to thin-bedded and is intercalated with the heterolithic tuff lithofacies that contains quartz amygdaloidal, aphyric basalt clasts and quartz and feldspar phyric rhyolite clasts that range from 2 to 24 cm long and 2 to 18cm in width (average size of 9 x 5 cm) (Devine, 2003). The "Railway volcanoclastic" unit is interpreted to be the time-stratigraphic equivalent of the coarser rhyolite and rhyolite-basalt breccia lithofacies at Millrock Hill (Stop 2.2), and the bedded tuff and heterolithic tuff lithofacies (Stop 3.3) at South Main. At these localities, the rhyolitic component of these lithofacies is interpreted to have been emplaced by submarine mass flows that were ultimately derived from syndepositional rhyolite domes.

On route to the lower Callinan stop, typical volcanoclastic lithofacies that comprise the Blue Lagoon member are examined at Stops 4.5 to 4.8 (Fig 9); lithofacies descriptions at each Stop are modified from Devine (2003).

Stop 4.5 is typical of the crystal-rich tuff and lapilli tuff lithofacies of the Blue Lagoon member. It contains 12 to 40% plagioclase crystals from 0.1 to 2 cm in size within a finer, tuff-sized, mafic matrix; locally the lapillistone facies is totally comprised of plagioclase crystals and is devoid of a finer matrix. The crystal-rich tuff and lapilli tuff lithofacies are crudely bedded, and conformably overly a matrix-supported tuff-breccia lithofacies that grades upward into the lapilli tuff lithofacies. The tuff breccia and lapilli tuff lithofacies contain clasts of feldspar phyric and aphyric basalt in a mafic, tuff-sized matrix containing up to 10 % plagioclase crystals. Possible mechanisms to explain the abundance of crystals include: pyroclastic fragmentation of highly crystallized (phyric) magma, primary and secondary eruptive fractionation, and or reworking of pre-existing, unconsolidated, volcanoclastic deposits, (i.e. Cas and Wright, 1987). The feldspar crystal-rich tuff and lapilli-tuff units are interpreted to have been

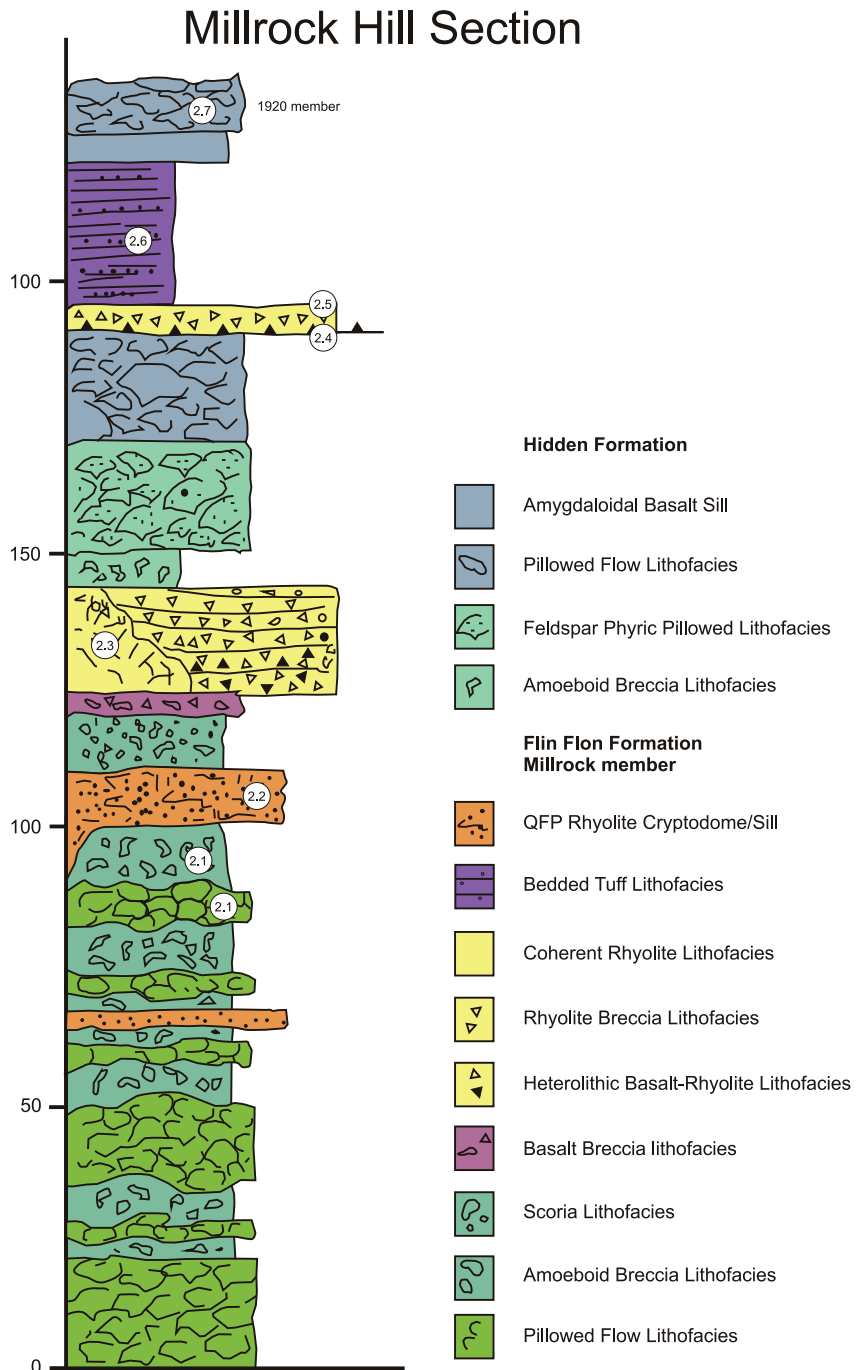


Figure 24. Idealized stratigraphic section through the Millrock member at the Smelter section showing the lithofacies and stop locations.

derived by pyroclastic fragmentation of crystal-rich magmas, such as those that produced the intercalated pillowed flows, which have a plagioclase phenocryst content of 12-20% (Devine, 2003). The higher crystal content of the volcanoclastic lithofacies as compared their coherent extrusive lithofacies is interpreted to reflect crystal concentration processes during explosive submarine pyroclastic eruptions (sorting during eruption column generation and collapse) and their subsequent emplacement by subaqueous, pyroclastic flows and, where plagioclase crystals are the only component and bedforms do not indicate re-working or mass flow transport, by pyroclastic fall (Gibson et al., 2009a; submitted).

Located some 100 m east and up-section from Stop 4.5, a coarse, heterolithic, block-rich lithofacies at Stop 4.6 occurs at the top of the Blue Lagoon member. The coarse volcanoclastic lithofacies contains plagioclase-phyric, basalt blocks in a fine, recrystallized, tuff-sized matrix containing 5% plagioclase crystals. Depositional units range from 3 to 4m in thickness, and are poorly size sorted and chaotic. These features suggest transportation by mass flows and, along with the occurrence of clasts of breccia (feldspar-phyric blocks in a feldspar-rich matrix) up to 1.5 m in size, suggest derivation from the redeposition of pre-existing volcanoclastic deposits (Fig. 9). The mass flows may have been triggered by synvolcanic faulting, during subsidence, which generated debris flows composed of previously emplaced volcanoclastic deposits.

The coarse heterolithic block-rich lithofacies at Stop 4.6 is conformably overlain by thin bedded to laminated tuff and crystal tuff lithofacies of the Millrock member at Stop 4.7. The lithofacies weather a rusty brown color due to oxidized sulphides and occurs approximately 100m up-dip of the Dan VMS occurrence. Plagioclase crystals within the tuffs abruptly decrease in abundance upwards, and are absent in the uppermost portion of the thin-bedded tuff. The Millrock bedded tuff lithofacies is now buried by construction debris, but similar bedded tuffs displaying flame, ball and pillow structures, as well as cross-bedding are well exposed some 100 m to the north at Stop 4.8. However, at Stop 4.8 the bedded tuff lithofacies is underlain by a coarse, heterolithic breccia lithofacies of the Millrock member that is identical to that at Stop 5.4. The continuation of the Millrock bedded tuff lithofacies between Stops 4.7 and 4.8, and the marked absence of Millrock Hill heterolithic breccia lithofacies at Stop 4.7, where the Millrock bedded tuff sits directly on the Blue lagoon member suggest the presence of a synvolcanic fault between Stops 4.7 and 4.8 (Fig 9). The absence of Millrock heterolithic basalt breccia lithofacies at Stop 4.7, suggests that it was uplifted relative to Stop 4.8 before the onset of Millrock member volcanism (Fig 9). Blue Lagoon detritus within the Millrock heterolithic breccia lithofacies at Stop 5.3 may have been derived from the Blue Lagoon member in the adjacent, uplifted block of Stop 4.7.

STOP 5. LOWER CALLINAN SECTION

Coordinates

Stop 5.1: UTM 6075705, 313535

Stop 5.2: UTM 6075560, 313753

Stop Descriptions

In this section, lithofacies typical of the Club, Blue Lagoon and Millrock members will be examined. At Stop 5.1, the Club member consists of three lithofacies, coherent rhyolite, rhyolite breccia and bedded tuff. The coherent rhyolite facies consists of massive, aphyric, aphanitic, rhyolite that is conformable, but in sharp contact with the overlying breccia lithofacies. The breccia lithofacies contains clasts of aphyric rhyolite in a fine, tuff-sized, mafic matrix. The lithofacies is thick bedded, typically normally graded and the rhyolite clasts have identical trace and REE compositions to the underlying coherent rhyolite lithofacies (Devine, 2003). The range in size and abundance of rhyolite fragments, and the absence of other clast types indicates that the rhyolite clasts have not been transported a great distance, and are derived from a single source. This coupled with their angular and blocky form, and the occurrence of in situ brecciated or jigsaw fit clasts suggests the clasts are a product of autoclastic fragmentation, and that they were emplaced by mass flows along the flanks of the growing flow dome represented by the underlying coherent lithofacies (Devine, 2003). Multiple normally graded beds suggest depositional units were emplaced quickly, one after another, through successive periods of dome growth and collapse. The fine, tuff-sized mafic matrix has a separate mafic provenance and may have ultimately been derived from contemporaneous explosive basalt volcanism.

The bedded tuff lithofacies conformably overlies the rhyolite breccia facies and is texturally similar to the mafic tuff matrix of the latter lithofacies. The bedded tuff lithofacies is interpreted to be a product of explosive basaltic

volcanism and to have been emplaced by fall (suspension) and low concentration mass flows. The contact with the overlying Blue Lagoon member is conformable, sharp and defined by the abrupt appearance of plagioclase crystals within the mafic tuff.

The purpose of Stop 5.2 is to examine multi-generational peperite that developed where feldspar phyric and aphyric basaltic dykes and sills intruded massive, crudely bedded, crystal tuff lithofacies of the Blue Lagoon member that contains 5 to 20% plagioclase crystals (<5 mm in size). The sparsely feldspar phyric, fine-grained sill is characterized by irregular, aphanitic chilled contacts and numerous fractures that increase in abundance and decrease in spacing towards the sill-crystal tuff contact. Irregular to fluidal apophyses of the sill extend into the crystal tuff, where they are fractured, in situ brecciated, and brecciated to form blocky peperite; the peperite is interpreted to be a product of quench fragmentation during emplacement of the sill into the wet, unconsolidated tuffs (Gibson et al., 2003a).

The crystal tuff away from the sill contact contains irregular, wispy and brecciated fragments of aphyric basalt that lack the feldspar crystals found within the adjacent sill. The wispy, fluidal to amoeboid clasts of aphyric basalt are not associated with a coherent intrusion and are interpreted to be an earlier formed, fluidal (blocky) peperite, which formed by the total disintegration of an initial basalt magma that was emplaced into the unconsolidated crystal tuff (Gibson et al., 2003a).

Basalt sills exposed on the immediately adjacent outcrop to the east crosscut earlier sills and rarely develop peperite (UTM 6075580, 313765). Their contacts with the crystal tuff are more uniform and straight, which suggests that at this stage the crystal tuff was essentially lithified and that there were no significant rheological differences between the tuff and earlier sills (Gibson et al., 2003a). This outcrop also displays a sharp but irregular contact between the Blue Lagoon crystal tuff lithofacies and a 75 m thick heterolithic breccia lithofacies of the Millrock member. Although conformable, the base of the Millrock lithofacies is erosive as it scours into, and contains fragments of the underlying crystal-rich beds of the Blue Lagoon member; the contact is also folded about a northwest-trending fold axis (parallel to the D₂ Hidden Lake Syncline). The Millrock heterolithic breccia lithofacies (UTM 6075575, 313795) is framework supported and contains wispy- to plate-like to angular blocks and lapilli of amygdaloidal, aphyric basalt and minor clasts of feldspar phyric basalt and crystal tuff in a fine, tuff-sized matrix that contains up to 5% plagioclase crystals, which decrease in abundance with distance from the contact (Devine, 2003). The breccia lithofacies is crudely bedded and normally graded. A tentative interpretation for the monolithic basalt breccia lithofacies is that it is a product of phreatomagmatic pyroclastic eruptions that developed in response to the emplacement of basalt magma into unconsolidated and wet Blue Lagoon crystal tuff (Gibson et al., 2003a). The heterolithic breccia lithofacies was transported and emplaced by high concentration mass flows and may represent a primary pyroclastic deposit or a re-deposited, syneruptive equivalent. Aphanitic, aphyric sparsely amygdaloidal basalt dykes and sills that intrude the lithofacies have distinct autobrecciated margins with peperite. These intrusions are identical in texture and composition to the aphanitic aphyric basalt clasts within the lithofacies, and are interpreted to have intruded their own, unconsolidated volcanoclastic deposits (Gibson et al., 2003a).

Hazard: This exposure occurs along the edge of the outcrop, above a cliff.

STOPS 5.3 to 5.5:

Coordinates

Stop 5.3: UTM 6075518, 313910

Stop 5.4: UTM 6075595, 313934

Stop 5.5: UTM 6075625, 313970

Stop Descriptions

The purpose of Stops 5.3 to 5.5 is to examine heterolithic breccia and bedded tuff lithofacies that comprises the Millrock member in the Callinan fault block (section 8 of Figs 8 and 9). The lithofacies at Stops 5.3 to 5.5 and the location of the substops are shown in Figure 9. At Stop 5.3, the crystal tuff lithofacies of the Blue lagoon member consists of crudely bedded, plagioclase crystal tuff and lapilli tuff similar to those observed at Stops 4.1 and 4.5. The contact with the Millrock member is not exposed, but is interpreted to be conformable. Note that this outcrop is interpreted to be a thrust fault repeat of the same contact exposed to the west at Stop 5.2. The inferred thrust fault lies in the valley floor and is not exposed.

At Stop 5.4, the heterolithic breccia lithofacies is similar to that at Stop 5.2, and it attains a maximum thickness of 150 m. It consists of framework supported beds (80% clasts) that are moderate to poorly sorted, range from 0.4 to 6m in thickness, and contain clasts of angular, wispy- to plate-like, aphyric, aphanitic basalt, feldspar phyric basalt, and minor medium- grained gabbro that range up to 1.4 m in size, within a finer, tuff-sized, mafic matrix that contains <1% feldspar crystals (Devine, 2003). The upper portion of the lithofacies fines abruptly and then continuously from thick- to medium-bedded lapillistone and lapilli tuff to thin-bedded and laminated mafic tuff, with cross bedding and scours particularly well developed within the finer-grained, tuff beds. Thin (<20 cm) lenses of crystal tuff and blocks of crystal tuff occur near the transition from lapilli tuff to tuff.

The relatively large thickness (up to 150 m) and confined lateral extent of this lithofacies suggest its emplacement into a distinct fault-block basin (the Callinan fault block). The lack of thinner, fine-grained beds between the coarser tuff breccia and lapillistone beds and the disorganized clast fabric with respect to bedding suggests these units were emplaced quickly and by high-concentration mass flows. They are interpreted to be syneruptive, resedimented, pyroclastic deposits (Devine, 2003). The presence of numerous aphanitic, aphyric basalt clasts that are angular, irregular, and have unbroken shapes and slightly chilled margins suggest this unit may have formed by initial phreatomagmatic explosive eruptions with subsequent syneruptive redeposition (as proposed for the similar lithofacies at Stop 5.2; Gibson et al., 2003a). The crystal tuff lenses and blocks of crystal tuff within the upper most beds of this lithofacies are interpreted as detritus derived from Blue Lagoon member in the adjacent fault block to the south (Stops 4.6 and 4.7) that was uplifted and exposed by faulting prior to or during Millrock member volcanism (Gibson et al., 2009a). As at Stop 5.2, the aphanitic, aphyric basalt dykes and sills that intrude the heterolithic breccia lithofacies have autobrecciated margins with peperite, and are interpreted to have intruded their own, unconsolidated volcanoclastic deposits (Gibson et al., 2003a).

The bedded tuff lithofacies at Stop 5.5 also defines the top of the Millrock member and consists of thin-bedded to laminated mafic tuff and lesser, lighter coloured felsic tuff; soft sediment slump structures are common. The tuff is plane bedded, although some beds show erosive lower contacts, and is intruded by basalt sills. The bedded tuff lithofacies weathers a rusty red-brown colour and occurs approximately 250m up-dip and plunge from the Callinan VMS deposit.

The bedded tuff lithofacies defines the top of the Millrock member in all structural blocks from Millrock Hill (and south) to Callinan in the north where it ranges in thickness from 5 to 50 m (+) thickness (Fig. 7). It is dominantly composed of basalt tuff, but locally contains a minor rhyolitic “tuff” component towards its base (Tardif, 2003). It also contains minor lapilli-sized scoria and lesser lithic clasts, feldspar crystals, and beds containing accretionary lapilli. It is typically plane bedded, but locally cross bedded, and often displays structures attributed to soft-sediment deformation during slumping. The shear volume of bedded tuff, its significant areal extent, ubiquitous occurrence in all fault blocks, and its basaltic composition, which is identical to the composition of associated basalt flows (no geochemical evidence for input of external detritus), are consistent with an origin through pyroclastic eruptions (Fig. 12; mixed strombolian magmatic and hydrovolcanic eruptions; Gibson et al., 2009a; submitted). Bed forms suggest it was emplaced by suspension sedimentation and low concentration mass flows. The occurrence of accretionary lapilli indicate the eruption column was, at least in part, subaerial and the common occurrence of cross bedding and less commonly ripples suggests reworking by bottom currents during hiatuses in eruption and deposition (Gibson et al., 2009a; submitted).

STOP 6. BEAVER ROAD ANTICLINE

The stops through the Beaver Road anticline will demonstrate: 1) field evidence for defining primary synvolcanic subsidence, 2) the relationship between volcanism, subsidence, and hydrothermal alteration, 3) the influence of primary synvolcanic structures on later deformation, 4) how strata composed predominately of massive flows deform and fold; and 5) features characteristic of thrust faults and their reactivation. The locations of the substops are shown in Figures 25-27.

STOPS 6.1 to 6.10

Coordinates

Stop 6.1: UTM 6071210, 313892

Stop 6.2: UTM 6071550, 313910

Stop 6.3: UTM 6071900, 313968

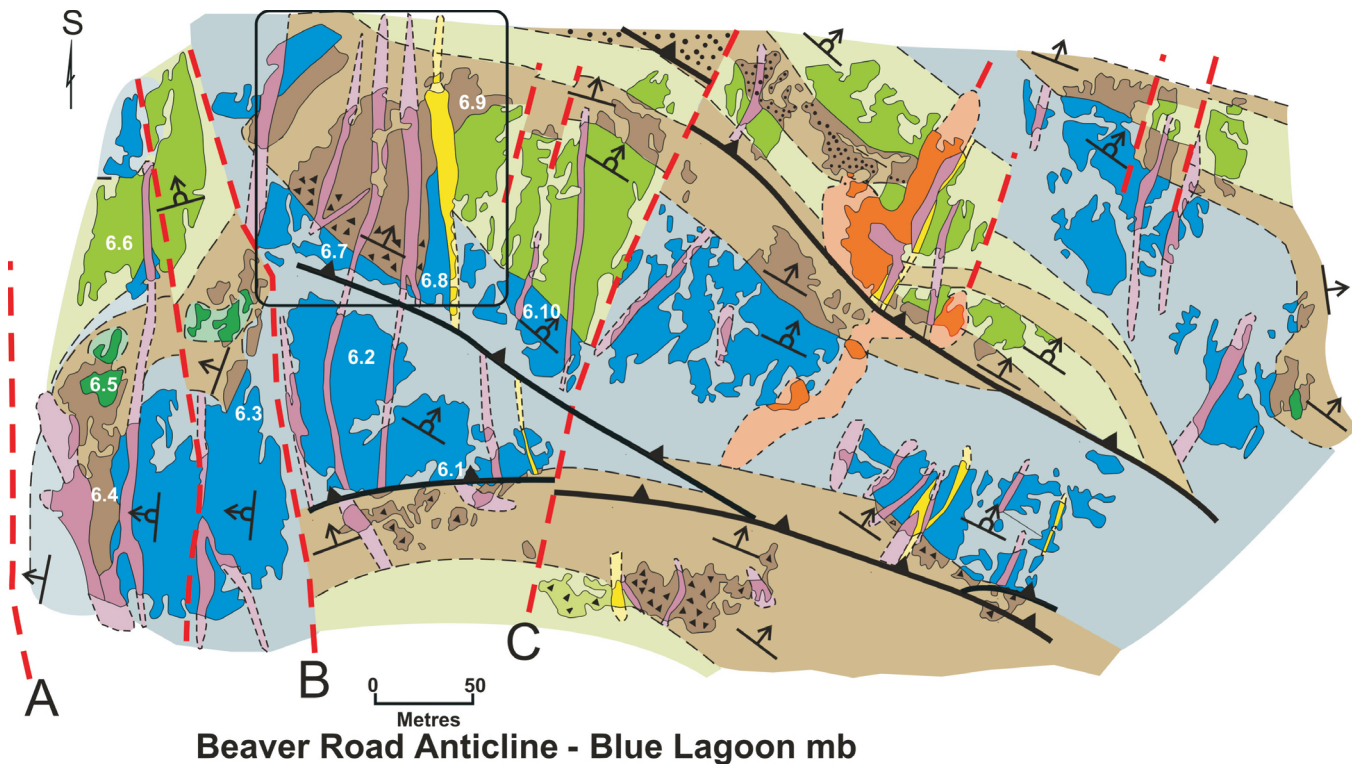


Figure 25. Simplified geology and structure within the Blue Lagoon member at the Beaver Road Anticline showing Stop locations (after Gibson et al., 2007). Units are as follows; light green with black triangles = coarse basaltic volcanoclastic lithofacies; brown = volcanoclastic lithofacies comprised of coarse block-rich and megabreccia facies, massive crudely bedded tuff and well bedded tuff lithofacies with variable amounts of feldspar crystals and scoria (black dots); blue = feldspar phyrlic pillowed basalt lithofacies (10-15 % feldspar); green = aphyric to sparsely feldspar phyrlic (<5 % feldspar) basaltic pillowed lithofacies; purple, yellow and orange = basaltic, rhyolitic and Boundary intrusion dykes. Area within circle is illustrated in detail in Figure 26.

Stop 6.4: UTM 6071230, 314085

Stop 6.5: UTM 6071156, 314038

Stop 6.6: UTM 6171082, 314050

Stop 6.7: UTM 6071095, 313915

Stop 6.8: UTM 6071092, 313893

Stop 6.9: UTM 6071035, 313850

Stop 6.10: UTM 6071135, 313825

Stop Descriptions

At Stop 6.1 a basaltic tuff lithofacies is separated from feldspar phyrlic pillowed lithofacies of the Blue Lagoon member by a shallow, south-dipping fault that clearly truncates dykes within both lithofacies and flow contacts within the pillowed lithofacies. The fault is interpreted to be a thrust fault because it has a bedding-parallel shear foliation and a down-dip, SE-plunging, stretching lineation and is similar in strike and dip to the D_4 Railway-Club Lake thrust faults (Lewis et al. 2007). A mafic dyke in the hanging wall of the fault underwent a clockwise rotation into the fault, and the shear foliation within the thrust fault is overprinted by dextral shear bands and asymmetrical Z-shaped drag folds, suggesting that it was reactivated as a dextral transcurrent fault during D_6 . The thrust fault is offset along a north-northwest trending steeply dipping fault labeled B in Figure 25 which, along with other similarly oriented faults, are parallel to the Flin Flon Lake Fault (A in Fig. 25). The Flin Flon Lake Fault is poorly exposed but a 3D reconstruction of the subsurface geology by Schetselaar et al. (submitted), suggests that the fault is an early, west-directed, D_3 thrust fault that was later reactivated as a transcurrent shear zone as indicated by dextral and sinistral shear fabrics in several parallel and adjacent minor faults.

The feldspar phyrlic pillowed lithofacies at Stop 6.2 is typical of the Blue Lagoon member. Note the well-developed pillow selvages, minor interpillow hyaloclastite and shallow south dip of the flow. The pillows contain 12 to 15% plagioclase crystals. Continuing 30 m to the north the pillows have a sharp but irregular contact with an overlying breccia containing angular to irregular (amoeboid) fragments in a hyaloclastite matrix. The breccia is inter-

puted to be a flow top breccia to the underlying pillowed flow. The contact between the pillows and breccia trends west-northwest, parallel to other flow contacts within this fault block.

The traverse from Stop 6.2 to Stop 6.3 transects the north-northwest trending Fault B, which is not exposed as it occupies the low ground between the two outcrops (Fig. 25). Fault B coincides with a significant change in the attitude of the flows, where strata at Stop 6.2 to the west, strike west-northwest and dip shallowly to the south whereas strata at Stop 6.3 to the east, strike north-northeast and dip steeply to the southeast; the horizontal movement along the fault is sinistral (Fig. 30). This abrupt and rapid change in the orientation of strata which, in part, defines the Beaver Road anticline is actually more in response to faulting and than folding as folding would manifest itself by a gradual change in the orientation of bedding.

At Stop 6.4, the contact between the feldspar phyric pillowed lithofacies and the overlying volcanoclastic lithofacies comprised of thin-bedded to laminated tuff and coarse, block-rich tuff breccia confirms the north-trending, steeply southeast dipping and facing orientation of the strata as does the bedding within the volcanoclastic lithofacies. Aphyric basalt sills and dykes within the volcanoclastic lithofacies have peperite along their contacts indicative of their synvolcanic emplacement.

At Stop 6.5, two large blocks (approx. 10 m x 10 m) of aphyric pillowed basalt occur within the volcanoclastic lithofacies (Fig. 25; a third and larger block occurs 25m to the west) and this unit is interpreted to be a megabreccia, deposited by high concentration mass flows (debris flows) generated by the collapse of fault scarp walls during or after subsidence. Again the strike and dip of strata are the same as at Stops 6.3 and 6.4.

The aphyric pillowed basalt lithofacies at Stop 6.6 strikes west-southwest and dips shallowly and faces to the south. This change in bedding orientation from that at underlying Stops 6.3-6.5 is abrupt, occurs directly above the volcanoclastic unit examined at Stop 6.5, and is interpreted to define a primary, angular unconformity between strata within the same fault block (Fig. 25). Thus, the abrupt change in the orientation of strata from Stop 6.2 to Stop 6.3 is a result of synvolcanic faulting along Fault B. No doubt subsequent deformation resulted in some rotation of the fault blocks and the reactivation of Fault B, but the D₂ Beaver Road Anticline as illustrated on previous maps is due, in part, to block rotation during synvolcanic faulting and subsidence (Gibson et al., 2007).

The feldspar phyric pillowed flows at Stop 6.7 are similar to those at Stop 6.2, but here they are in sharp but conformable contact with an overlying volcanoclastic lithofacies that is characterized by a coarse, block-rich tuff breccia, comprised mainly of broken pillows at the base, that grades upwards into finer lapillistone, lapilli tuff and tuff within a tuff-sized matrix containing abundant feldspar crystals (Fig. 25, 26). Medium- to thin-bedded to lam-

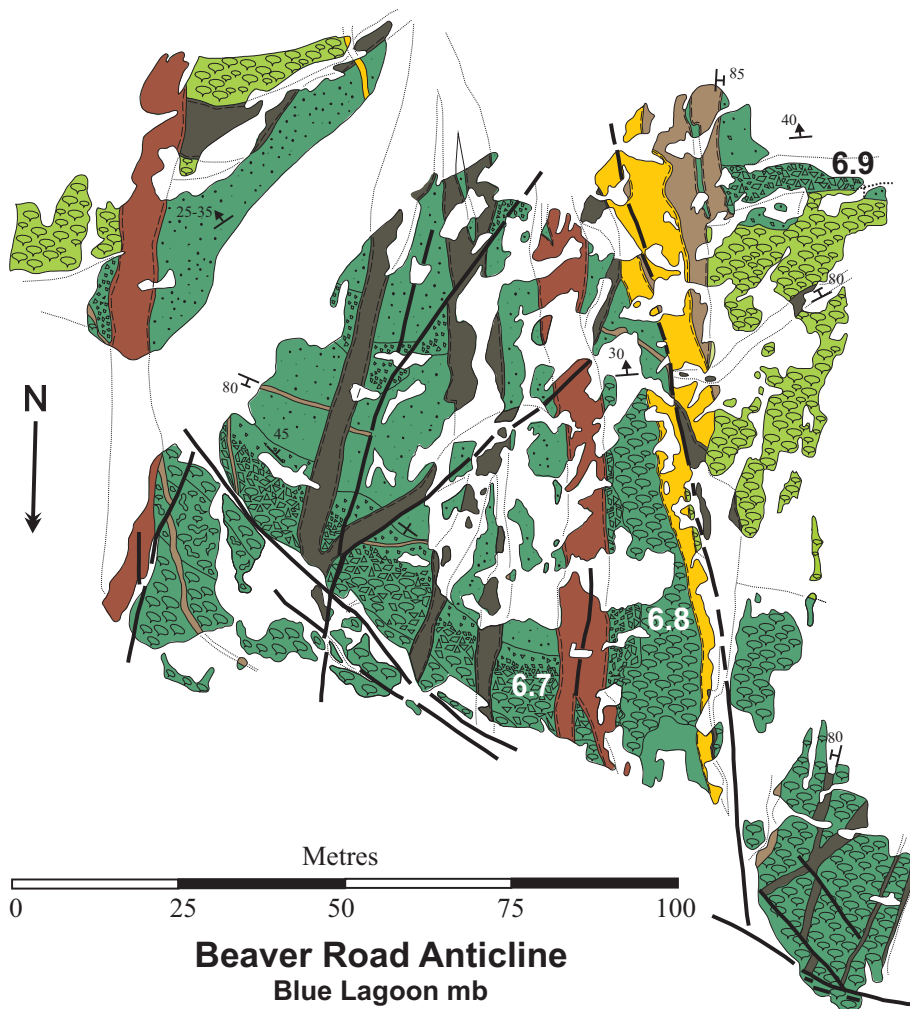


Figure 26. Details of synvolcanic graben in Figure 30 showing Stop locations (after Gibson et al., 2007). Map units as follows: dark green with pillow symbol = feldspar phyric pillowed lithofacies; dark green with fine black dots = basaltic megabreccia, breccia, and tuffs with variable amounts of feldspar crystals; light green = sparsely feldspar phyric pillowed lithofacies; and shades of brown and yellow = basaltic and rhyolitic dykes.

inated basaltic tuff containing variable amounts of scoria, lithic lapilli and feldspar crystals occurs at the top of the volcanoclastic lithofacies. The volcanoclastic lithofacies at Stop 6.7 is correlated with that at Stops 6.3, 6.4 and 6.5 (Fig. 25). Several types and generations of basalt dykes and an aphyric rhyolite dyke crosscut the pillowed and volcanoclastic lithofacies; some of the basalt dykes have irregular and locally peperitic contacts with the volcanoclastic lithofacies.

At Stops 6.8, and 6.9 the contacts between the volcanoclastic lithofacies and adjacent pillowed lithofacies are examined (see details in Fig. 26). The contact between the volcanoclastic lithofacies and feldspar phyric pillowed flow at Stop 6.7 trends northwest, whereas at Stop 6.8 the contact abruptly changes orientation to north-south, where it is at a high angle to bedding within the adjacent volcanoclastic lithofacies. This change in orientation continues to the south where it separates the volcanoclastic lithofacies from the aphyric pillowed lithofacies, which conformably overlies the feldspar phyric pillowed lithofacies. This north-south contact between the volcanoclastic unit and the feldspar phyric and aphyric basalt lithofacies is interpreted to be a primary, synvolcanic fault scarp wall (Fig. 31 and 32; Gibson et al., 2006). However, at Stop 6.9 the volcanoclastic – aphyric pillowed lithofacies contact abruptly changes strike and returns to a northwest orientation, and bedding within the volcanoclastic lithofacies is now parallel to the contact, and to other flow contacts in the same fault block indicating that it is conformable (Fig. 25). Also note that the strike extent of the aphyric pillowed facies is limited by the primary, north-northeast trending fault scarp to the east, and by the north-northeast trending Fault C to the west. This complex relationship between lithofacies, abrupt changes in strike, and conformable versus unconformable contacts can be explained by successive episodes of synvolcanic faulting, subsidence and volcanism (Fig. 26; Gibson et al., 2006). As illustrated in Figure 26, initial faulting and subsidence is interpreted to have resulted in the development of a localized structural basin or graben within the feldspar phyric pillowed flows. Volcanism that accompanied or immediately followed subsidence resulted in the emplacement of an aphyric, pillowed basalt flow within the graben. Subsequent faulting, manifest by the reactivation of an earlier fault (the synvolcanic fault scarp in Fig. 26) and the development of a new, parallel fault to the east resulted in the formation of a step like basin, which was subsequently filled by the volcanoclastic lithofacies such that coarse debris collected at the base of the graben and the finer tuffs and bedded tuffs extend beyond the limits of the small graben defined in Figure 27 to define a larger synvolcanic structural basin within what is now the Beaver Road anticline (Fig. 25). Collapse of this basin during synvolcanic subsidence along Fault B resulted in tilting of strata within this block, and the megabreccias examined at Stop 6.5.

Epidote-quartz alteration occurs through the basaltic flows, but is locally concentrated in two areas. The first being in the pillowed lithofacies immediately adjacent to the primary synvolcanic fault scarp at Stop 6.8. The second is at Stop 6.10 where a 1 m wide, north-northeast trending zone of epidote-quartz alteration crosscuts the feldspar phyric pillowed lithofacies. In both examples, the zone of intense and pervasive epidote-quartz alteration is disconformable, either adjacent to or oriented parallel to synvolcanic faults, and are interpreted to represent high-temperature hydrothermal up-flow zones.

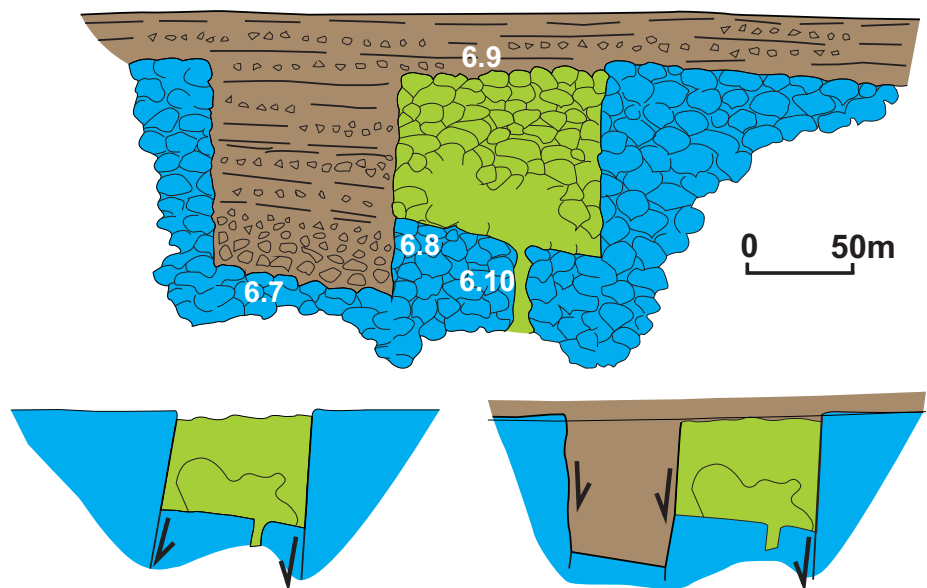


Figure 27. Pre-dyking and pre-folding reconstruction of the area in Figures 25 and 26 showing Stop locations; color legend as in Figure 30 (after Gibson et al., 2007).

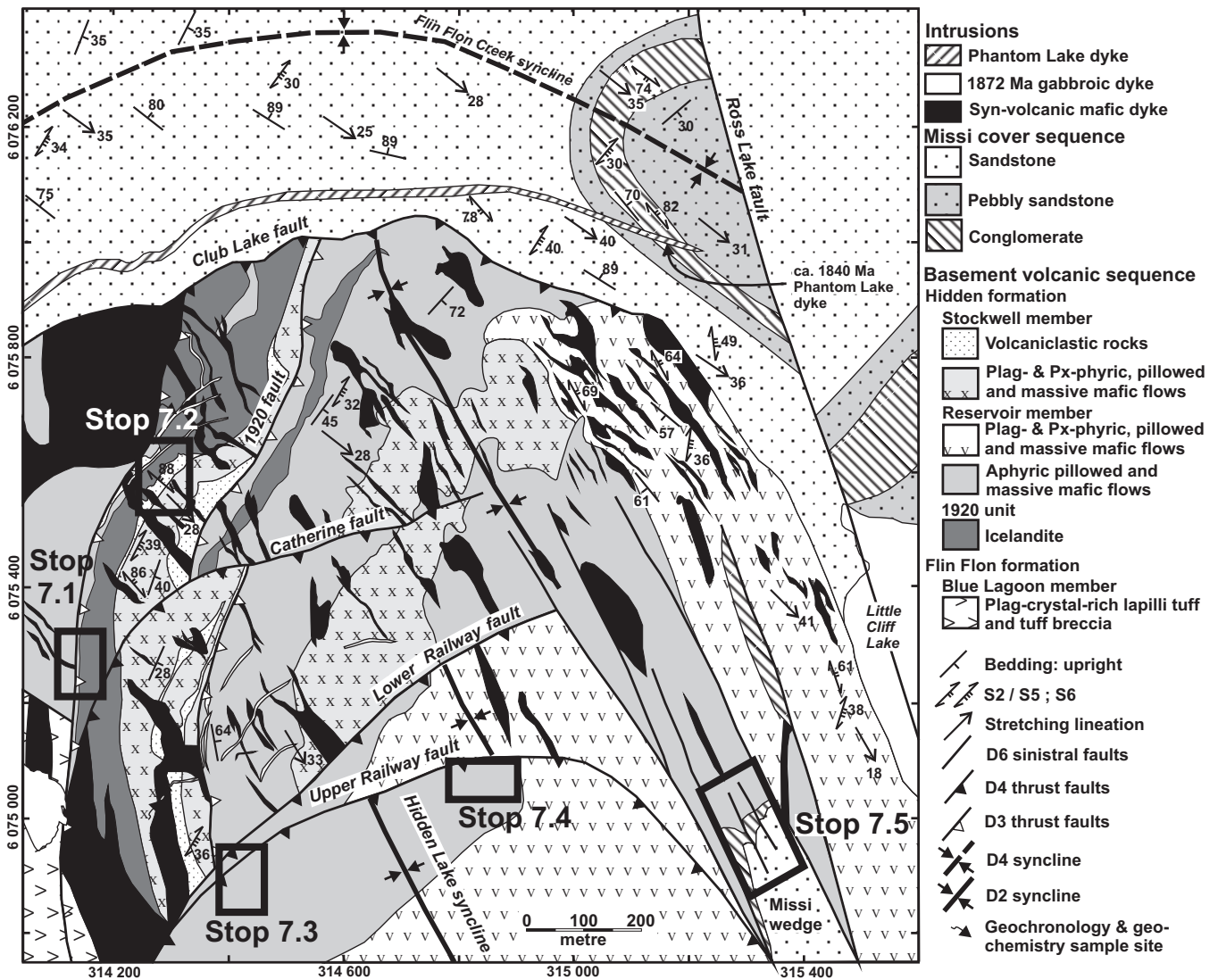


Figure 28. Geology and structure of the Hidden formation within the Hidden lake Syncline showing the location of Stops 7.1 to 7.5 (after DeWolfe et al., 2009).

DAY 4: FLIN FLON DISTRICT

STOP 7: UPPER CALLINAN SECTION

This traverse is a continuation of the Lower Callinan section (Stop 5) and focuses on coherent andesitic and basaltic flows of the Hidden formation and key structural elements, including the Railway Thrust Faults. The location of Stops 7.1, 7.2, 7.3, 7.4 and 7.5 are shown on Figure 28. On the walk to Stop 7.1 you will cross several large outcrops that contain thin (<1 metre) screens of the bedded tuff lithofacies (as at Stop 5.5), sometimes containing quartz crystals and quartz phyric rhyolite lapilli, between the basalt and basaltic-andesitic sills which, coupled with the common occurrence of peperite, has been cited as evidence to indicate that these thick sills were emplaced into the unconsolidated, wet, Millrock member bedded tuff lithofacies during the initial stages of Hidden formation volcanism (Gibson et al., 2003b; DeWolfe et al., 2009a). The numerous basaltic and basaltic-andesitic dykes and sills encountered constitute part of a “sheeted dyke-sill complex” that defines a significant zone of extension and a volcanic centre within Callinan Block and in the larger Flin Flon cauldron (Gibson et al., 2003b ;2007; submitted).

STOP 7.1: Columnar jointed vent facies of the 1920 member cryptoflow

Coordinates

UTM 6075231, 314122

Stop Description

The 1920 member occurs at the base of the Hidden formation and here consists of a coherent basaltic andesite that, along with an overlying volcanoclastic lithofacies, occupies and defines a localized fault-bounded subsidence basin (DeWolfe et al., 2009a,b). The overburden to the east of this outcrop represents a thrust fault of the same generation of the Railway fault. Directly in front of this fault in the vertical face of the large outcrop is an aphyric basaltic unit (base of outcrop and a dark green colour) in contact with the 1920 member (upper portion of outcrop and a dark grey-blue colour). The contact between the two units is sharp and characterized by discontinuous lenses of strongly quartz-epidote altered tuff. Near the centre of this outcrop is the feeder dyke for the 1920 member cutting upwards through the underlying basalt and fanning upwards and outwards away from the vent forming a columnar jointed, massive facies of the 1920 member. If you climb up on top of the outcrop you can observe the columnar joints in a cross sectional view. As you walk to the northeast along the line outcrops you are walking oblique to strike moving upwards through stratigraphy (Fig. 28). In addition to numerous flow banded, synvolcanic dykes you will notice the presence of very irregular, seldom laminated, inclusions of quartz-epidote altered tuff within the 1920 member. In some areas there is a very complex relationship between the tuff and the basaltic andesite forming a chaotic mixture of the two rock types, or peperite, which suggests that the 1920 member was emplaced as a high level, synvolcanic sill into wet, unconsolidated tuff just below the seafloor. Follow the outcrops up and to the northeast for approximately 280 metres.

STOP 7.2: Facies transitions within the 1920 member: Field evidence for emplacement as a cryptoflow

Coordinates






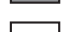
UTM 6075578, 314252

Stop Description



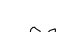
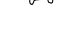

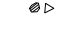



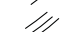
At this location the 1920 member displays a vertical facies transition from massive, coherent basaltic andesite at the base, or northwestern edge of outcrop, to in situ breccia to peperite, all by the host volcanoclastic unit present at the southeastern margin of the outcrop (Figs. 28-29; DeWolfe and Gibson, 2011).

The in situ breccia facies occurs near the top of the coherent unit and its contact with the underlying massive facies is gradational. Within the in situ breccia facies the basaltic andesite fragments have an angular or blocky shape, and a jigsaw-puzzle fit. The fine-grained, dark grey, granular-textured matrix contains angular to cusped shards of basaltic andesite. Moderate to strong epidote-quartz alteration manifests itself as 5–50 cm, light green to light brown, rounded patches in this area. Massive lobes (< 1 m to 3 m) of basaltic andesite

LEGEND

-  Feldspar porphyritic mafic dykes and sills
-  Feldspar and pyroxene porphyritic mafic dykes and sills
-  Fine- to medium-grained mafic dykes and sills
-  Feldspar-rich, coarse-grained dykes and sills
-  1920 unit: Basaltic andesite cryptoflow
-  Mafic volcanoclastic rocks

SYMBOLS

-  Tuff breccia
-  Weak, patchy epidote-quartz alteration
-  Strong, patchy epidote-quartz alteration
-  Columnar jointing
-  Included Tuff
-  Peperite
-  Lapillistone
-  Lapilli-tuff
-  Tuff
-  Lobe

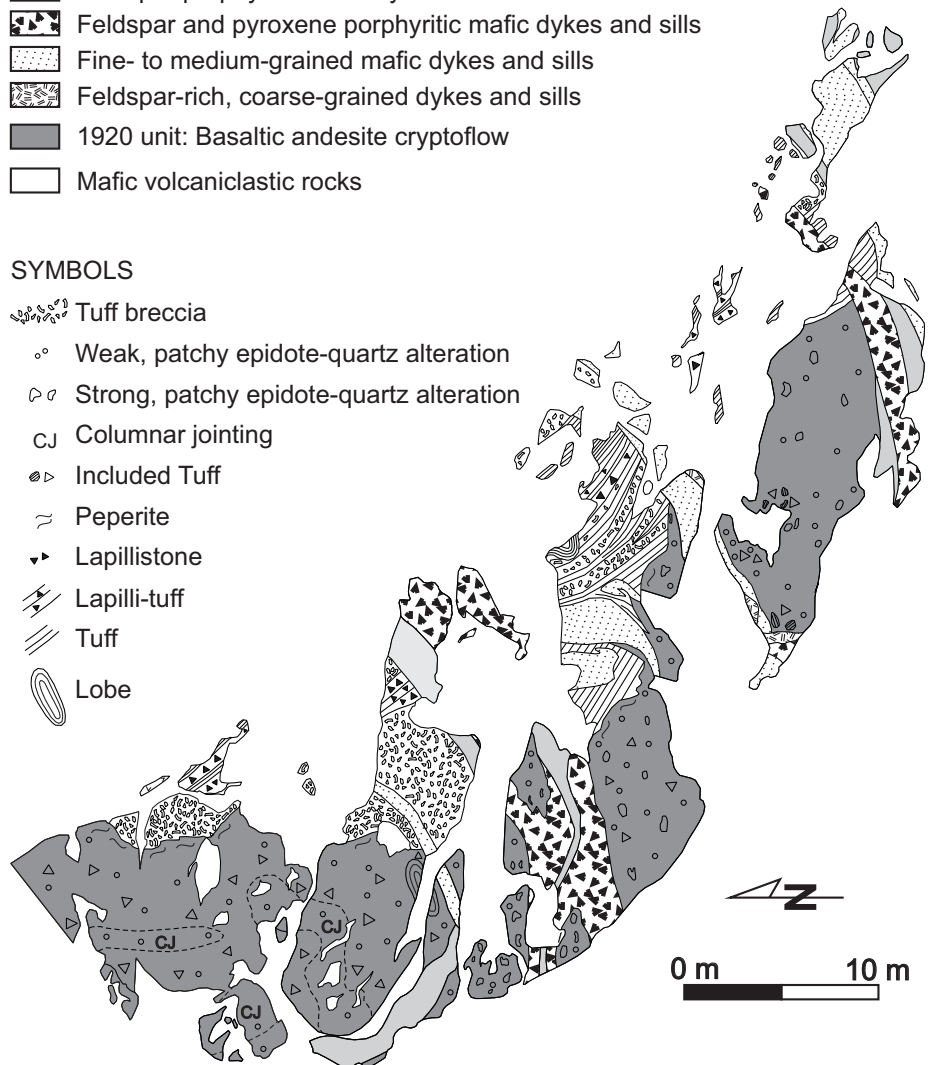


Figure 29. Geology of the 1920 unit at Stop 7.2 (after DeWolfe and Gibson, 2011).

are also present within the in situ breccia facies. The lobes have a 1-2 cm wide, dark grey chilled margin, a concentration of elongate quartz-filled amygdules in bands parallel to the lobe margins, and contain irregular to fluidal shaped inclusions (1-25 cm) of tuff.

The in situ breccia facies grades upwards into a peperite facies and this gradation is marked by a change from basaltic andesite fragments with a jigsaw puzzle fit and minor tuff between clasts, to smaller basaltic andesite fragments that are blocky to fluidal in shape within a tuff and hyaloclastite matrix. Locally the peperite is in sharp, but irregular contact with the host-volcaniclastic rocks consisting of tuff-breccia, or intercalated mafic lapilli-tuff and tuff.

Given that the 1920 member's different lithofacies, textures and structures, and their organization within the unit, including contact relationships, are similar to those observed in subaqueous mafic flows, it is referred to as a cryptoflow. The 1920 member was emplaced into volcanoclastic deposits that accumulated within a synvolcanic graben (DeWolfe and Gibson, 2011).

STOPS 7.3 to 7.5 - Post-Missi structures in the hinge of the Hidden Lake syncline

STOP 7.3: Sheared rhyolitic Tuff breccias of the Millrock member along the Upper Railway fault

Coordinates

UTM 6074830, 314395

Stop Description

The Upper Railway fault is the southern splay of the north-directed Railway thrust fault, which is one of several post-Missi, east-striking, D₄ thrust faults that cut across the hinge of the Hidden Lake syncline and that imbricated the VMS-hosting Millrock member.

As you walk towards a small cliff south of the railroad, the Upper Railway fault is well exposed on horizontal outcrop surfaces and at the base of the cliff as a 10 m wide shear zone that follows a horizon of polymictic tuff breccia and bedded tuff of the Millrock member (Figs. 28, 30). The tuffs are stratigraphically overlain by mafic

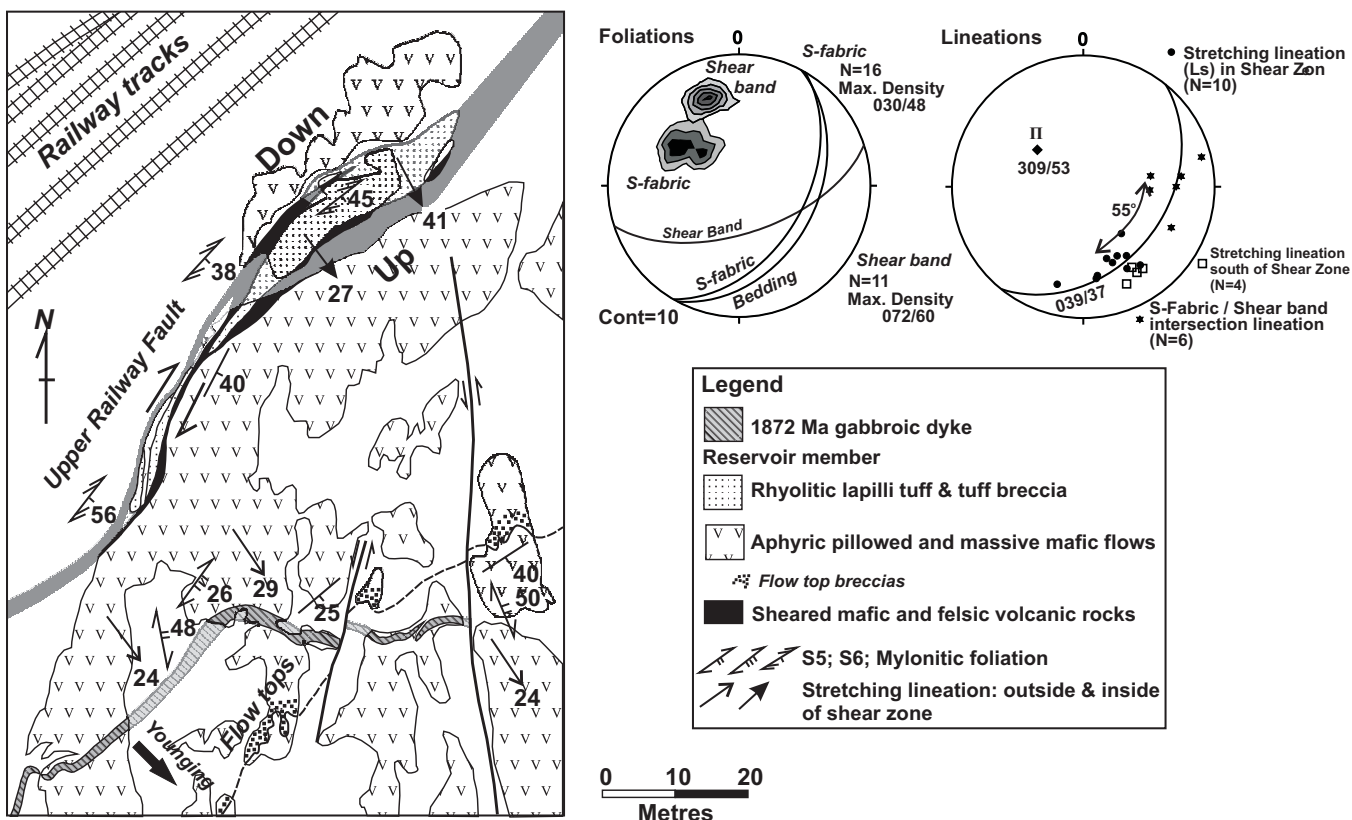


Figure 30. Details of the geology and structure of the Railway thrust faults at Stop 7.3 (after Lafrance et al., submitted).

massive flows of the Reservoir member and structurally underlain by the same unit. The shear zone is characterized by a strong mylonitic S-foliation and stretching L-lineation defined by biotite and by the flattening and elongation of the clasts. The lineation plunges 30° to 50° to the SE, down the dip of the NE-striking mylonitic fabric. Kinematic indicators along the shear zone are at first sight puzzling because they are best developed on horizontal outcrop surface. Dextral asymmetrical strain shadows around cascades of folded quartz veins and penetrative, closely-spaced (<1 cm), steeply-dipping, dextral shear bands overprint the mylonitic foliation. The intersection lineation between the shear bands and mylonitic foliation pitches within 55° of the down-dip stretching lineation along the mylonitic foliation plane (see stereonet plot in Fig. 30), suggesting that the Upper Railway fault originated as a dip-slip shear zone that was later reactivated as a dextral transcurrent shear zone during D₆.

Shear sense indicators related to the formation of the mylonitic S-foliation and down-dip stretching lineation are observed on vertical, west-facing, outcrop surface parallel to lineation and perpendicular to foliation. Along this surface, the S-foliation changes orientation in anticlockwise sense as it passes from tuff breccia layers to less competent, finer-grained, tuff layers, suggesting reverse, south-side-up thrust movement along the shear zone. The orientation of the stretching lineation along the shear zone is similar to that of the regional stretching lineation in the volcanic rocks south and north of the fault. The regional stretching lineation is interpreted as a composite structure that formed during D₄ thrusting and that was subsequently modified during D₅ along the limbs of the Hidden Lake syncline.

Climb up the cliff or hill and then walk for roughly 15 minute or 400 metres eastward along the crest of the hill.

STOP 7.4: Sheared 1840 Ma Phantom Lake dykes and 1872 Ma gabbroic dykes along the Upper Railway fault

Coordinates

UTM 6075075, 314820

Stop Description

Four hundred metres east of the last outcrop, the Upper Railway fault is further exposed along strike as an array of <5 m wide, S-dipping (50°-60°), shear zones that host strongly foliated dykes (Fig. 31). The shear zones have a strong mylonitic foliation and down-dip, SE-plunging, mineral stretching lineation, which are similar in style and orientation to those observed at the previous stop. The southernmost shear zone can be traced for 40 m in a north-easterly direction along the contact between the flow-top breccia of an underlying massive mafic flow and the polygonal-jointed base of an overlying massive flow. It then changes orientation and cuts across bedding to become parallel to an east-striking, andesitic to dacitic dyke (08-FF-12 in Fig. 31), which has a similar REE pattern as ca. 1840 Ma Phantom Lake dykes. Another dyke (08-FF-14), which is similar in major element and REE composition to ca. 1872 Ma gabbroic dykes, is deformed within a parallel shear zone along the northern edge of the outcrop. These overprinting relationships suggest that the Upper Railway fault formed either during or after the emplacement of ca. 1840 Ma Phantom Lake dykes and it therefore postdates the deposition of the older Missi cover sequence.

The dykes and mylonitic foliation are folded by Z-shaped F₆ folds with an axial plane, NNE-striking, S₆ cleavage and overprinted by dextral shear bands. This confirms that the D₄ Upper Railway fault was reactivated as a D₆ dextral shear zone as observed at the previous stop.

Walk 400 m in a south-easterly direction to the first occurrence of Missi conglomerate.

STOP 7.5: Missi wedge

Coordinates

UTM 6074955, 315300

Stop Description

The Missi wedge records the complete post-Missi deformation history of the Flin Flon mining district. It consists of shallowly-dipping Missi conglomerate and sandstone, which unconformably overlie steeply-dipping, pillowed,

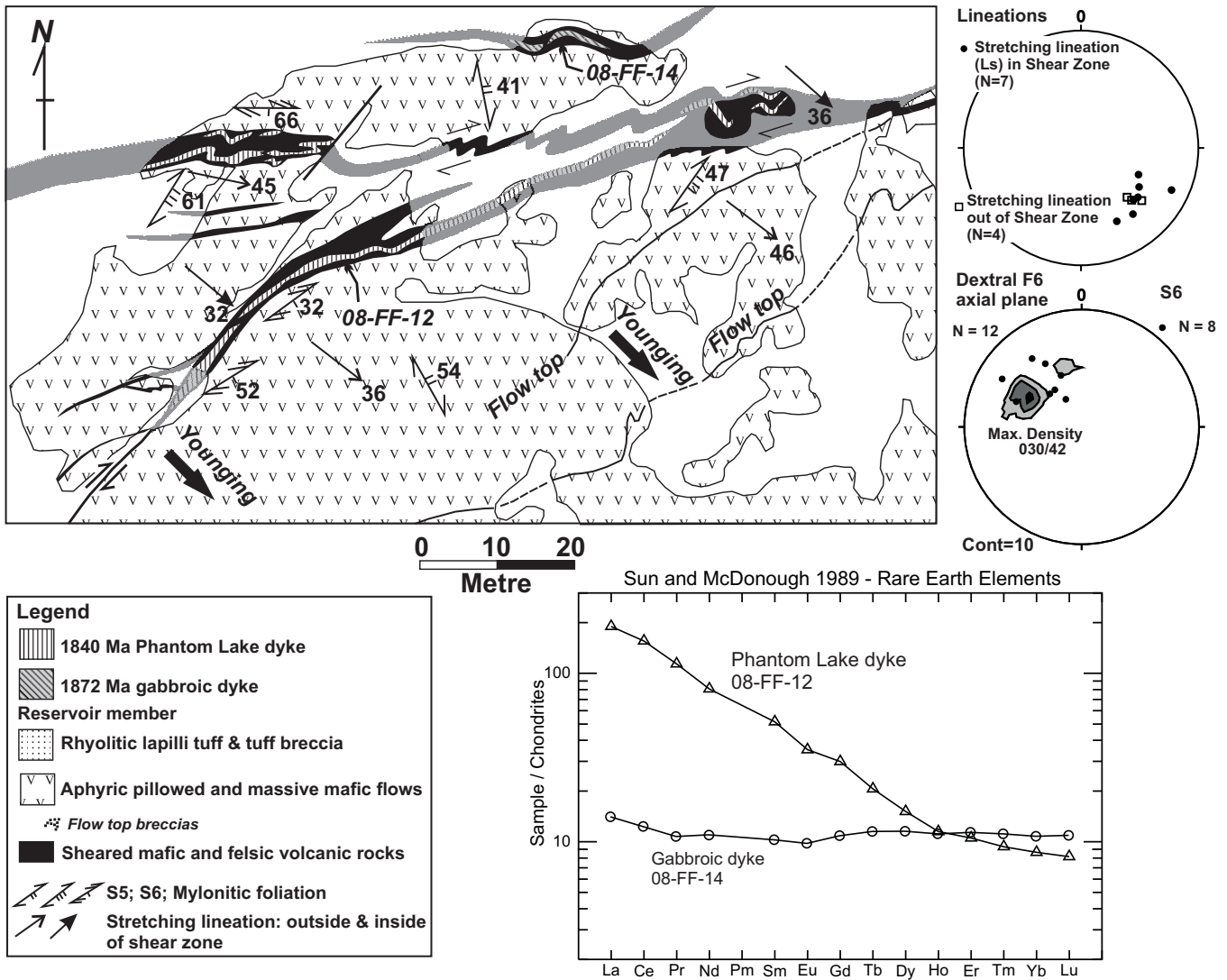


Figure 31. Geology and structure of the Upper Railway thrust fault at Stop 7.4 (after Lafrance et al., submitted).

mafic volcanic rocks along the east limb of the pre-Missi F2 Hidden Lake syncline. Both volcanic rocks and younger Missi rocks contain a SE-plunging stretching lineation, which is spectacularly expressed by strongly elongate pebbles in conglomerate. As its orientation is similar to that of the stretching lineation along the Upper Railway thrust fault and surrounding volcanic rocks, it is interpreted to have formed during the same D₄ event.

The Missi wedge was subsequently folded by upright F₅ folds and overprinted by their axial plane S₅ cleavage. F₅ fold axes are roughly parallel to the stretching lineation which acted as a structural anisotropy that controlled the nucleation of the folds. The folds and cleavage formed during an ENE-directed compression event (D₅) that produced the first regional NNW-striking cleavage (S₅) across the basement-cover rocks and that reactivated the limbs of the Hidden Lake syncline and other NW-striking planar structural anisotropies as dextral shear zones.

The folded and lineated Missi wedge is transected by an array of 0.5 m to 1 m thick, milky white, quartz veins (Fig. 32). The veins are subvertical and strike north-south. They have fibrous-textured margins, massive blocky centres, and chlorite laminae with a spacing of ~ 1 cm. Thin, 1-2 cm thick, fibrous, extensional quartz veins are oriented 30° to 40° clockwise of the thicker laminated veins. Striations along chlorite laminae within the thicker veins, the dextral rotation of the lineation and Z-shaped folding of the extensional veins next to the thicker laminated veins suggests that the thick laminated quartz veins formed as dextral shear veins. The attitude of the two sets of veins suggest that the maximum and minimum principal stresses, σ_1 and σ_3 , were horizontal and oriented parallel and perpendicular, respectively, to the extensional veins, and intermediate principal stress σ_2 was vertical and equal in magnitude to lithostatic pressure.

The veins formed during multiple repeated cycles subdivided in four stages similar to those suggested by Sibson et al. (1987) and Robert et al. (1995) for reverse faults. During pre-rupture **Stage 1**, σ_1 , σ_3 , and fluid pressure increase across the shear veins. If fluid pressure increases faster than the differential stress ($\sigma_1 - \sigma_3$), extensional veins form at low differential stress (i.e. $(\sigma_1 - \sigma_3) < 4T$, where T is the tensional strength of the rock) in the wallrocks of the shear veins. The formation of extensional veins buffers fluid pressures and allows the wallrocks adjacent to the shear veins to deform ductilely resulting in Z-shaped folding of the extensional veins and dextral dragging of the stretching lineation. During **Stage 2** rupture, further increases in the principal stresses and differential stress (i.e. $(\sigma_1 - \sigma_3) > \sim 8T$) acting across the shear veins result in rupture, slip reactivation of the shear veins, and the formation of striations along chlorite laminae. The transient sudden decrease of the principal stresses σ_1 and σ_3 acting across the shear veins produces a switch in the orientation of the maximum principal stress σ_1 from horizontal to vertical as the magnitude of the maximum horizontal stress drop below lithostatic pressure. During **Stage 3** sealing of the shear veins, the shear veins open as extensional fractures under vertical σ_1 and increasing fluid pressures due to the migration of fluids from the surrounding wallrocks into the open fractures. Since the fluid pressure within the open fractures is less than in the surrounding wallrocks, the decrease in quartz solubility at lower pressures causes quartz to precipitate as fibers and/or blocky equant grains sealing the open fractures. During post-rupture Stage 4, the depleted fluid pressure and lower stresses adjacent to the shear veins are slowly restored as Stage 4 grades into Stage 1.

The shear veins are offset and deformed within late NNW-striking faults bounding the Missi wedge. The veins underwent anticlockwise rotation within these fault zones and are fringed by sinistral drag folds while other narrow quartz veins are offset by sinistral shear bands. Because the shear veins cut across older D_4 and D_5 structures, the bounding NNW-striking faults are interpreted as sinistral D_6 structures. The attitude of the S_6 cleavage, which is best observed at the previous stop, suggests that the compression direction was roughly ESE-WNW during D_6 . Thus during D_6 compression, the E- to NE-striking Upper Railway fault was reactivated as a dextral shear zone and NNW-striking contacts between volcanic and Missi rocks at the Missi wedge were reactivated as sinistral faults or shear zones.

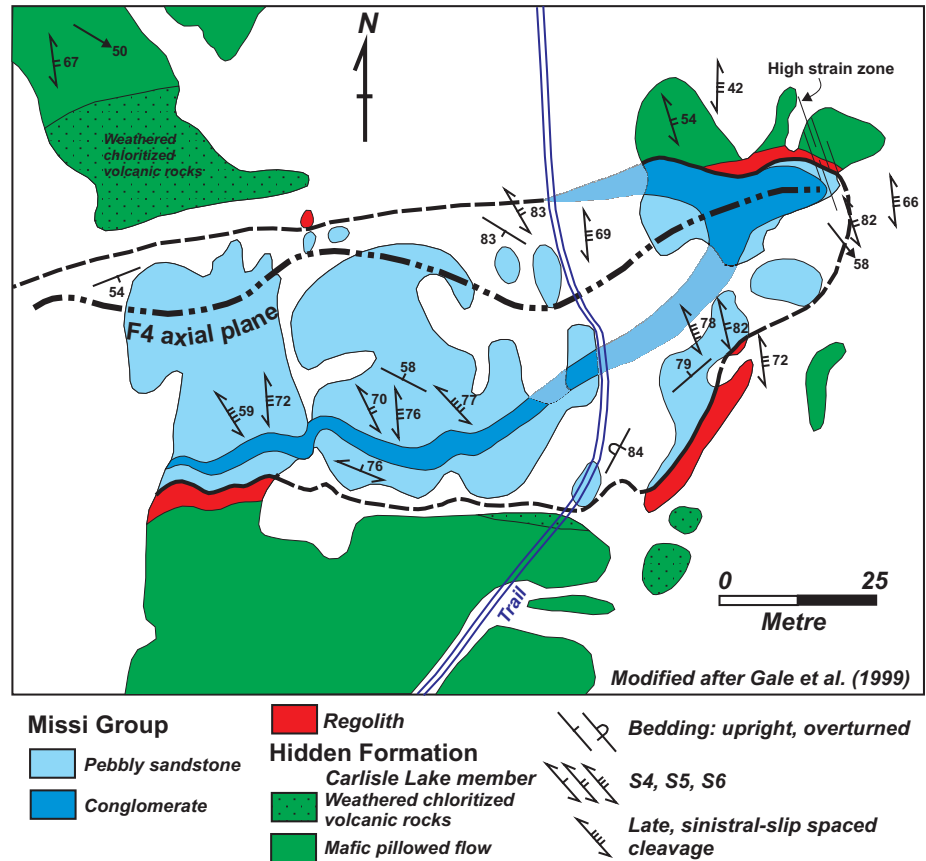


Figure 32. Geology and structure of the "Missi Wedge" area (after Lafrance et al., submitted).

DAY 5 A: FLIN FLON DISTRICT

STOP 8: 777 UNDERGROUND TOUR

Due to changing conditions underground it is not possible to exactly map out what stops and faces will be accessible on the day of the tour. What follows is a general description.

The 777 deposit was discovered in 1993 and was the third major deposit found within the Millrock member of the Flin Flon district. Drilling from underground in the Callinan mine was designed to test the down plunge extent of the Callinan ore body and to follow-up minor sulphide mineralization previously intersected in surface drill hole 4Q-64. The deposit was named after the discovery hole, diamond drill hole CX-777, which provided the first major intersection of the new orebody. The 777 deposit is situated between 900 and 1600m below the city of Flin Flon.

The 777 Mine is currently accessed via a five compartment production shaft which hosts twin 16.5 tonne production skips, a 100-man main cage for men and materials, main cage counter weight and an auxiliary hoist for moving up to 6 men. This main shaft is 1540 m deep and is 6.7 m in diameter. The shaft has five main shaft stations, with an internal ramp linking all infrastructure. The 777 North Mine Project is currently under construction, this project will provide a ramp from surface and 300 tons per day of additional mill feed. 777 hosts 21.9 Mt and is projected to produce a further 1.49 million tonnes grading 2.07g/t Au, 27.88g/t Ag, 2.80% Cu, and 4.20% Zn in 2011. It is expected to produce until 2020 from reserves of 13,553,610 tonnes grading 2.07 g/t Au, 28.77 g/t Ag, 2.36% Cu, and 4.51% Zn combined proven and probable reserves. (as of January 1, 2010.).

Table 2: Ore Reserves at the 777 Mine as of January 1, 2010.

| 777 Mine | Tonnes | Au g/t | Ag g/t | Cu % | Zn % |
|----------|-----------|--------|--------|------|------|
| Proven | 4,492,023 | 2.12 | 25.92 | 3.23 | 3.76 |
| Probable | 9,061,587 | 2.05 | 30.18 | 1.94 | 4.88 |

Mine Geology

The ore is hosted in rhyolitic and basaltic volcanic lithofacies of the Millrock Member of the Flin Flon formation. Basaltic flow and intrusive lithofacies of the overlying Hidden formation occur in the hanging wall to the deposit (Figs. 33 and 34). At 777 the Millrock member is subdivided into 4 map units (Fragmental ‘Andesite’, Chlorite Schist, Quartz Porphyry Rhyolite, and Mafic/Felsic Tuffs). Andesite is a mine term used for the light coloured, typically altered, effusive volcanics that geochemically are classified as basalts. Lithofacies within each of these mine units, and the overlying Hidden formation are described below.

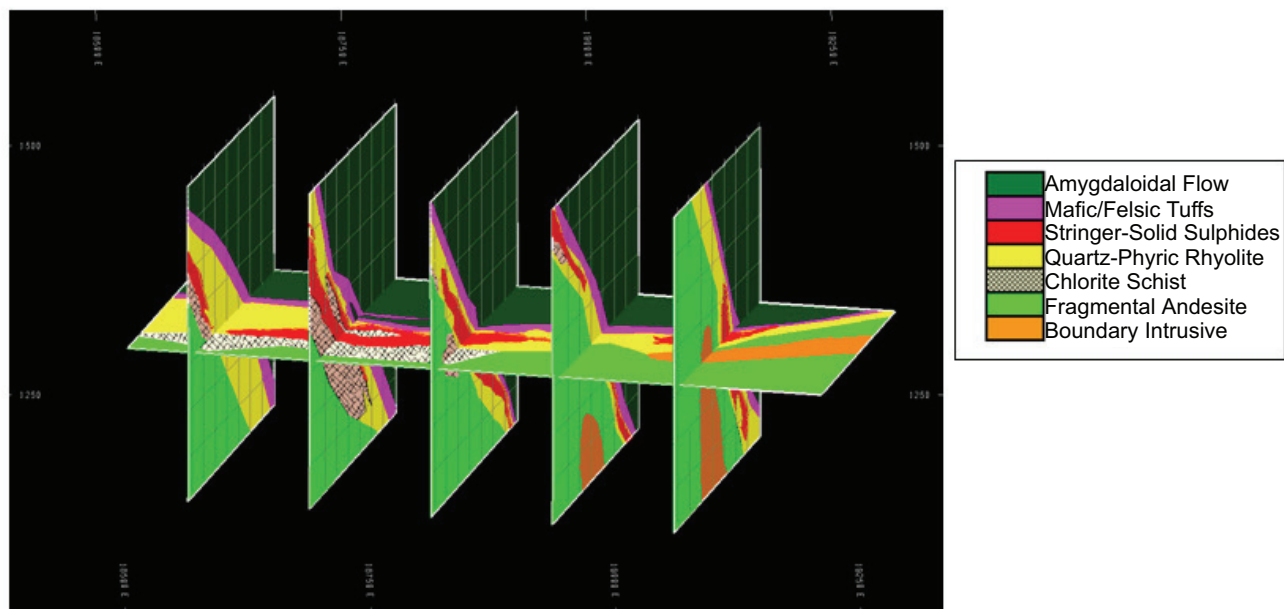


Figure 33. Generalized 3D Geology of the 1262m level of the 777 Deposit. Fragmental andesite, quartz-porphyry rhyolite, and tuffs of the 1.89 Ga Millrock member are upward facing and steeply east dipping. Amygdaloidal mafic flows of the ca. 1.88 Ga Hidden Formation lie in the hangingwall. Footwall ‘pipe’ alteration defined by the chlorite schist lies underneath the ore body and is now tabular in shape due to superimposed multiple deformation phases. Younger 1.85 Ga gabbroic intrusions of the Boundary Intrusive suite occur lie in the footwall.

777 1082mL DEVELOPMENT PLAN GEOLOGY WITH CURRENT MINE WORKINGS

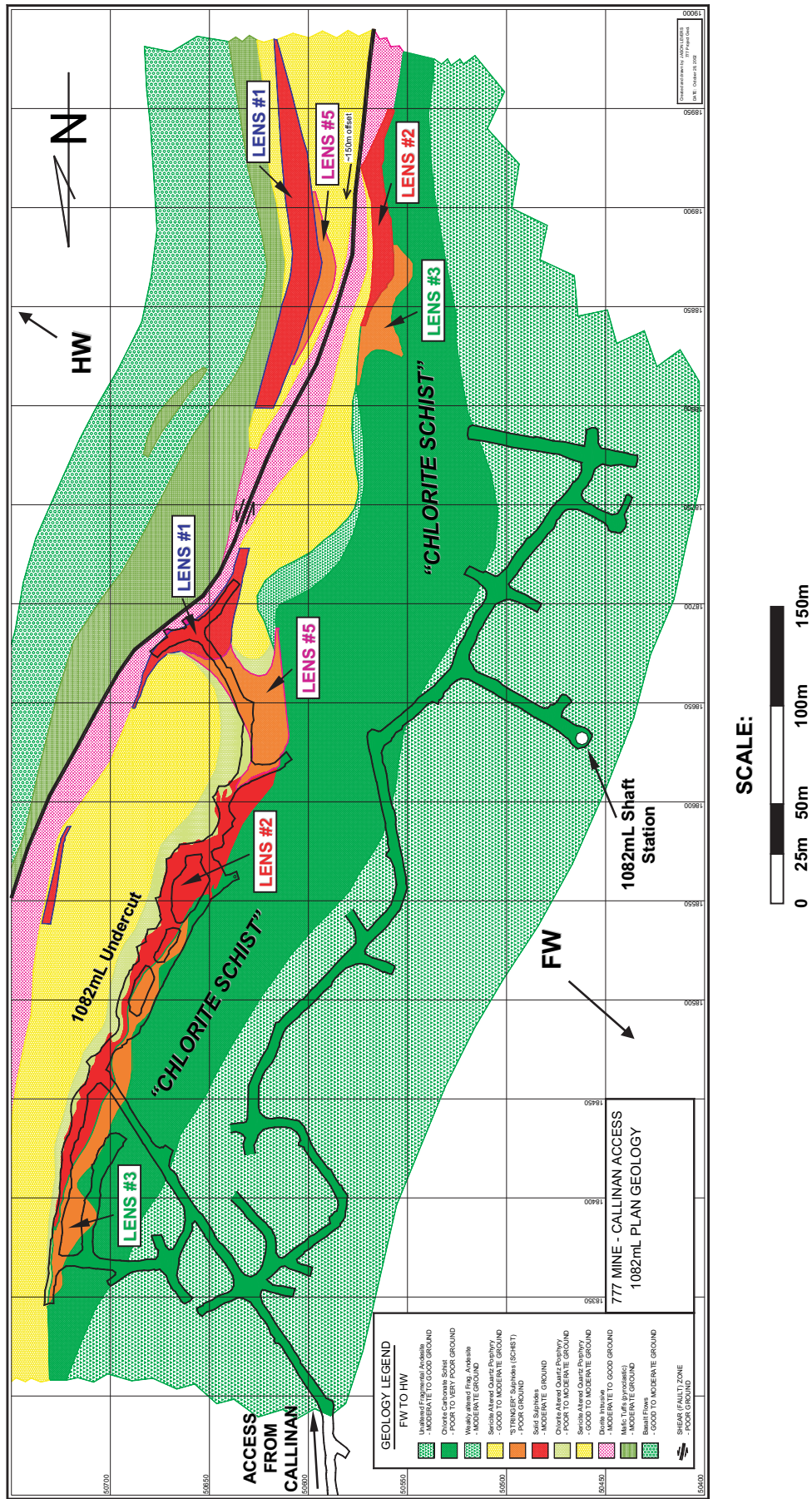


Figure 34. Geological map of the 1082 m level, including Stop #1 and mine map units

The “Fragmental Andesite unit” consists of dark green, fine-grained to aphanitic, amygdaloidal aphyric and sparsely feldspar phyric basalt clasts within a finer-grained, light to medium green basaltic matrix (Fig. 34). The basalt clasts are sub angular to well rounded, and range in size from 1-10 cm. The “Chlorite Schist unit” consists of near massive chlorite with sections of very strongly foliated and chloritized mafic and felsic volcanoclastic lithofacies (Fig. 34). It has a pronounced schistose fabric. Locally this unit contains pyrrhotite, chalcopyrite, magnetite mineralization, and it occurs only within the footwall to the 777 deposit. Sulphide Zones 15, 50, and 70 occur in this unit. The Chlorite schist unit is interpreted to be the hydrothermally altered equivalent of the Fragmental Andesite unit (locally the Quartz Porphyry Rhyolite unit) and, as such defines the footwall alteration pipe to the 777 deposit. Its stratabound nature, with respect to the strata, is interpreted to result from transposition during deformation.

The ore is hosted in the “Quartz Porphyry Rhyolite (QP) unit” (Fig. 34). The QP unit consists of coherent and volcanoclastic lithofacies. The volcanoclastic lithofacies contain subangular to subrounded fragments of QP in a finer-grained matrix that also contains quartz crystals. The massive sub units and the matrix material consists of aphanitic to very fine grained rhyolite with up to 10% blue to clear quartz eyes with trace plagioclase phenocrysts. Minor to pervasive chlorite and sericite alteration is present throughout. The “Mafic/Felsic tuff” unit consists of mafic, and lesser felsic tuff and volcanoclastic lithofacies that conformably overlies the QP unit (denoted as “Tuffs” in Fig. 34). The mafic (and lesser felsic) tuff lithofacies consists of massive, thick to medium bedded tuff and thinly bedded to laminated tuff. The volcanoclastic lithofacies contain lapilli-sized clasts of QP rhyolite, chlorite and or sericite altered QP rhyolite, amygdaloidal and massive sulphide in a finer-grained, mafic tuff-sized matrix. The Tuffs unit marks the top of the Millrock member. The “Flow unit” marks the base of the conformably overlying Hidden formation. It consists of a coherent basalt lithofacies that is fine-grained to aphanitic, aphyric, massive and distinctly amygdaloidal (up to 15% white amygdules filled with quartz and carbonate). Plagioclase and mafic phenocrysts occur locally as do epidote-quartz alteration patches. The Flow unit is interpreted to consist of basaltic flows and sills.

The Massive Sulphide

The 777 ore zones are divided into North, South and West Zones. All 3 zones occur within the same stratigraphic interval and are associated with the same lithofacies as described above but the West zone lies within a lower thrust slice. On average, the sulphide lenses strike 010° and dip to the east at 45° . All zones have a relatively shallow plunge that trends at -35° towards 140° . Horizontal widths through the deposit range from 2.5 to 70m in thickness. Thicker widths are observed where two or more of the ore lenses overlap. There are a total of seven distinct sulphide lenses within with the 777 deposit. Zones 10, 15, 20 and 30 occur in the North Zone, while Zones 40, 50, 60, and 70 occur in the South Zone. The sulphide lenses have been distinguished on the basis of grade and ore type, as well as their spatial location. Zone 10 contains variable concentrations of pyrrhotite, pyrite, and chalcopyrite. Locally, minor sphalerite, arsenopyrite, chalcocite, and chlorite are present. Zones 15, 50, and 70 are hosted within the Chlorite Schist unit. They generally contain pyrrhotite, and chalcopyrite, with minor amounts of sphalerite, pyrite, arsenopyrite, and magnetite. Zones 30, 40, and 60 are Zn rich (High Zinc Lens) and contain variable concentrations of pyrite, sphalerite, and chalcopyrite. Locally, minor pyrrhotite, magnetite, and arsenopyrite are present.

Underground Tour

A number of stops are planned on the tour to showcase each of the main underground map units, the sulphide lenses themselves and the some of the major structures, including the thrusts (Fig. 35). Where stops occur and specific details will be finalized in the days before the field trip depending on mine conditions and scheduling.

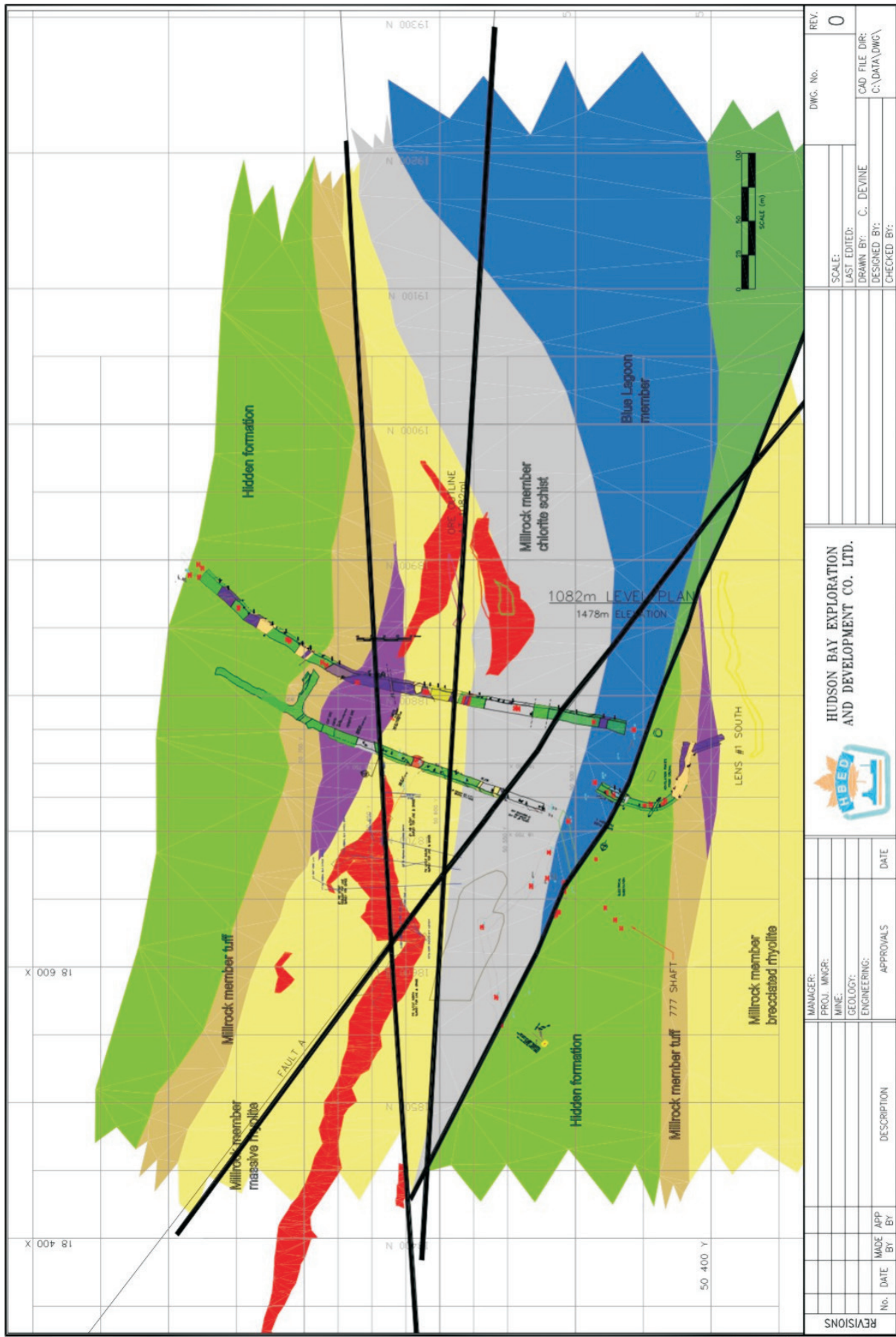


Figure 35. Thrust fault placing Blue Lagoon footwall lithofacies overtop of Hidden formation basalts, 1080 m level. Photo, mapping by C. Devine, HBED.

STOP 9: HANGING WALL TO THE SCHIST LAKE AND MANDY ORE BODIES

The Schist Lake and Mandy VMS deposits are located on the western edge of the Northwest Arm of Schist Lake, approximately 4 km southeast of the town of Flin Flon, and are currently inactive (Fig. 4). Field observations suggest a major, synvolcanic structure is present in the rocks structurally overlying the Schist Lake and Mandy deposits and is defined by the following: a) an abrupt lateral change in lithofacies from dominantly volcanoclastic in the south to dominantly flow in the north, b) a synvolcanic dyke that transitions upwards into a thin pillowed flow along this structure, and c) the presence of a megabreccia (south side) and megapillows (north side) proximal to this structure lower in stratigraphy and a spatter rampart deposit higher in stratigraphy (DeWolfe, 2009). The megabreccias, megapillows and spatter rampart are all indicative of a vent proximal environment. The synvolcanic structure most likely acted as both a magma and fluid pathway whilst accommodating movement associated with both primary subsidence, related to volcanism, and later deformation.

STOP 9.1: Lava tubes and megabreccias within the Hidden formation: Evidence for vent proximity

Coordinates

UTM 6069380, 317125

***Hazards:** Very steep outcrop. Use caution if approaching the southeastern margin of the large outcrop to the south. A moderate level of fitness is required to reach this field stop as the ski trail is quite steep in places (30 m of elevation gain from road to field stop).*

Stop Description

As you approach the outcrops from the ski trail you will notice that there is a marked topographic feature, a narrow gully, separating a large outcrop to the north from a larger outcrop to the south. The northern outcrop contains a large basaltic lava tube surrounded by basaltic pillows, whilst the southern outcrop is dominated by breccias with a thin pillowed flow on top (Fig. 36). This lateral facies transition is abrupt and marked by an aphyric mafic body, approximately 1-2 m wide, that locally cross cuts bedding lower in the stratigraphy, and changes orientation becoming parallel to bedding higher in the stratigraphy. This change in orientation corresponds with a change from massive to pillowed facies; therefore, this unit is interpreted to represent an aphyric mafic dyke, cross cutting the megabreccia and feeding a thin, pillowed flow that was extruded on top of the breccia. This dyke, because it separates the megabreccia and other volcanoclastic units to the south from the basaltic flows to the north, is interpreted to have been emplaced along a synvolcanic fault, which marks the northern boundary of a subsidence structure into which the megabreccias and other volcanic debris flows were deposited. Although there is evidence of minor shearing along this dyke, pillows are not truncated, and the vertical offset of the underlying plagioclase crystal-rich volcanoclastic unit along this structure is on the order of only a few metres, suggesting that this is a primary volcanic fault that has been reactivated by later deformation.

STOP 9.2: Spatter rampart and synvolcanic dykes within the Hidden formation: Evidence for vent proximity

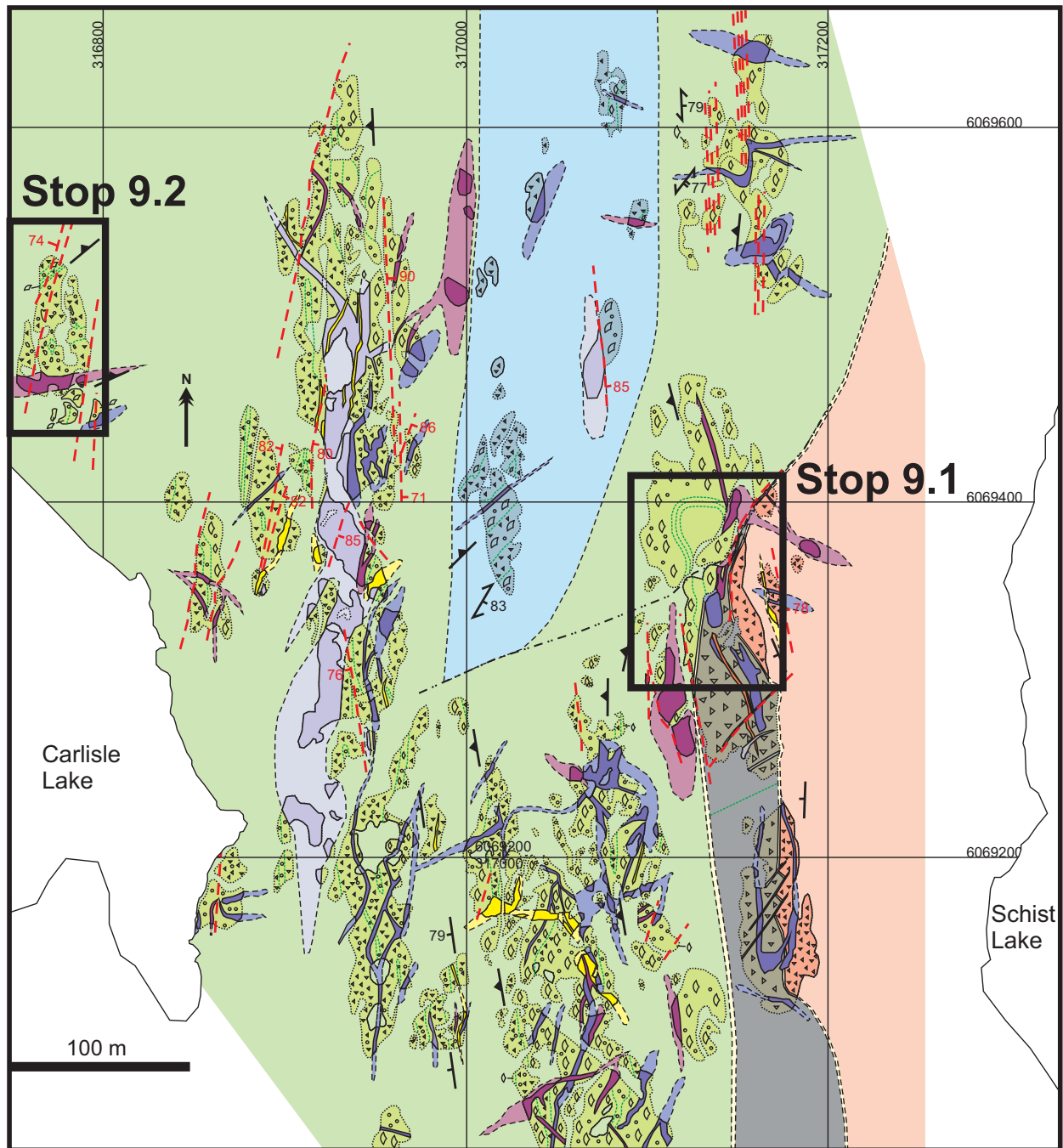
Coordinates

UTM 6069480, 316780

Stop Description

Coarse, fluidal breccias with minor (<10%) thin pillowed and massive flows extend approximately 450 m along strike, and have maximum thickness of 90 m. The breccia is clast supported with a reddish-brown, fine-grained tuff matrix, and is commonly intruded by thin massive to pillowed aphyric mafic sills, which can be observed on the northern tip of this outcrop.

This fluidal breccia unit is interpreted to be a spatter deposit that lies above the synvolcanic structure observed at the last stop. A synvolcanic dyke, utilizing a similar synvolcanic feature occurs on the western margin of this outcrop. This synvolcanic dyke is ~2 m wide and 'sills-out' horizontally into the surrounding spatter deposit. Where the dyke propagates laterally, parallel to bedding, spatter or bombs, amoeboid blocks of aphyric, quartz-amgydaloidal basalt, are larger and more abundant proximal to the dyke (vent) and decrease in size and number away from the dyke (vent).



LEGEND

- | | | |
|--|---|---------------------------------------|
| Felsic dykes | Plagioclase porphyritic basalt | Outcrop |
| Aphyric mafic dykes and sills | Aphyric basalt | Lithological contact (known/inferred) |
| Aphyric intermediate sills | Mafic tuff breccia to megabreccia - north of facies contact | Facies contact (known/inferred) |
| Plagioclase- (+/- pyroxene)-phyric mafic dykes and sills | Plagioclase crystal-rich volcaniclastic unit | Synvolcanic fault (interpreted) |
| | | Fault |
| | | Bedding |
| | | Flow contact (top known) |

Figure 36. Geology and structure of the Hidden formation along the east limb of the Hidden Lake Syncline showing the location of Stops 9.1 and 9.2 (after DeWolfe, 2009).

STOP 10. CLIFF LAKE PLUTON

Based on a U-Pb zircon age of 1859 +/- 22 Ma, the Cliff Lake Pluton was originally interpreted as single, multi-phase quartz tonalite – quartz gabbro intrusion that was younger than host volcanic strata of the Hooke Lake Block (1891 +/-17 Ma) and to VMS hosting strata of the Flin Flon Block (approx 1888 +/- 2 Ma) (Bailes and Syme; 1989; Kremer and Simard, 2007; Simard 2007). However, a recent U-Pb zircon age for the quartz gabbro phase along the west margin of the intrusion yielded an age of 1888 +/- 1 Ma, within error of the age of strata within Flin Flon and Hooke Lake Blocks (Rayner et al., 2010). The Cliff Lake Pluton and Hooke Lake Block are now divided into two intrusions and two blocks, the Western Hooke Lake Block and the Eastern Hooke Lake Block, that are separated by the Hooke Lake Fault (Figs. 4 and 6). Based on recent U-Pb zircon ages, volcanic strata of the western Hooke Lake block are now interpreted to be “time equivalent” to strata of the Flin Flon Block. The younger, eastern quartz leucotonalite intrusion was emplaced into volcano-sedimentary strata of the Eastern Hooke Lake Block, whereas the older, western intrusion, consisting of quartz tonalite and quartz gabbro phases was emplaced into the Western Hooke Lake Block, and into strata of its own volcanic pile during a period of magmatic resurgence that followed cauldron subsidence and Flin Flon VMS deposit formation (Gibson et al., 2009b; submitted). The west or upper margin of the intrusion is, in part, enveloped within a high temperature (?) reaction zone.

STOP 10.1: Contact between the Cliff Lake Pluton and the Hooke Lake Block

Coordinates

UTM 6075241, 317788 and UTM 6075242, 317758

Stop Description

Stop 10.1 is at the contact between the quartz tonalite phase (UTM 6075241, 317788) of the Cliff Lake Pluton and a pillowed flow (UTM 6075242, 317758) of the Hooke Lake Block (Fig. 37). The tonalite contains numerous mafic xenoliths that define a crude layering and near the contact the tonalite is weakly chlorite and epidote altered. The adjacent pillowed flow to the west is pervasively silicified and the silicification is overprinted by epidote-quartz and a later chlorite alteration that is localized along east-west trending shears and fractures. The silicification zone extends for several 100 metres from the intrusion-volcanic contact, but the epidote-quartz and chlorite alteration are restricted to within 10s of metres of the contact.

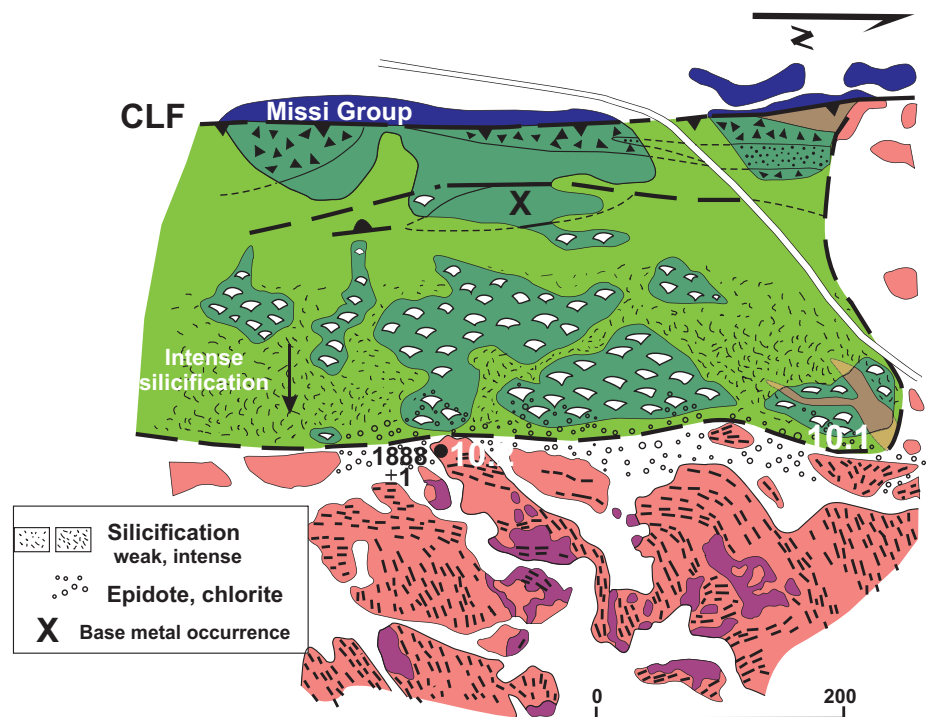


Figure 37. Contact between the Cliff lake Pluton (western phase) with a pillowed flow lithofacies within the Western Hooke Lake Block showing the Location of Stop 10 (after Gibson et al., 2009b). Map units are as follows: the pink and purple = tonalite and quartz-gabbro phases of the Cliff Lake Pluton, and the black dashed lines denote aligned concentration of mafic xenoliths; the darker green = basaltic lithofacies, with the white pillowed symbols = pillowed lithofacies, the black triangles = volcaniclastic lithofacies and the uniform green = massive lithofacies,; the dark blue = Missi Group sedimentary strata.

STOP 10.2: Contact between the Cliff Lake Pluton and the Hooke Lake Block

Coordinates

UTM UTM 6075010, 317771

Stop Description

Stop 10.2 is the same contact as at Stop 10.1 except here a highly fractured and epidote –quartz and chlorite altered quartz gabbro, along with the quartz tonalite (locally with Fe-staining) is in contact with the silicified pillowed

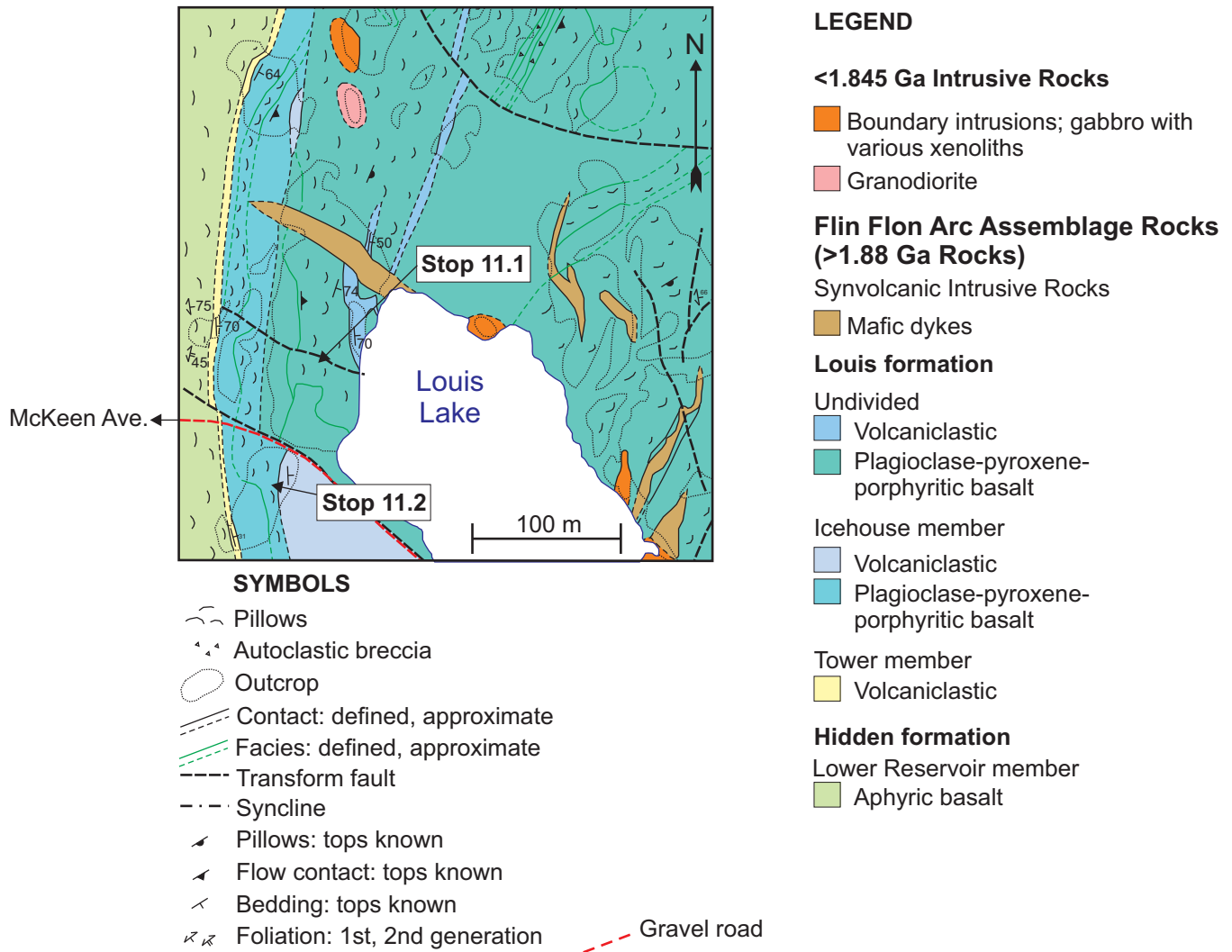


Figure 38. Geology and structure of the Louis formation (Ice House member at Louis Lake) showing the location of Stops 11.1 and 11.2 (after DeWolfe, 2008).

flows. The latter are pervasively epidote-quartz and chlorite altered for several metres from the contact. A pegmatitic phase of the quartz gabbro at this locality yielded the 1888 +/- 2 Ma U-Pb zircon age (Fig. 37). The locations of the next two stops are shown in Figures 4 and 38 and descriptions are from DeWolfe (2008).

STOP 11. ICEHOUSE MEMBER, LOUIS FORMATION, NEAR LOUIS LAKE

STOP 11.1: Massive and pillows lava flows of the Icehouse member

Coordinates

UTM 6071565, 315460

Stop Description

The Louis formation consists, from oldest to youngest, of the Tower member, Icehouse member and undivided plagioclase and pyroxene phyrific basaltic flows (Fig. 7). On this outcrop there are two lava flows exposed (Fig. 38). All units in the area strike north and face east. The flows are part of the undivided portion of the Louis formation. The western most flow is massive and its flow-top marked by an increase in quartz amygdule content from 5 to 30% (<1–5 cm) over its upper 5 m. The contact with the overlying pillowed flow is sharp, but irregular. Pillows are <1 m in size, have thin (<=2 cm) selvages, and contain 5–10% quartz amygdales (<1 cm). Finely laminated, epidote-quartz-altered mafic tuff commonly occurs between the pillows. At the southern edge of this outcrop there is

domain of massive lava that is in sharp contact, along strike, with the pillowed flow, but it does not truncate the pillows (Fig. 38). To the west this massive domain is in sharp contact with the lower massive flow. The margin of the massive domain shows a decrease in grain-size suggesting it is a chilled contact. This domain of massive basalt, which is not laterally continuous, is interpreted to be a lava tube, feeding the surrounding basaltic flows. Walk west to the next outcrop. This outcrop consists of a massive basaltic flow overlain by a pillowed basaltic flow of the Icehouse member (Fig. 38). Continue to the west where the next outcrop is a small exposure of mafic tuff and lapilli tuff beds of the Tower member overlying aphyric basalt of the Hidden formation (Fig. 38).

STOP 11.2: Pillow lavas, pillow breccia and overlying volcanoclastic rocks of the Icehouse member

Coordinates

UTM 6071468, 315430

Stop Description

At the western edge of this outcrop is the mafic tuff – lapilli-tuff of the Tower member that is overlain by massive and pillowed lava flows of the Icehouse member. The massive lava flow is in sharp contact with the overlying pillowed lava flow (Fig. 38). The upper margin of the pillowed flow is irregular and broken, with a gradation over a distance of 1 m from intact pillows to pillow breccia to an overlying, normally graded, crudely bedded, heterolithic volcanoclastic unit (Fig. 38). At the base of the volcanoclastic unit there is a large block (2 m x 0.75 m) of bedded tuff with very irregular margins. Overall, the volcanoclastic unit contains 50% lapilli-sized, round, aphyric to plagioclase and pyroxene phyric basalt clasts. The tuff-sized matrix is reddish brown and contains abundant plagioclase (20–25%) and pyroxene (15%) crystals. The lower 5 m of the unit is a clast supported tuff breccia bed, containing 20% large blocks (6.4–50 cm) of plagioclase and pyroxene phyric, quartz amygdaloidal basalt and 5–10%, angular to subrounded blocks of aphyric rhyodacite. The next 3–5 m marks a transition from a clast-supported tuff breccia to a matrix-supported tuff breccia bed. In this interval, there are only 5% large plagioclase-pyroxene phyric pillow fragments (>10 cm), 3–5% aphyric rhyodacite clasts (rounded and ≤15 cm), and 10–20% lapilli-sized, aphyric to plagioclase-pyroxene phyric basalt fragments. The upper 10 m of the volcanoclastic unit is a matrix supported lapillistone bed that contains 30% round, lapilli-sized basalt clasts and 5–10% subrounded, aphyric rhyodacite clasts in a mafic, tuff-sized matrix. The poorly sorted, massive to crudely bedded tuff breccia to lapillistone unit is interpreted to have been emplaced as a mass flow that was restricted to a localized basin (DeWolfe, 2008).

VOLCANOLOGICAL AND STRUCTURAL SETTING OF PALEOPROTEROZOIC VMS DEPOSITS IN THE CHISEL-LALOR LAKES AREA AT SNOW LAKE

Introduction

Located at the east end of the exposed Paleoproterozoic Flin Flon Domain (Intro belt figure), the Snow Lake area is dominated by 1.84–1.81 Ga fold-thrust-style tectonics and by a southwest-verging allochthon of volcanic rocks (Snow Lake arc assemblage). The area comprises a lithologically and structurally diverse sequence of deformed and metamorphosed volcanic, sedimentary and intrusive rocks, and contains 8 of the belt's 27 producing and past-producing base metal mines. These include the Chisel North Zn-Cu mine, 7 past-producers, and the newly discovered Lalor Lake deposit.

The volcanogenic massive sulphide (VMS) deposits occur in an approximately 6 km thick volcanic succession (Figs. 39, 40 (Snow Lake arc assemblage) that records a temporal evolution in geodynamic setting from a 'primitive arc' (Anderson sequence), to a 'mature arc' (Chisel sequence) and then to an 'arc-rift' (Snow Creek sequence) (Bailes and Galley 1999). The VMS-hosting Anderson and Chisel sequences contain evidence of intra-arc rifting. Evidence in the Anderson sequence this includes the occurrence of boninite, low-Ti basalt and isotopically juvenile rhyolite flows, an association that has been attributed in both modern and Phanerozoic arcs to high-temperature hydrous melting of refractory mantle sources in an extensional and/or proto-arc environment. According to Crawford et al. (1989), boninitic and refractory magmas are a reflection of zones of extremely high heat flow because, to form, they require high heat of fusion. This rock association has been linked with VMS deposits (Swinden 1996) and this may reflect a common genetic affiliation with zones of high heat flow, rifting and attendant increase in fluid circulation and geothermal activity (Bailes and Galley, 1999, and references therein). In the Chisel sequence evidence is indirect, and includes voluminous volcanoclastic detritus; prominent synvolcanic dyke sets; and the local presence of highly fractionated, differentiated magma series. VMS deposits in both sequences are spatially associated with juvenile rhyolite complexes, synvolcanic intrusive rocks (dominated by two large trondhjemitic bodies) and extensive areas of rocks that underwent synvolcanic hydrothermal alteration.

Structural History

Structural studies carried out in the Flin Flon Domain have identified deformation events spanning early accretion (1.88–1.87 Ga) to late tectonic continental

collisions (1.83–1.77 Ga; Lucas et al., 1996). Deformation events that would have accompanied the pre-1.85 Ga tectonic accretion and amalgamation have yet to be recognized in the Snow Lake area. The oldest recognized structures (D_1) in the area, best developed in successor arc supracrustal units such as the Burntwood Group sedimentary rocks, are <1.84 Ga in age. Four deformation events have been recognized in the Chisel-Anderson lakes area (D_1 – D_4 ; Krause and Williams, 1998). The first two (D_1 and D_2) are interpreted to result from the southwest tectonic transport of rocks from the Kisseynew Domain over the Flin Flon Domain (Krause and Williams, 1999) and are characterized by tight isoclinal folding and associated low-angle 'thrust' faults (e.g., McLeod Road Fault). The D_3 event is interpreted to result from northwest-southeast transpressional shortening that accompanied syn- to post-peak regional metamorphism (Connors et al., 1999). It is largely manifested by upright, open to closed F_3 folds (e.g., Threehouse Lake synform) and associated, steeply dipping faults (e.g., Berry Creek Fault). The D_4 structures are east-trending open upright folds that overprint F_3 folds (Connors, 1996; Krause and Williams, 1998).

VMS Mineralization in the Snow Lake Camp

VMS deposits at Snow Lake are subdivided into two distinct types: Cu-Zn-rich (Cu-Zn, Cu-Zn-Au) and Zn-Cu-rich (Zn-Pb-Cu-Ag) types. The Cu-Zn-rich deposits occur principally in the Anderson sequence and the Zn-Cu-rich deposits, the focus of this fieldtrip, occur in the Chisel sequence.

Cu-Zn-rich deposits in the Anderson sequence (Fig. 40) occur, almost entirely, within the Anderson-Stall and Daly rhyolite complexes. All of the past-producing deposits occur in the former rhyolite. The Anderson, Stall and Rod orebodies contain an aggregate 10.1 million tonnes of ore with an average grade of 4.15% Cu, 0.53% Zn, and averaged 1.5 g/t Au (Bailes and Galley, 1996).

Five Zn-rich VMS deposits (Chisel-Lalor VMS system) occur in the Chisel sequence, approximately 2 km stratigraphically above its base and at the contact between the Lower and Upper parts of the Chisel sequence. Chisel, Chisel North, Lost and Ghost contained an aggregate 10.6 Mt (production plus reserves) grading 0.42% Cu and 10.06% Zn, and between 30 to 60 g/t Ag and 0.4 to 1.7 g/t Au. Drilling so far on the newly discovered Lalor Lake deposit has defined an indicated base metal resource of 13.3 Mt grading 0.66% Cu, 8.87% Zn, 1.6 g/t Au and 24.9 g/t Ag with an inferred base metal resource of 4.8 Mt grading 0.58% Cu and 9.25% Zn, with 1.3 g/t Au and 26.2 g/t Ag, as well as an inferred precious metal resource of 5.4 Mt of 4.7 g/t Au, 30.6 g/t Ag with 0.47% Cu and

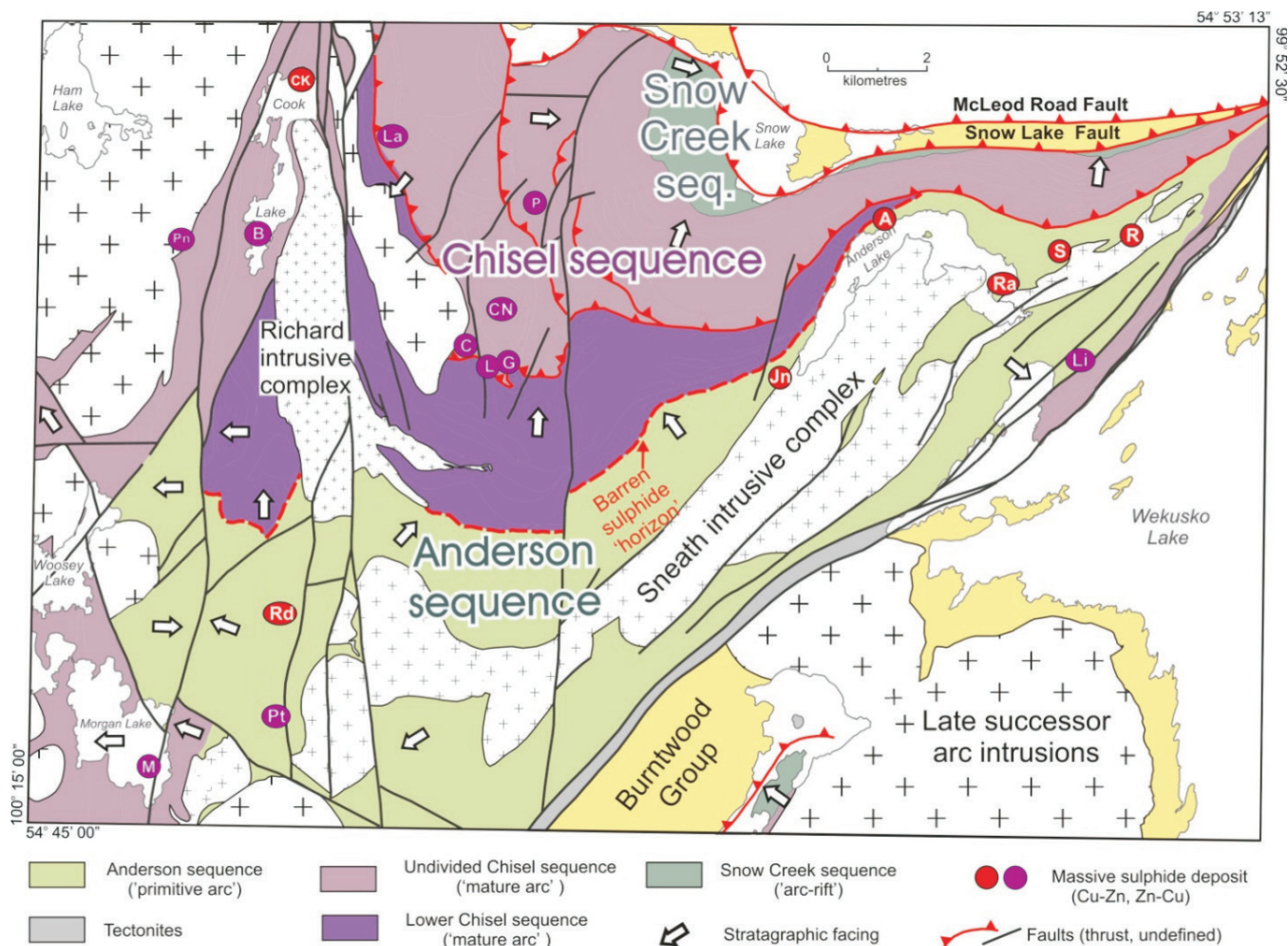


Figure 39: Plan view of the 1.89 Ga Anderson ('primitive arc'), Chisel ('mature arc') and Snow Creek ('arc-rift') sequences of the Snow Lake arc assemblage. The two large synvolcanic intrusive complexes, Sneath and Richard, belong to the Anderson and Chisel sequences, respectively. The ca. 1.84–1.83 Ga sedimentary Burntwood Group rocks are composed of detritus derived from volcanic and intrusive rocks of the Flin Flon Domain. Arrows show facing directions of supracrustal rocks. The late successor arc intrusive rocks truncate the ca. 1.84 Ga thrust faults (teeth) and are themselves cut by ca. 1.78 Ga normal faults (solid lines). Filled circles and ovals (red, Cu-Zn; purple, Zn-Cu) show distribution of VMS deposits: A, Anderson Lake; C, Chisel Lake; CK, Cook Lake (located just north of map boundary); CN, Chisel North; G, Ghost Lake; La, Lalore; Li, Linda; L, Lost Lake; M, Morgan Lake; Pt, Pot Lake; P, Photo Lake; Pn, Pen; Rd, Raindrop; R, Rod; Ra, Ram; S, Stall Lake. The 'Foot-Mud horizon' (thick red dashed line) is a pyritic, fine-grained volcanoclastic unit located at the contact between the Anderson ('primitive arc') and Chisel ('mature arc') sequences.

0.46% Zn (May 1, 2010). All five deposits overlie the Powderhouse dacite and local discrete rhyolite flow complexes. These deposits are characterized by dolomite that later regional metamorphism recrystallization has converted to coarse-grained calc-silicate assemblages similar to those commonly displayed by magmatic skarn deposits (Galley and Ames, 1998).

The Photo Lake VMS deposit is a Cu-Zn-Au massive sulphide mineralization within the upper Chisel sequence. It occurs within a thick section of rhyolite (Bailes and Simm, 1994). The current interpretation is that the Photo Lake VMS deposit occurs in the hangingwall structural panel to the Chisel-Lalore VMS system and may be part of a separate and unrelated VMS forming event (Bailes et al., 2009).

Regional-Scale Synvolcanic Alteration Zones associated with the Snow Lake VMS Deposits

The Snow Lake arc assemblage contain prominent zones of alteration that visibly affect approximately 25% of the volcanic strata and associated synvolcanic intrusions (Fig. 41). The alteration zones, formed by synvolcanic 1.89 Ga hydrothermal activity, were subsequently recrystallized during 1.81 Ga regional metamorphic episode and can be readily recognized by their unique metamorphic mineral assemblages that include centimetre-scale, euhedral crystals of chlorite, phlogopitic biotite, amphibole, muscovite, garnet, staurolite, andalusite, kyanite, sillimanite and gahnite. Three periods of robust hydrothermal activity are identified within the Snow Lake arc assemblage (Bailes and Galley, 1996).

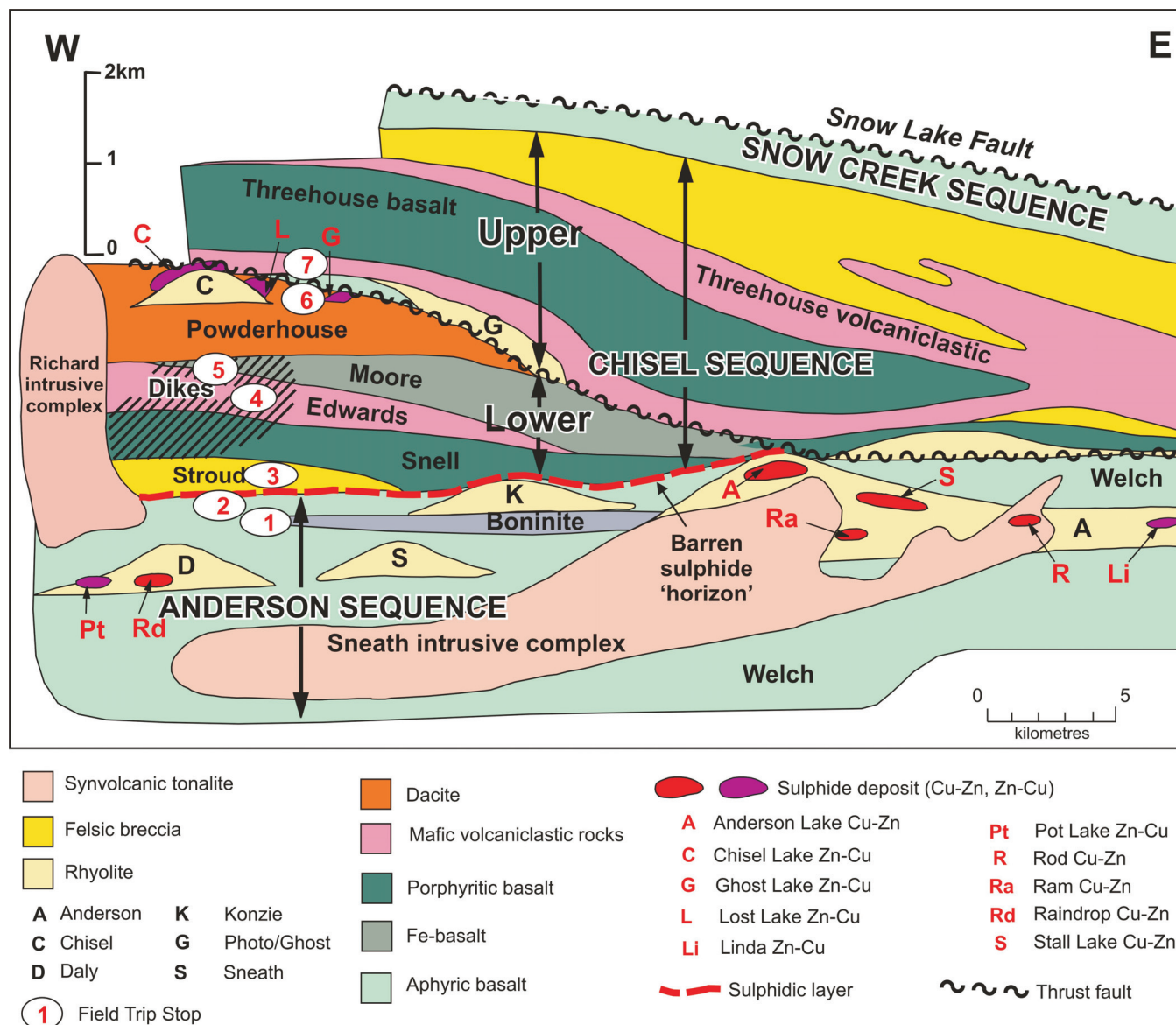


Figure 40. Schematic stratigraphic section showing the major rock formations of the Snow Lake arc assemblage after Bailes and Galley (in press). The modified from Bailes and Galley (1996, 1999).

The first, and oldest, (Fig. 41) is focused within the Anderson–Stall and Daly felsic extrusive complexes, and is interpreted to be genetically related to formation of the Anderson, Stall and Rod Cu-Zn VMS deposits, in the former complex, and the Raindrop and Pot Lake base metal occurrences, in the latter (Fig. 41). This hydrothermal activity also affected the underlying Sneath intrusive complex, most typically as ‘fracture-controlled’ zones of alteration, where it is interpreted to result from ‘collapse’ of the hydrothermal system into the subvolcanic intrusion as it cooled. Alteration caused by this hydrothermal activity includes both stacked, semi-conformable zones, 3–5 km long and as much as 1000 m in total thickness, and discordant alteration ‘pipes’ that commonly terminate upsection at known VMS deposits and occurrences. The alteration zones

are truncated by a late phase of the Sneath intrusive complex, which is considered evidence of the coeval nature of the volcanism, alteration and plutonism.

The second hydrothermal event took place at the end of Anderson sequence volcanism. This hydrothermal activity resulted in a 300–500 m thick zone of silica and epidote addition to Welch basalt at the top of the sequence (Fig. 41) directly underlying the ‘Foot-Mud tuff-exhalite’. Both the alteration and the Foot-Mud exhalite have the same strike length as the underlying Sneath subvolcanic intrusion.

The third hydrothermal event is located within Lower Chisel volcanic rocks (Fig. 41) and, in particular, with dykes of the ‘Powderhouse’ dacite and early phases of the Richard intrusive complex. Alteration, which is largely confined to the Edwards mafic vol-

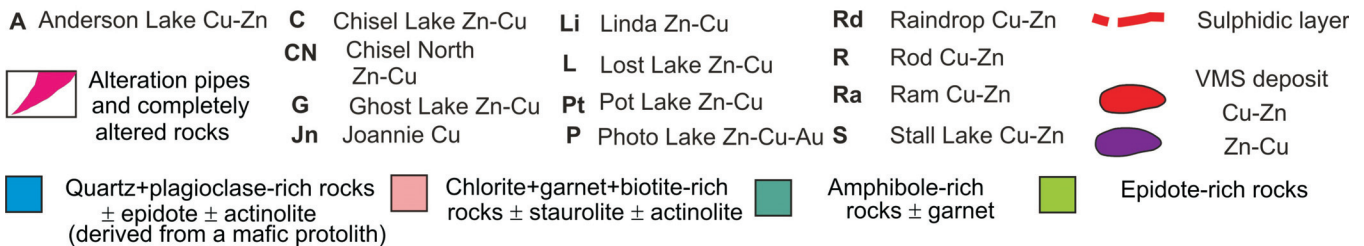
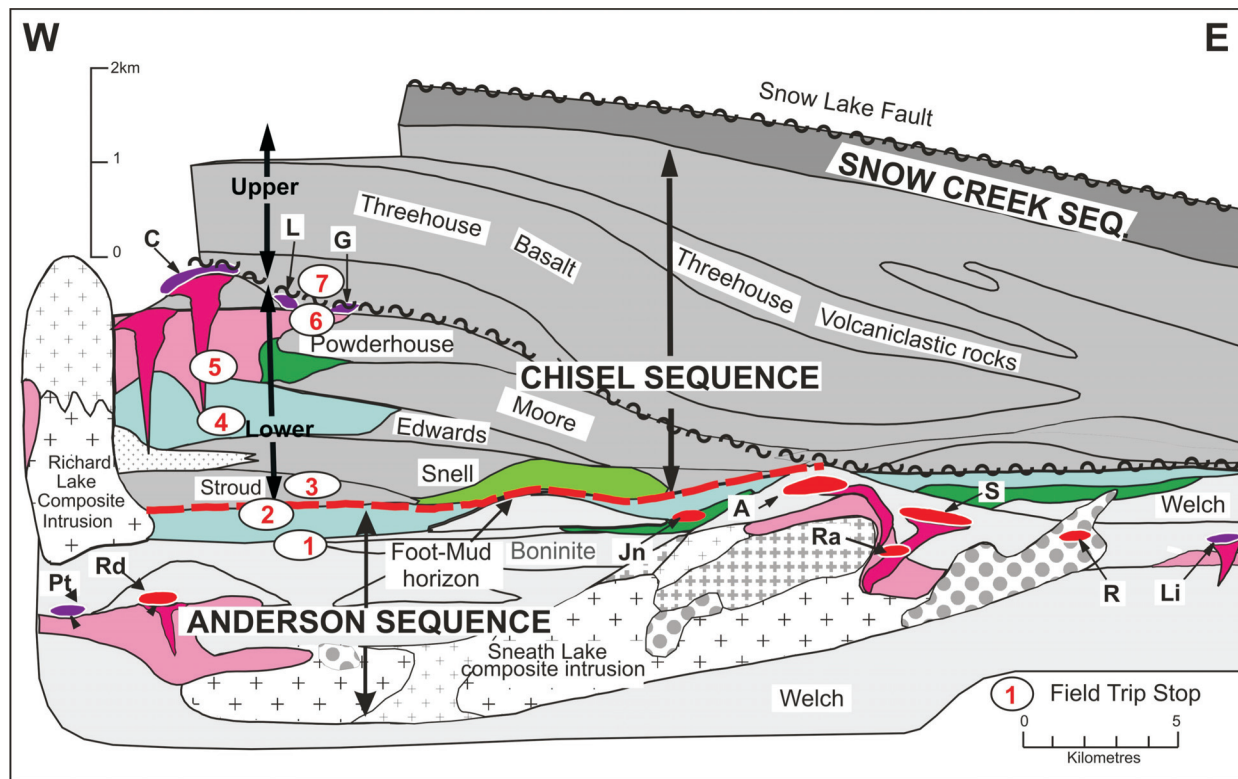


Figure 41. Schematic stratigraphic section showing the major zones of alteration affecting the Snow Lake arc assemblage after Bailes and Galley (in press). The arrows identify the three sequences (Anderson, Chisel (with lower and upper subdivisions), Snow Creek) recognized by Bailes and Galley (2007).

caniclastic rocks, is interpreted to be synvolcanic and related to generation of VMS deposits, as it only affects strata underlying the Chisel–Chisel North–Ghost–Lost–Lalor VMS horizon. The alteration zone is truncated to the west by late phases of the Richard intrusive complex and by late faults.

Geology and Alteration Features in the Chisel–Lalor Lakes Area, Snow Lake Arc Assemblage

During this part of the fieldtrip we will examine a section which begins in the upper part of the Anderson

sequence and ends at the mine-hosting portion of the Chisel sequence. The stops will emphasize features produced by the footwall hydrothermal alteration system below the Chisel VMS deposits, and provide evidence for the stratigraphic and tectonic setting of the VMS deposits. The extent of hydrothermal alteration within this section of the mature arc has been defined both mineralogically (Fig. 41) and isotopically (Taylor and Timbal, 1998). Many of the stop descriptions are modified from Galley and Bailes (2002).

DAY 5 B: SNOW LAKE AREA**STOP 12: WELCH LAKE BONINITE, ANDERSON SEQUENCE****STOP 12.1: Three flows on the Welch formation****Coordinates**

UTM 6072978; 0429289

Stop Description

At Stop 12.1 (Figs. 40, 42) three well preserved north-facing mafic flows will be examined. The lowermost flow displays the chemical characteristics of a high-Ca boninite (Stern et al., 1995a; Bailes and Galley, 1999), and the overlying two flows display boninite-like litho-geochemistry (e.g. higher MgO, Ni and Cr values than most tholeiitic rocks at Snow Lake). Three locations marked by circled letters will be examined.

STOP 12.1, Location A: “High-Ca boninite”**Coordinates**

UTM 6072978; 0429289

Stop Description

The “high-Ca boninite” (flow 1) is over 35 m thick, aphyric, pillowed, and a distinctive pale pistachio green weathering colour. Pillows are blocky, display narrow (<5 cm) selvages, are 30-80 cm in diameter, contain 10-15% quartz and carbonate amygdales (0.5-3 mm), and are surrounded by light tan coloured, recrystallized inter-pillow hyaloclastite. A 1 m wide synvolcanic porphyritic mafic dyke, which intrudes between but never across pillows, is texturally identical to the overlying flow 3.

STOP 12.1, Location B: Contact between flows 1 and 3**Coordinates**

UTM: 6072972; 0429281

Stop Description

The contact between flow 1 and 3 is covered by a narrow (<0.5 m wide) gully. The upper 4 m of flow 1 displays higher vesicularity and thicker domains of interpillow hyaloclastite than at location A. Flow 3 is easily distinguished from flow 1 by its pyroxene (amphibole-replaced)-plagioclase phyric character, medium to dark grey green weathering colour, and smoothly curving pillow morphologies. Pillows in flow 3 are locally imbricated consistent with flow transport from SW to NE (present geographic coordinates). Pillows in flow 3 display narrow selvages and up to 1 cm of rusty weathering interpillow hyaloclastite. Pillow size is relatively constant. Southwest of location B, flows 1 and 3 are separated by up to 6 m of laminated mafic scoria tuff and lapilli tuff which includes a narrow porphyritic pillowed flow that is locally only one pillow thick.

STOP 12.1, Location C: Contact between flows 3 and 4**Coordinates**

UTM: 6072989; 0429272

Stop Description

Flows 3 and 4 are separated by a 0.3-3 m unit of mafic scoria tuff and lapilli tuff that displays both reverse and normal size grading, and, in one locality, current lamination; the latter indicates the same SW to NE component of

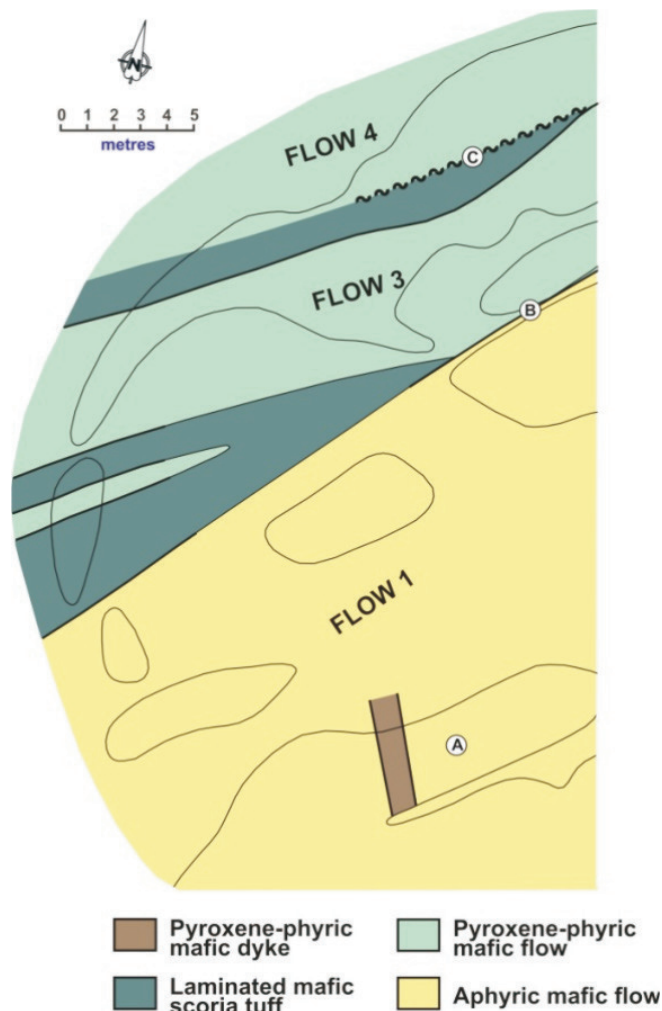


Figure 42. Series of boninite and boninite-like flows in the Welch formation of the Anderson sequence.

transport as the pillow imbrication in flow 3. The tuff/lapilli tuff contains local accessory clasts that are identical to the underlying flow. Flow 4 is similar in textural and composition to flow 3, but has a slightly lower phenocryst population than flow 3 and contains 1-3% quartz-filled radial pipe vesicles (up to 5 cm in length) that are not observed in flow 3.

STOP 12.2: Silicified/feldspathized Welch Lake basaltic andesite and Foot-Mud sulphide

Coordinates

UTM 6073390; 0428802

Stop Description

Stop 12.2 (Figs. 40, 42) provides a particularly photogenic and well preserved example of a silicified/feldspathized aphyric pillowed basaltic andesite. The silicification /feldspathization alteration is part of a larger zone located at the very top of the Anderson primitive arc sequence and is directly overlain by Foot-Mud sulphidic sedimentary rocks. As the overlying Chisel sequence is unaffected by this prominent silicification/feldspathization which is itself cross cut by the Chisel sequence Richard Lake subvolcanic intrusion (Figs. 39,40), supports the interpretation by Skirrow (1987) and Skirrow and Franklin (1994) that it formed very close to, or at, the paleo-seafloor.

Proceeding west (along strike) by trail from the road, weakly to moderately silicified/feldspathized pillows are crossed on route to the intensely altered pillowed flow at Stop 12-2. Primary features are well preserved and include excellent pillow shapes, thermal contraction cracks, amygdales, and interpillow hyaloclastite. Prominent white weathering zones of intense silicification/feldspathization form a complete ring around the inner margin of pillows, and enclose less altered or epidotized pillow cores. Strongly gossaned sulphidic sedimentary rocks of the Foot-Mud horizon are located just northeast of the outcrop. Detailed mapping (1:10 scale) by Surka (2001) defined eight alteration facies and two varieties of interpillow hyaloclastite.

Surka (2001) also examined the relative mass change of elements by comparing the altered rocks to least altered equivalents. His objective was two-fold. First was to establish whether the alteration represented a simple redistribution of elements in a closed system or whether the alteration took place in an open system with introduction and loss of elements. Second was to determine the mobility of metal ions during alteration and to establish the potential of this alteration to generate VMS mineralization. Surka concluded that SiO₂ and K₂O were added, and Fe₂O₃^T, Cu and Zn were lost during alteration of the basalt at this location. A rough calculation of the amount of metals lost from this zone during alteration was determined to be 17.5 Mt Cu and 1.0 Mt Zn or 583 Mt of 3% Cu and 17.5 Mt of 6% Zn. However, there is no way of knowing whether the metals were concentrated by the resultant mineralized hydrothermal fluids or were lost in the seawater column and deposited as widespread but sub-economic sulphides in the Foot-Mud horizon.

STOP 12.3: Stroud Lake felsic breccia

Coordinates

UTM 06073516; 0428973

Stop Description

The change from the Anderson primitive arc to Chisel mature arc sequences is abrupt and characterized change from a sequence dominated by subaqueous mafic flows (Stops 12.1 and 12.2; Fig. 40, 43) to one dominated by units composed of heterolithologic volcanoclastic detritus (Stops 3 to 7). It is also marked by distinctive changes in the geochemical character of associated mafic flows (discussed below). These mafic flows display anomalously high Th contents and the highest apparent proportion of "old" Nd (-0.4 to +2.4 δNd), of all the arc rocks in the Flin Flon belt. Stern et al. (1992, 1995) attribute these features to intracrustal contamination.

David et al. (1996) analyzed zircons from a sample taken from a 1 m thick felsic wacke bed of the Stroud Lake breccia located at the southern end of the outcrop at Stop 3 (Location A, Fig. 44). The sample yielded two zircon sample populations. One suite defined a discordia line with an upper intercept of 1892 ±3 Ma, interpreted to be the age of crystallization of felsic material forming the felsic wacke. Within error this age is identical to that determined for the Sneath Lake (1886±17/-9 Ma) and Richard Lake (1889±8/-6 Ma) tonalite plutons, consistent with their interpretation as subvolcanic intrusions (Bailes et al., 1991). The second population yielded inversely discordant Pb-Pb ages of 2652 Ma and 2674, and Pb-Pb discordant ages of 2715 Ma, 2823 Ma and 2691 Ma that David

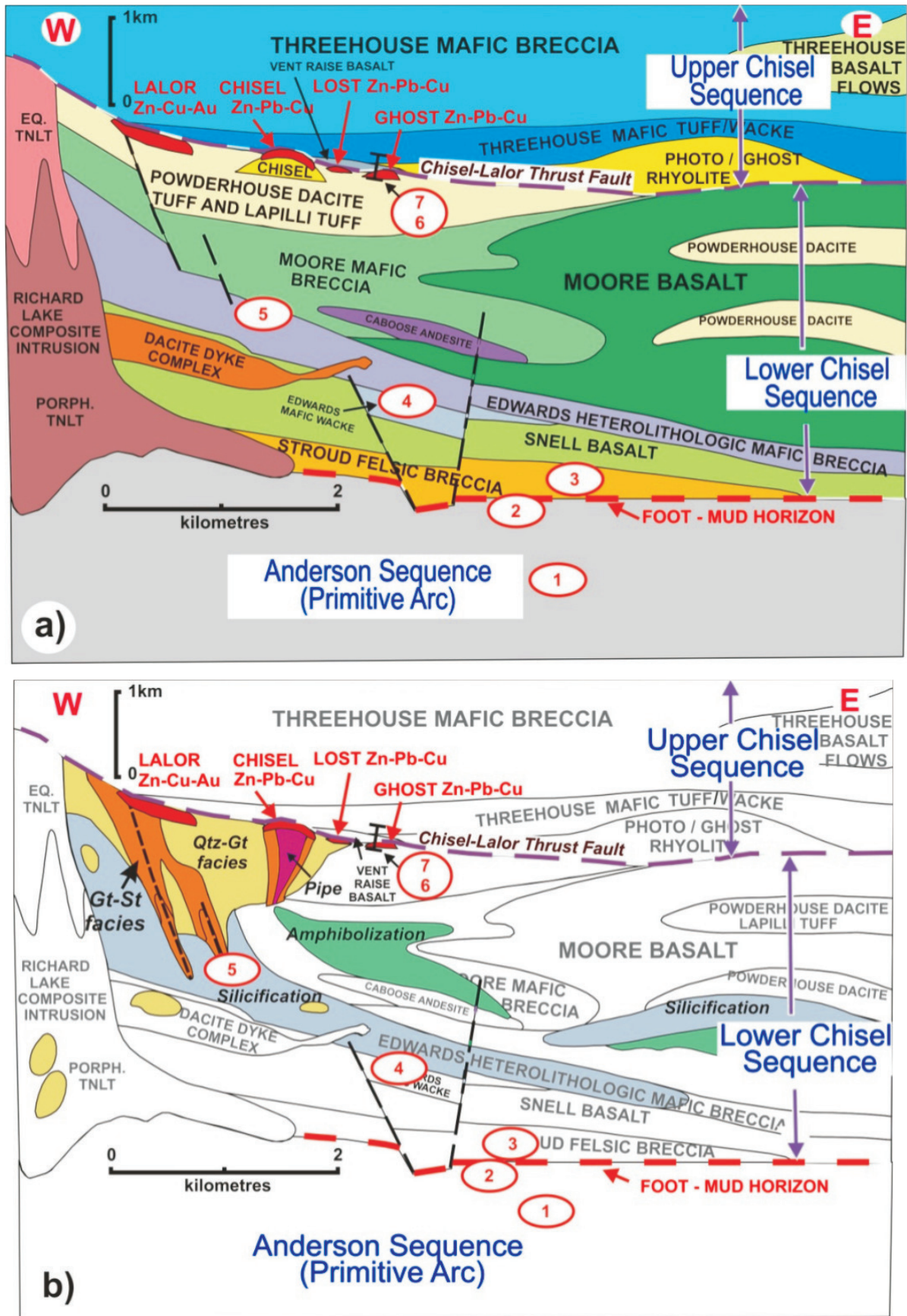


Figure 43. Schematic cross section through the Chisel sequence showing a) stratigraphic units and b) domains of altered rocks. Note the Chisel-Lalor thrust fault at the contact between the Lower Chisel and Upper Chisel sequences.

et al. (1996) interpret as inherited. The ca. 2.7 Ga inherited zircons support the interpretation by Stern et al. (1992) that the high proportion of “old” Nd in the intercalated Snell mafic flows is due to intracrustal contamination, possibly through contamination by Archean crust in the basement to the Snow Lake arc segment or within an underlying subducting plate. The coarsely porphyritic felsic blocks in the 18 m thick bed are texturally and geochemically indistinguishable from the megacrystic trondhjemite phase of the underlying Sneath Lake sub-volcanic intrusion. This suggests that the Stroud Lake felsic breccia may have been derived by uplift and erosion of the underlying Anderson primitive arc sequence coincident with outpouring of the isotopically anomalous Snell Lake mafic flows.

At this stop, located 50 m above the base of the Chisel sequence, a 29 m section of north-facing, well-bedded, monolithologic to heterolithologic felsic breccia and wacke is exposed (Fig.43, 44). The southern 11 m consists of <5 cm and up to 2.6 m thick beds of intermediate to felsic wacke that display bed forms and sedimentary structures characteristic of turbidity and fluidized sediment flows. Normal size grading, scour channels, rip-ups, syn-sedimentary faults, load structures and beds with A, AB and ABD Bouma zonation are present. The northern 18 m of the outcrop consists of a single (?) felsic bed characterized by distinctive, large quartz and plagioclase phenoclasts. The lower 8.5 m of this bed is massive and texturally uniform with 10% quartz phenoclasts (2-15 mm) and 15-20% plagioclase phenoclasts (2-5 mm) in a fine grained matrix. The upper 9.5 m is clearly fragmental and includes a wide variety of subangular to sub-rounded felsic blocks (<30 cm), including some that are

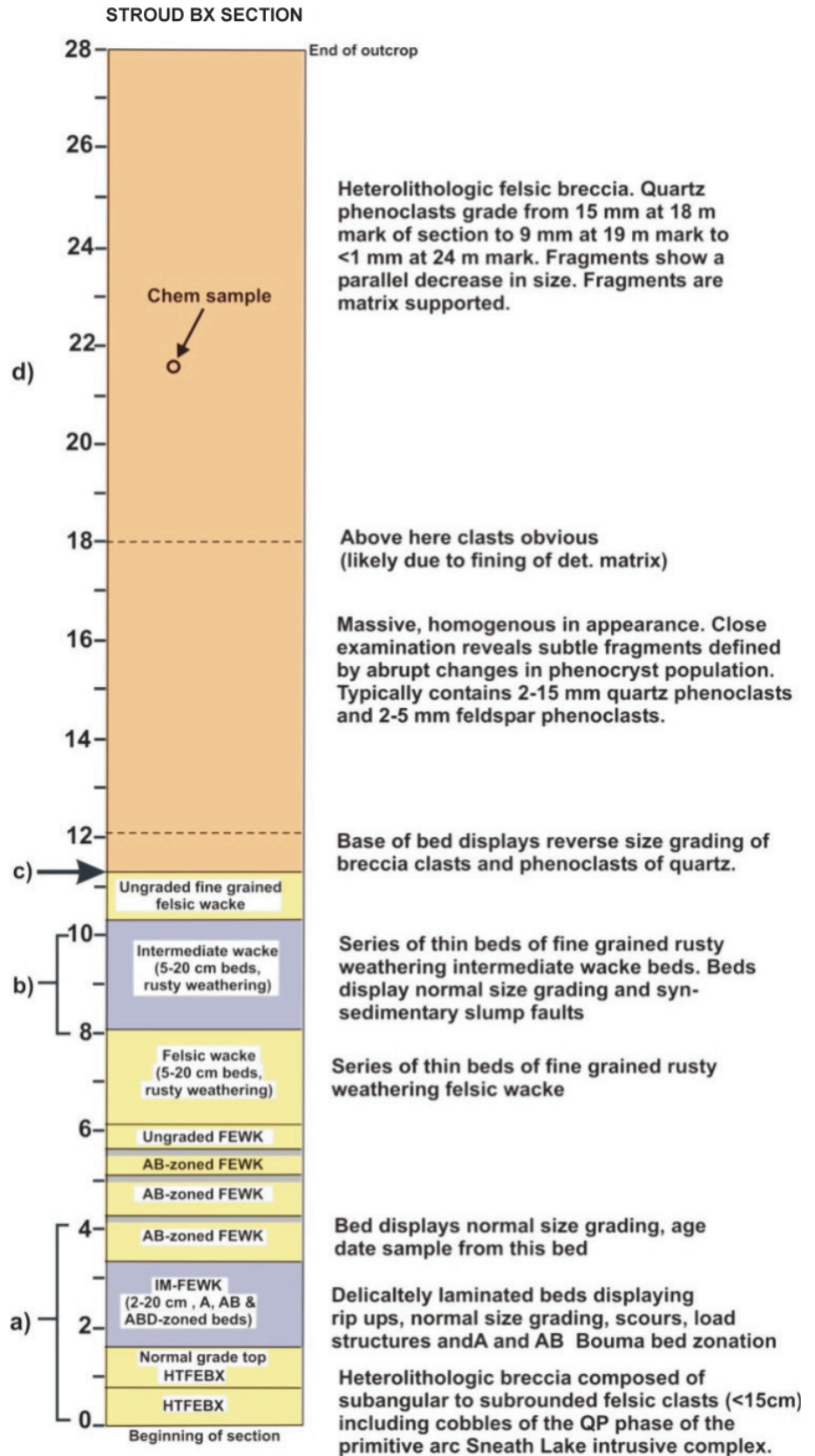


Figure 44. Stratigraphic section of Stroud felsic breccia exposed at Stop 3.

texturally identical to the lower 8.5 m of the bed. The felsic blocks, as well as phenoclasts of quartz and plagioclase in the intervening detrital matrix, all display normal size grading. The top of the bed is fine grained felsic sandstone.

STOP 12.3, Location A

Stop Description

The two heterolithologic felsic breccia beds at this location are matrix-supported and include subangular to sub-rounded quartz-plagioclase phyric rhyolite and trondhjemite clasts, as well as rip-up clasts of intermediate to mafic siltstone. The matrix to these beds is composed of 1-4 mm quartz phenoclasts, 2-4 mm plagioclase phenoclasts, and 2-8 mm lithic felsic to mafic clasts. The detrital matrix of these beds is normally size graded.

The intermediate to mafic siltstone and wacke beds overlying the felsic breccia beds are 2-20 cm thick and display delicate layering, normal size grading, rip-ups, scour channels, and A and AB Bouma bed zonation. Disseminated pyrite in these beds has oxidized to produce a rusty weathered colour.

The 1 m thick AB Bouma zoned felsic wacke bed is composed of an 80 cm graded division composed of 1-4 mm felsic clasts and 2-6 mm mafic lithic clasts, and a 20 cm top of delicately laminated fine sand and silt. This bed contains rare, up to 4 cm cobbles of quartz megacrystic trondhjemite. This is the bed dated by David et. al. (1996). The dating sample site is located at UTM 06073521/0428968.

STOP 12.3, Location B

Stop Description

This 2 m thick unit of intermediate mafic wacke and siltstone is well bedded at a scale of 2-23 cm, displays A and AB Bouma zonation, and normal size grading. Abundant delicate faults at high angles to the layering are interpreted as syn-sedimentary as they are discontinuous up section.

STOP 12.3, Location C

Stop Description

At this location the reverse graded 1 m base of a >18 m thick bed of felsic breccia is exposed. Reverse grading is displayed by both quartz phenoclasts in the matrix and by larger matrix-supported felsic blocks. Up section the felsic blocks, which are subtly defined by clusters of large quartz phenocrysts, are less obvious and the bed appears homogenous.

STOP 12.3, Location D

Stop Description

As the matrix fines, individual blocks of coarsely quartz-plagioclase phyric rhyolite and tonalite are increasingly evident in this thick bed. The felsic blocks are typically sub-rounded, matrix-supported and part of a distinctly heterolithologic felsic clast population. Clasts include aphyric rhyolite and a variety of quartz megacrystic and plagioclase porphyritic rhyolite and tonalite. A geochemical sample from one of the clasts at this locality displays identical geochemistry to that of the underlying Sneath Lake subvolcanic intrusion.

STOP 12.4: Silicification/feldspathization associated with dacite dykes in the Edwards Lake formation

Coordinates

UTM 6074231; 0428608

Stop Description

The Edwards Lake formation is up to 1200 m thick (Fig. 6a). The lower 550 m consists of fine grained mafic volcanoclastic sediments (observed at this Stop). The upper 650 m consists of heterolithologic mafic breccias. As much of this volcanoclastic formation is altered (Figure 6b) it has been interpreted to have been a hydrothermal aquifer (Skirrow, 1987; Bailes and Galley, 1996, 1999; Skirrow and Franklin, 1994). The alteration is spatially associated with an array of subvolcanic mafic to felsic sills, dykes and plugs that intrude both the Edwards Lake volcanoclastics and the underlying Snell Lake mafic flows. Most prominent among the synvolcanic intrusions is a swarm of aphyric and plagioclase phyric dacite dykes (Figure 6a) that are interpreted as the initial phase of the Richard

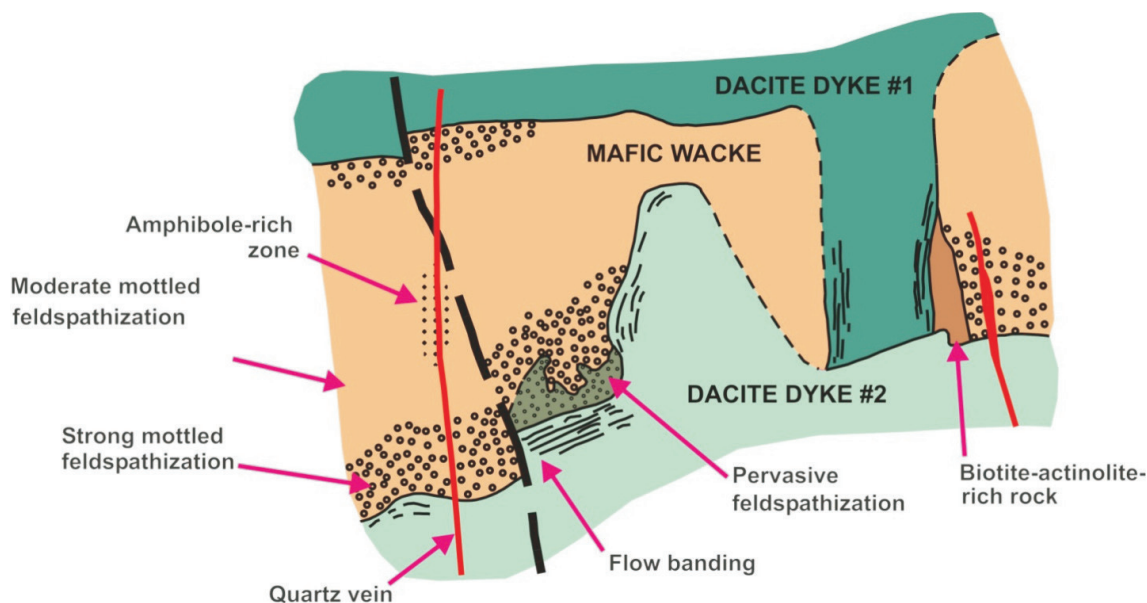


Figure 45. Sketch of relationship between dacite dykes and silicification/feldspathization at Stop 4.

Lake subvolcanic intrusion. The dacite dykes are identical in texture and chemistry to the Powderhouse dacite (Fig. 6a), which directly underlies the Chisel-Lost-Ghost-North Chisel-Lalor Zn-Cu-Pb-Ag sulphide deposits (Bailes and Galley, 1999; 2007).

At this stop (Fig. 45) we will examine silicified/feldspathized, fine-grained mafic wackes of the Edwards Lake formation and demonstrate the relationship between this alteration and dyke emplacement. The mafic wackes are typically massive and featureless, such that altered varieties are difficult to distinguish from the dykes.

At this stop the dacite intrusions are sheet-like bodies, cross-cut bedding, and have sharp, commonly flow-banded margins; there are several generations of intrusions. They are creamy white in colour and are plagioclase-phyric with a fine grained groundmass of quartz, plagioclase and minor biotite. Plagioclase phenocrysts are commonly enveloped or partially replaced by biotite giving dykes a spotted appearance. Adjacent to dacite dykes the mafic volcanic wacke is weakly to intensely silicified/feldspathized (Fig. 45) and is a mottled shades of grey in colour, composed of plagioclase, quartz and hornblende, and is slightly darker in colour than the adjacent dacite dykes (e.g., Fig. 45).

The lighter colour of the mafic wackes adjacent to the dacite dykes is an example of another type of silicification/feldspathization within the Snow Lake alteration systems (Fig. 41, 44). As opposed to the same alteration viewed at Stop 12.2, the alteration observed here is a product of deep sub-seafloor fluid-rock interaction. The dacite dykes are the intrusive equivalent of the Powderhouse dacite, and this implies that the alteration took place at depths of up to 2 km below the paleo-seafloor (Fig. 44). Another difference is that this silicification/feldspathization occurs at the base of a layered, semi-conformable alteration system interpreted to represent a series of seawater-rock interactions that took place over 2000m below the seafloor. This is evidence for the generation of a mature, convective hydrothermal system at the top of the Powderhouse dacite sill-dyke swarm that produced the Chisel-Chisel North-Lost-Ghost-Lalor Zn-Pb-Cu-Ag VMS deposits.

Evidence for the maturity and higher temperatures involved in the generation of this semi-conformable zone of silicification and feldspathization is the lower $\delta^{18}\text{O}$ values (<6 per mil) as compared to an increase in $\delta^{18}\text{O}$ values relative to unaltered volcanic strata for the same alteration at Stop 12.2 (Taylor and Timbal, 1998). This indicates that the silicification and feldspathization are due to high temperature (>350°C) seawater-rock interactions. This is the temperature range expected for the development of a robust, metal-producing convective hydrothermal system (Seyfried and Bishoff, 1977; Rosenbauer and Bischoff, 1983; Alt, 1995; Galley, 1993).

Permission is required from HBMS to access the Chisel Open Pit. Roads used to access this outcrop are in poor repair and caution is advised.

STOP 12.5: Highly altered Moore Lake mafic breccia*Coordinates*

UTM 6076595, 047895

Stop Description

The permeable nature of volcanoclastic rocks of the Edwards and Moore formations played an important role in the hydrology of the hydrothermal system that formed the semi-conformable alteration zone observed previously at Stop 12.4. Alteration in the eastern portion of the semi-conformable zone at Stop 12.4 is associated exclusively with volcanoclastic rocks of the Edwards Lake formation, but to the west it also affects the overlying Moore and Powderhouse formations. This is interpreted to be due to: (1) increasing primary permeability of the overlying Moore formation, accompanying a westerly facies change from massive and pillowed flows to more permeable flow breccia and debris flow deposits; and (2) the presence of a series of north-trending and crosscutting synvolcanic faults that may have focussed hydrothermal fluid discharge (Bailes and Galley 1996). At this stop we will examine Moore Lake formation mafic breccias which have been affected by both semi-conformable alteration and focussed, fault-controlled (?) alteration. At Stop 12.5 we will see evidence for the synvolcanic faulting that focused metal-enriched fluids to the seafloor to form the Chisel Zn-Pb-Cu-Ag VMS deposit.

At Stop 12.5 an east-trending unit of variably feldspathized/silicified monolithologic Moore Lake formation mafic volcanic breccia (Fig.41, 43) is cross-cut, at a high angle, by a prominent zone of chlorite-rich altered rocks characterized by abundant porphyroblasts of staurolite and garnet in a chlorite-biotite-rich groundmass. The cross-cutting chlorite-rich alteration zone is likely related to a synvolcanic fault. In other places these faults host dacite feeder dykes to the overlying Powderhouse formation, along with localizing intense Fe-Mg metasomatism.

Least altered breccias at this stop include complete pillows as fragments and broken pillow pieces, and are interpreted to be pillow fragment breccias derived from cold fragmentation and slumping of Moore Lake basalt flows. Chemical analyses of pillow fragments from this breccia display the prominent light REE enrichment that characterizes Moore Lake basalt flows. We will first examine the least altered breccias in the centre of the outcrop (location A) and then proceed to the most altered portion at the east end of the outcrop (location B).

STOP 12.5, Location A: Silicified/feldspathized and chlorite-rich altered mafic monolithologic breccia*Coordinates*

UTM 6075801, 0427304

Stop Description

The breccia at this location is coarse with many fragments up to 40 cm in diameter and rare blocks up to 1 m in size. It is composed of medium grey, light grey and white weathering blocks of variably feldspathized/ silicified aphyric mafic fragments. The primary mafic composition of fragments is manifest by their morphology; most are broken pieces of pillows, some are complete pillows, and one large block comprises a piece composed of several intact pillows. Many fragments contain quartz amygdals. Rare slabby fragments of altered laminated mafic tuff (interflow sediments?) are present; they must have been lithified prior to incorporation into the breccia.

Pillow fragment clasts range from relatively unaltered medium grey to white weathering blocks composed almost entirely of quartz and feldspar. Many fragments are zoned with a less altered core (composed of amphibole, garnet, quartz, and fine grained plagioclase) and a 1 to 3 cm wide white weathering rim (composed of quartz, feldspar, minor amphibole and magnetite). Inter-fragment matrix is a completely recrystallized mixture of black amphibole, anhedral garnet, plagioclase, quartz and minor euhedral magnetite.

Alteration of breccias at location A probably occurred in two stages. The early stage involved feldspathization/silicification during which Fe and Mg were removed and SiO₂ was added, essentially replacement of mafic pillow fragments by quartz and feldspar. Zones of feldspathization/silicification completely rim margins of broken pillows indicating that this alteration post-dated deposition of the breccia. The second stage consisted of the addition of Fe and Mg and is represented by garnet, amphibole and chlorite-rich rocks. This alteration began with the overgrowth of permeable interfragment domains, and proceeded to alter the previously silicified pillow fragments. The alteration becomes more intense to the east such that at location B, the breccia is overprinted by Fe- Mg-rich minerals such as garnet, chlorite and amphibole. Initially, the garnet-chlorite-amphibole alteration-assemblage is confined to the interfragment domains (i.e. zones of high permeability) but as location B is approached the fragments themselves are also affected. The altered breccia just west of the staurolite-bearing zone is a garnet-amphibole-biotite-rich rock with numerous white quartzo-feldspathic fragments. The inter-fragment domains are com-

posed amphibole, biotite, garnet and plagioclase. The fragments contain up to 5% garnet but virtually no other ferromagnesian minerals.

STOP 12.5, Location B: Staurolite-garnet-chlorite-biotite-rich altered rocks

Coordinates

UTM 6075801, 0427340

Stop Description

The strongly altered staurolite-rich rocks at location B form a cross-cutting north-trending zone (Figure 6b). The contact of this alteration zone is rapidly gradational to the west into less altered equivalents exposed at location A. The most strongly altered rocks are characterized by subhedral to euhedral honey brown to dark brown staurolite porphyroblasts (up to 5 cm long). In this zone, fragments are much less conspicuous than to the west, and where preserved are composed of quartz and feldspar with up to 50% anhedral garnet. The remainder of this zone is composed of 20% subhedral to euhedral staurolite, anhedral to euhedral garnet, biotite, chlorite, and 50% fine-grained quartz and plagioclase. It is not surprising that this rock was misidentified as a pelitic schist by early geologists (Harrison, 1949).

STOP 12.6: Surface expression of the Chisel "mine horizon" (at the Ghost mine vent raise)

Coordinates

UTM 6076505, 0428922

Stop Description

Outcrops in the immediate vicinity of the Ghost Lake mine vent raise display the surface expression of the Chisel-Lalor Thrust Fault (Figs. 43, 47). At this locality the thrust fault is marked by a 30cm wide recessive zone of foliated rocks between a 30-60 cm thick unit of coarse heterolithic felsic fragmental rocks to the east and a 120 m thick mafic flow to the west. In the Ghost Lake Mine this felsic fragmental unit may be up to 10m thick where it commonly occurs adjacent to the massive sulphide zone (N. Provens, pers. com., 1987). The felsic breccia is underlain to the east by laminated (340°/83°) and graded intermediate volcanoclastic rocks of the Powderhouse formation. The felsic fragmental unit is interpreted to be part of the Powderhouse tuff-breccia bed that 1.4 km to the west southwest (Fig. 46) is up to 100 m thick and occurs at the base of the Powderhouse formation. The absence of overlying Powderhouse dacite tuff above the felsic breccia is due to removal of the overlying strata by the Chisel-Lalor thrust. The Ghost lake orebody is within 100 m of surface at Stop 12.6 where the felsic fragmental unit is matrix-supported and consists of quartz-feldspar phryic felsic fragments up to 45 by 18 cm in size. Fragments have highly irregular to sub-rounded shapes,

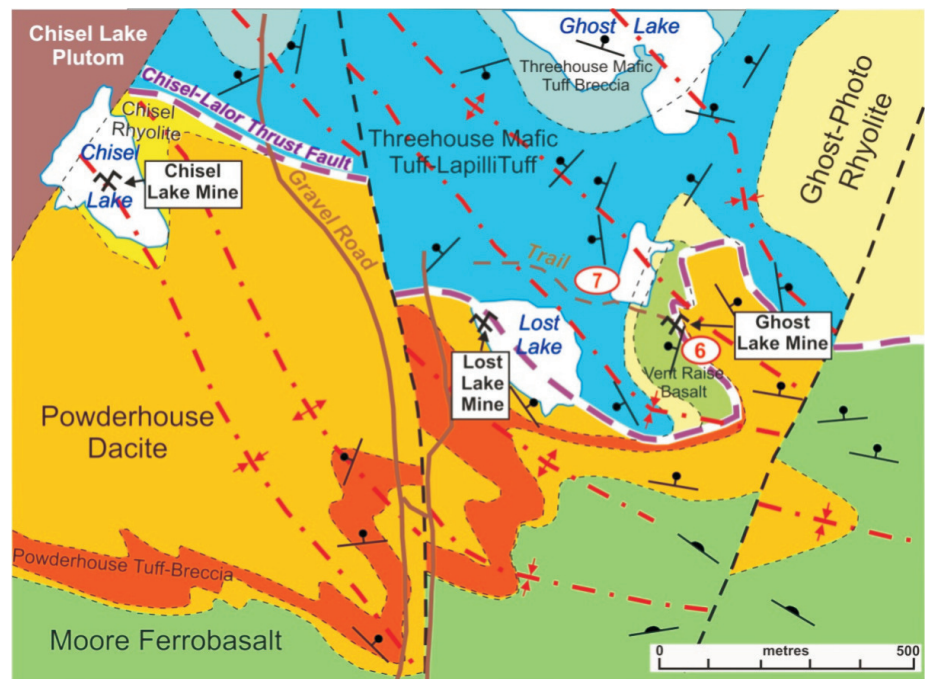


Figure 46. Plan view of the geology in the vicinity of the Chisel Lake, Lost Lake and Ghost Lake VMS mines. Stops 6 and 7, which are accessed by a trail that leads to the abandoned Ghost Lake mine, allow examination of the contact between the Lower and Upper Chisel sequences. At Stop 6 the contact, which is exposed in outcrop, is a narrow, <30 cm wide foliated recessive zone, interpreted to be the Chisel-Lalor thrust fault. At Stop 12-7 a well-preserved outcrop of the Threehouse mafic tuff displays abundant primary structures demonstrating the Threehouse formation rocks at this location evolved by erosion and downslope basinal deposition of a shoaling volcanic edifice in a shallow marine environment.

some with silicic margins up to 1 cm thick. A thicker unit of the felsic breccia is exposed on the southwest shore of Lost Lake at UTM 428476E/6076514N. Intermediate sedimentary rocks in the footwall are well layered and display many primary sedimentary structure including size grading, parallel lamination, convolute lamination, scours, and flame structures. Bed thickness range from 15 cm to 1.2 m. Bouma B and AB bed zonation predominates.

The overlying mafic flow is pillowed but selvages are poorly defined. Quartz amygdalae up to 1 cm in diameter are present. The basal 2 m of the flow is intensely brecciated with quartzo-feldspathic cement. This breccia zone is up to 11 m thick at a locality 30 m to the north. The top several metres of the flow are exposed in small outcrops in a low area to the west (south of the road). Here the flow comprises mainly flow top amoeboid breccia. The upper contact of the flow with the overlying Threehouse mafic volcaniclastic rocks is not faulted and locally displays peperite. The overlying Threehouse mafic tuff dips shallowly to the west (strike 060° and dip 15°). The mafic flow, locally named the Vent Raise basalt, is geochemically identical to the Balloch Lake basalt that occurs in the hanging wall thrust panel above the Lalor Lake VMS deposit.

STOP 12.7: Threehouse mafic volcaniclastic rocks

The Threehouse formation consists of an approximately 50m thick unit of well-bedded, mafic tuff and lapilli tuff followed up section by several hundred metres of poorly bedded, scoria-rich mafic tuff-breccia and lithologically diverse suit of matrix supported mafic bombs and clasts, with rare rhyolite fragments (e.g., UTM428288E/6077035N). Although many of the rocks stratigraphically below the Threehouse formation volcaniclastic rocks are intensely altered in the Chisel Open Pit and elsewhere, the Threehouse formation rocks everywhere are remarkably unaffected by alteration. The Threehouse mafic volcaniclastic rocks exposed at Stop 12.7 are part of the 50 metre interval of well-bedded, mafic tuff that forms the base of the Threehouse formation (Fig. 43a).

STOP 12.7, Location A: Large scour channel and bomb sag in mafic wacke

Coordinates

UTM 6076584, 0428868

Stop Description

The outcrop at location A is best observed on a ledge part way down the cliff face and looking west. Here well bedded mafic tuffs display excellent graded bedding, a large scour channel, load structures and a bomb sag with lee side cross bedding.

STOP 12.7, Location B: Cross bedded mafic wacke

Coordinates

UTM 6076580, 0428831

Stop Description

This outcrop is composed of well bedded, laminated and normally graded mafic tuff and lapilli tuff characterized by prominent trough cross bedding. The bed forms and primary sedimentary structures for this outcrop are sketched in Figure 47. Bed bases are typically composed of granular mafic tuff and lapilli tuff composed of phenoclasts of plagioclase and amphibole-replaced pyroxene. Pebble lags of coarse pyroxene (amphibole-replaced) phenoclasts occur along foreset laminae in some cross bed sets.

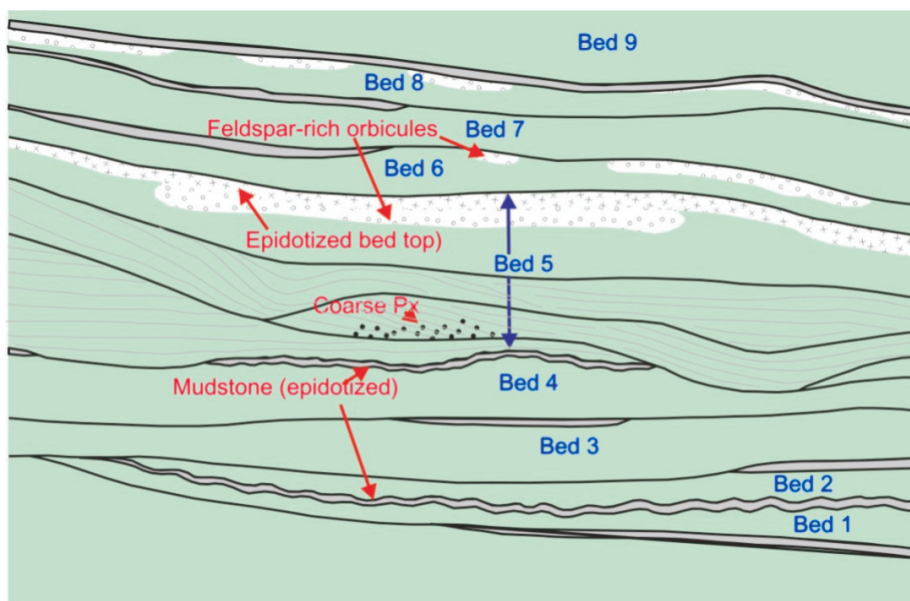


Figure 47. Sketch of outcrop at Stop 12-7 showing well bedded Threehouse mafic volcaniclastic rocks with numerous primary features. Beds are typically normally size graded.

Bed tops are typically fine grained and epidotized. Mafic mud tops to beds, which are commonly completely epidote-replaced, locally display asymmetrical ripples with mud drapes. Orbicular feldspathic domains, which resemble accretionary lapilli, are interpreted to be alteration they crosscut bedding. Besides phenoclasts the lapilli tuff is composed of dark angular shards, abundant scoria and local cored bombs.

The bed forms at this outcrop suggest deposition occurred in either a fluvial and/or inter-tidal environment coincident with a shoaling active volcano. In either interpretation, the environment of deposition was subaerial or very shallow marine. This is in sharp contrast to the subaqueous environment displayed by the underlying Lower Chisel sequence. Heterolithic, matrix-supported, mafic breccias higher in the Threehouse formation (not exposed here) form beds up to 30 m thick that likely represent debris flow deposits triggered by wave undercutting of the emergent portions of the volcano and deposition in basin areas surrounding the central edifice(s).

REFERENCES

- Alt, J.C., 1995, Subseafloor processes in mid-ocean ridge hydrothermal systems, *Seafloor Hydrothermal Systems: Physical, Chemical, Biological, and Geological Interactions*, AGU Geophysical Monograph 91, p. 85-114.
- Alt, J.C., 1999, Hydrothermal alteration and mineralization of oceanic crust: Mineral geochemistry and processes: *Reviews in Economic Geology*, 8, p.133-155.
- Ambrose, J.W., 1936, Progressive kinematic metamorphism in the Missi Series, near Flin Flon, Manitoba: *American Journal of Science*, v. 32, 5th series, p. 257-286.
- Ames, D. E., Tardif, N., Galley, A. G., Gibson, H. L. and MacLachlan, K., 2003, Hangingwall stratigraphy and hydrothermal signature of the Paleoproterozoic Flin Flon-Triple 7-Callinan VMS deposits: FF-TGI: Geological Association of Canada, Geological Association of Canada: Mineralogical Association of Canada, Vancouver, BC, Canada, May 26-28, 2003, Program with Abstracts, vol. 28.
- Ames, D.E., Tardif, N., MacLachlan, K. and Gibson, H. L., 2002, Geology and hydrothermal alteration of the hanging wall stratigraphy to the Flin Flon-777-Callinan volcanogenic massive sulphide horizon (NTS 63K12NW and 13SW), Flin Flon area, Manitoba: in Report of Activities 2002, Manitoba Industry, Trade and Mines - Geological Services, p. 20-34.
- Ansdell, K.M., 1993, U-Pb zircon constraints on the timing and provenance of fluvial sedimentary rocks in the Flin Flon and Athapapuskow basins, Flin Flon Domain, Trans-Hudson Orogen, Manitoba and Saskatchewan: in *Radiogenic Age and Isotopic Studies: Report 7*, Geological Survey of Canada, Paper 93-2, p. 49-57.
- Ansdell, K.M., Kyser, T.K., Stauffer, M. and Edwards, G., 1992, Age and source of detrital zircons from the Missi Group: a Proterozoic molasse deposit, Trans-Hudson Orogen, Canada: *Canadian Journal of Earth Sciences*, v. 29, p. 2583-2594.
- Ansdell, K.M. and Norman, A.R., 1995, U-Pb geochronology and tectonic development of the southern flank of the Kisseynew Domain, Trans-Hudson Orogen, Canada: *Precambrian Research*, v. 72, p. 147-167.
- Ashton, K.E., Lewry, J.F., Heaman, L.M., Hartlaub, R.P., Stauffer, M. R., and Tran, H. T., 2005, The Pelican Thrust Zone: basal detachment between the Archean Sask Craton and Paleoproterozoic Flin Flon – Glennie Complex, western Trans-Hudson Orogen: *Canadian Journal of Earth Sciences*, v. 42, p. 685706
- Bailes, A.H., Bray, D., and Syme, E.C., 2003, Geology of the South Main Shaft area, Flin Flon, Manitoba, Manitoba Industry, Economic Development and Mines, Manitoba Geological Survey, Preliminary Map PMAP2003-7, scale 1:5000.
- Bailes, A.H. and Galley, A.G., 1996, Setting of Paleoproterozoic volcanic-hosted massive sulphide deposits, Snow Lake: in EXTECH I, A multidisciplinary approach to massive sulphide research: Rusty Lake-Snow Lake greenstone belt, Manitoba, (ed.) G.F. Bonham-Carter, A.G. Galley and G.E.M. Hall.: Geological Survey of Canada Bulletin, 426, p. 105-138.
- Bailes, A.H. and Galley, A.G., 1999, Evolution of the Paleoproterozoic Snow Lake arc assemblage and geodynamic setting for associated volcanic-hosted massive sulphide 88 deposits, Flin Flon Belt, Manitoba, Canada: *Canadian Journal of Earth Science*, 36, p. 1789-1805.
- Bailes, A.H., Galley, A.G., Paradis, S. and Taylor, B.E., submitted, Large synvolcanic alteration zones associated with Snow Lake VMS deposits, Flin Flon Belt, Manitoba, Canada: in Paleoproterozoic tectonics and ore deposits of the western Trans-Hudson orogen (eds, Pehrsson, S. and Gibson, H.): Special Volume of the Society of Economic Geologists.
- Bailes, A.H., Galley, A.G., Skirrow, R.G., and Young, J., 1996, Geology of the Chisel volcanic-hosted massive sulphide area, Snow Lake, Manitoba: Geological Survey of Canada: Manitoba Department of Energy and Mines, Mineral Resources Division, Open File, Open File Report 3262 95-4, scale 1:5000.
- Bailes, A.H., Gilmore, K., Levers, J. and Janser, B., 2009, The Lalor deposit surprise at depth: Manitoba Mining and Minerals Convention 2009, Winnipeg, Manitoba, November 19-21, 2009, Program, p. 57-58.
- Bailes, A.H. and Syme, E.C., 1989, Geology of the Flin Flon - White Lake area: Manitoba Energy and Mines, Geological Report GR87-1, 313 p + 1 geologic map at 1:20,000.
- Bailey, K. A., 2006, Emplacement, petrogenesis and volcanic reconstruction of the intrusive and extrusive Myo rhyolite complex, Flin Flon and Creighton, Saskatchewan: Laurentian University, Sudbury, 123 p.
- Bailey, K., Gibson, H.L., MacLachlan, K., Piercy, S. and Lafrance, B., submitted. Emplacement, Petrogenesis, and Reconstruction of the Paleoproterozoic Myo Rhyolite Complex within Flin Flon cauldron subsidence structure: Implications for subsidence history and VMS formation. Submitted to a Special Issue of Economic Geology entitled "Paleoproterozoic Tectonics and Ore Deposits of the Western Trans-Hudson Orogen".
- Banerjee, N.R., Gillis, K.M. and Muehlenbachs, K., 2000, Discovery of epidotes in a modern setting, the Tonga fore-arc. *Geology*, v.28, p. 151-154.
- Banerjee, N.R., and Gillis, K.M., 2001. Hydrothermal alteration in a modern supra-subduction zone: the Tonga fore-arc. *Journal of Geophysical Research*, v.106, p. 21737-21750
- Beccaluva, L. and Serri, G., 1988, Boninitic and low-Ti subduction-related lavas from intraoceanic arc-back arc systems and low-Ti ophiolites: a reappraisal of their petrogenesis and original tectonic setting: *Tectonophysics*, 14, p. 291-315.
- Bleeker, W., 1990, New structural-metamorphic constraints on Early Proterozoic oblique collision along the Thompson Nickel Belt, Manitoba, Canada: In: Lewry, J. F. and Stauffer, M. R. (eds) *The Early Proterozoic Trans-Hudson Orogen of North America*. Geological Association of Canada, Special Paper, v. 37, p. 5773.
- Bruce, E.L., 1918, Amisk-Athapapuskow Lake district: Geological Survey of Canada, Memoir 105, 91 p.
- Cas, R.A.F. and Wright, J.V., 1987, *Volcanic Successions: Modern and Ancient*. Allen and Unwin, 528p.
- Connors, K.A., 1996, Unraveling the boundary between turbidites of the Kisseynew Domain and volcano-plutonic rocks of the Flin Flon domain in the eastern Trans-Hudson Orogen, Canada: *Canadian Journal of Earth Sciences*, 33, p. 811-829.
- Coombe Consultants, 1984, Gold in Saskatchewan: Saskatchewan Energy and Mines, Saskatchewan Geological Survey, Open File Report 84-1.
- Corrigan, D., Galley, A.G., and Pehrsson, S., 2007, Tectonic evolution and metallogeny of the southwestern Trans-Hudson Orogen: In: Goodfellow, W. D. (ed.) *Mineral Deposits of Canada: A Synthesis of Major Deposit-types, District Metallogeny, the Evolution of Geological Provinces, and Exploration Methods*. Geological Association of Canada, Mineral Deposits Division, Special Publication v. 5, p. 881-902.

- Corrigan, D., Pehrsson, S., Wodicka, N., and de Kemp, E., 2009, The Palaeoproterozoic Trans-Hudson Orogen; a prototype of modern accretionary processes: in: Ancient orogens and modern analogues, Geological Society Special Publications, v. 327, 457-479.
- Crawford, A., Falloon, T.J. and Green, D.H., 1989, Classification, petrogenesis and tectonic setting of boninites: in Boninites, A.J. Crawford (ed.), Unwin Hyman, p. 1-49.
- David, J., Bailes, A. H., and Machado, N., 1996, Evolution of the Snow Lake portion of the Palaeoproterozoic Flin Flon and Kiseynew belts, Trans-Hudson Orogen, Manitoba, Canada: Precambrian Research, v. 80, p. 107-124.
- Devine, C., 2003, Origin and emplacement of volcanogenic massive sulphide-hosting, Paleoproterozoic volcanoclastic and effusive rocks within the Flin Flon subsidence structure, Manitoba and Saskatchewan, Canada: Laurentian University, Sudbury, 279 p.
- Devine, C., Gibson, H., Bailes, A., Galley, A., MacLachlan, K. and Gilmore, K., 2003, Origin and emplacement of VMS-hosting, Paleoproterozoic volcanoclastic rocks within the Flin Flon Subsidence Structure, Flin Flon, Manitoba and Saskatchewan. In, Abstract Volume 28, Geological Association of Canada/Mineralogical Association of Canada Joint Annual Meeting, Vancouver, Canada.
- Devine, C. A., Gibson, H. L., Bailes, A. H., MacLachlan, K., Gilmore, K. and Galley, A. G., 2002, Stratigraphy of volcanogenic massive sulphide-hosting volcanic and volcanoclastic rocks of the Flin Flon Formation, Flin Flon (NTS 763K12 and 13), Manitoba and Saskatchewan: in Report of Activities 2002, Manitoba Industry, Trade and Mines - Geological Services, p. 9-19.
- DeWolfe, Y.M. and Gibson, H.L., 2011, (Accepted November 2, 2010). The Facies Architecture of a Paleoproterozoic Basaltic-Andesite Intrusion, Flin Flon, Manitoba, Canada: The description and emplacement of a cryptoflow, intrusion. Bulletin of Volcanology.
- DeWolfe, Y. M., 2008, Physical volcanology, petrology and tectonic setting of intermediate and mafic volcanic and intrusive rocks in the Flin Flon volcanogenic massive sulphide (VMS) district, Manitoba, Canada: Growth of a Paleoproterozoic arc: Ph.D. thesis, Laurentian University, Sudbury, 269 p.
- DeWolfe, Y. M., 2009, Stratigraphy and structural geology of the hangingwall to the hostrocks of the Schist Lake and Mandy volcanogenic massive sulphide deposits, Flin Flon, Manitoba (part of NTS 63K12) in Report of Activities 2009, Manitoba Science, Innovation, Energy and Mines, Manitoba Geological Survey, p. 22-36.
- DeWolfe, Y. M. and Gibson, H. L., 2004, Physical description of the 1920 member, Hidden formation, Flin Flon, Manitoba (NTS 63K16SW): in Report of Activities 2004, Manitoba Industry, Economic Development and Mines, Manitoba Geological Survey, p. 24-35.
- DeWolfe, Y. M. and Gibson, H. L., 2005, Physical description of the Bomber, 1920 and Newcor Members of the Hidden Formation, Flin Flon, Manitoba (NTS 63K16SW): in Report of Activities 2005, Manitoba Science, Technology, Energy and Mines, Manitoba Geological Survey, p. 7-19.
- DeWolfe, Y. M. and Gibson, H. L., 2006, Stratigraphic subdivision of the Hidden and Louis Formations, Flin Flon, Manitoba (NTS 63K16SW): in Report of Activities 2006, Manitoba Science, Technology, Energy and Mines, Manitoba Geological Survey, p. 22-34.
- DeWolfe, Y. M., Gibson, H. L., Lafrance, B. and Bailes, A. H., 2009a, Volcanic reconstruction of Paleoproterozoic arc volcanoes: the Hidden and Louis formations, Flin Flon, Manitoba, Canada, Canadian Journal of Earth Science, v. 46, p. 481-508.
- DeWolfe, Y. M., Gibson, H. L. and Piercey, S. J. 2009b, Petrogenesis of the 1.9 Ga mafic hanging wall sequence of the Flin Flon, Callinan and 777 massive sulphide deposits, Flin Flon, Manitoba, Canada, Canadian Journal of Earth Science, v. 46, p. 509-527.
- Digel, S. and Gordon, T.M., 1995, Phase relations in metabasites and pressure-temperature conditions at the prehnite-pumpellyite to greenschist facies transition, Flin Flon, Manitoba, Canada: in Schiffman, P., and Day, H.W., eds., Low-Grade Metamorphism of Mafic Rocks, Geological Society of America Special Paper 296, p. 67-80.
- Fedorowich, J.S., Kerrich, R. and Stauffer, M.R., 1995, Geodynamic evolution and thermal history of the central Flin Flon Domain, Trans-Hudson Orogen: constraints from structural development, 40Ar/39Ar, and stable isotope geothermometry, Tectonics, v. 14, p. 472-503.
- Fisher, R. V., 1966, Rocks composed of volcanic fragments, Earth Science Reviews, v. 1, p. 287-298.
- Fisher, R. V. and Schmincke, H. U., 1984, Pyroclastic rocks: Springer-Verlag, Berlin, 472 p.
- Gale, D. F. G., Lucas, S. B., and Dixon, J. M., 1999, Structural relations between the polydeformed Flin Flon arc assemblage and Missi Group sedimentary rocks, Flin Flon area, Manitoba and Saskatchewan, Canadian Journal of Earth Sciences, v. 36, p. 1901-1915.
- Galley, A. G., 1993, Characteristics of semi-conformable alteration zones in volcanogenic massive sulphide districts: Journal of Geochemical Exploration, 48, p. 175-200.
- Galley, A. G., 1996, Paleoproterozoic volcanic-related massive sulphide deposits: Tectonic and depositional environments, The Gange, 54, p. 10-13.
- Galley, A. G. and Ames, D.E., 1998, Skarns associated with Precambrian VMS deposits: Geological Association of Canada, Abstracts with Programs, A-61.
- Galley, A. G., Bailes, A.H. and Kitzler, G., 1993, Geological setting and hydrothermal evolution of the Chisel Lake and North Chisel Zn-Pb-Ag-Au massive sulphide deposit, Snow Lake, Manitoba: Exploration and Mining Geology, 2, p. 271-295.
- Galley, A.G., Bailes, A.H., Paradis, S. and Taylor, B., 2002, Volcanogenic massive sulphide-related hydrothermal alteration events within the Paleoproterozoic Snow Lake Arc Assemblage, Geological Association of Canada-Mineralogical Association of Canada Joint Annual Meeting 2002, Saskatoon, Saskatchewan, Canada, Field Trip A2 Guidebook, 94 p.
- Galley, A.G., Syme, E.C., and Bailes, A.H., 2007, Metallogeny of the Paleoproterozoic Flin Flon Belt, Manitoba and Saskatchewan: in: Goodfellow, W.D., ed., Mineral Deposits of Canada: A Synthesis of Major Deposit Types, District Metallogeny, the Evolution of Geological Provinces, and Exploration Methods: Geological Association of Canada, Mineral Deposits Division, Special Publication No. 5, p. 509-531.
- Gibson, H.L., Devine, C., Lafrance, B., DeWolfe, M., A. Bailes, Pehrsson, S., Gilmore, K., and Simard, R. L., Submitted, Construction and evolution of the Paleoproterozoic Flin Flon cauldron subsidence structure: An example of ancient arc rifting and VMS metallogenesis. Submitted to a Special Issue of Economic Geology entitled "Paleoproterozoic Tectonics and Ore Deposits of the Western Trans-Hudson Orogen".

- Gibson, H.L., Lafrance, B., DeWolfe, M., Devine, C., Gilmore, K., and Pehrsson, S., 2009a. Volcanic Reconstruction and Post Depositional Modification of a Cauldron Subsidence Structure within the Flin Flon VMS District. In, Program with Abstracts, Prospectors and Developers Association of Canada, Annual Meeting, Toronto, ON.
- Gibson, H.L., Lafrance, B., DeWolfe, M., Devine, C., Gilmore, K., Pehrsson, S., and Simard, R-L., 2009b. The Volcanic and subvolcanic architecture of a VMS hosting cauldron subsidence structure at Flin Flon, Manitoba. In, Program with Abstracts, Manitoba Mining and Minerals Convention, Winnipeg, Manitoba.
- Gibson, H. L., DeWolfe, Y. M., Lafrance, B., Bailey, K., Devine, C., Simms, D., Gilmore, K., Bailes, A. H., Simard, R. L. and MacLachlan, K., 2007, The relationship between rifting, subsidence, volcanism and VMS deposits at Flin Flon, Manitoba: Manitoba Mining & Minerals Convention 2007, Winnipeg, Manitoba, p. 55.
- Gibson, H.L., Bailey, K., DeWolfe, M., Gilmore, K., Devine, C., Sims, D., Bailes, A. and MacLachlan, K., 2006, Evidence for cauldron subsidence at the Flin Flon Mining Camp: Implications for the location of volcanogenic massive sulphide deposits. In, Program with Abstracts, Saskatchewan Industry and Resources Convention, Saskatoon, Saskatchewan.
- Gibson, H. L., DeWolfe, Y. M., Bailey, K., Devine, C., Lafrance, B., Gilmore, K., Simms, D. and Bailes, A. H., 2005, The Flin Flon caldera: ore localization within a Paleoproterozoic synvolcanic subsidence structure defined through mapping: Manitoba Industry, Economic Development and Mines, Manitoba Mining & Minerals Convention 2005, Winnipeg, Manitoba, November 17-19, 2005, p. 49.
- Gibson, H. L., Ames, D. E., Bailes, A. H., Tardif, N., Devine, C., Galley, A. G., MacLachlan, K. and Gilmore, K., 2003a, Invasive flows, peperite and Paleoproterozoic massive sulphide, Flin Flon, Manitoba and Saskatchewan: Geological Association of Canada, Geological Association of Canada: Mineralogical Association of Canada, 2003 Joint Annual Meeting, Vancouver, Program with Abstracts, vol. 1, p. 28.
- Gibson, H. L., Devine, C., Galley, A. G., Bailes, A. H., Gilmore, K., MacLachlan, K. and Ames, D. E., 2003b, Structural control on the location and formation of Paleoproterozoic massive sulfide deposits as indicated by synvolcanic dike swarms and peperite, Flin Flon, Manitoba and Saskatchewan: Geological Association of Canada, Geological Association of Canada: Mineralogical Association of Canada, 2003 Joint Annual Meeting, Vancouver, Program with Abstracts, p. 28.
- Gibson, H. L., Bailes, A. H., Tourigny, G. and Syme, E. C., 2001, Geology of the Millrock Hill area, Flin Flon Manitoba Geological Survey, Geologic map 33, scale 1:500.
- Gibson, H. L., Morton, R. L. and Hudak, G. J., 1999, Submarine volcanic process, deposits, and environments favorable for the location of volcanic-associated massive sulfide deposits: in Volcanic associated massive-sulfide deposits: processes and examples in modern and ancient settings, C. T. Barrie and M. D. Hannington (eds.), Reviews in Economic Geology, vol. 8, p. 13-51.
- Gibson, H. L., Watkinson, D.H., and Comba, C.D.A., 1983, Silicification: Hydrothermal alteration in an Archean geothermal system within the Amulet Rhyolite formation, Noranda, Quebec: Economic Geology, 78, p. 954-971.
- Gill, J.B. and Whalen, P., 1989, Early rifting in an oceanic island arc (Fiji) produced shoshonitic to tholeiitic basalts: Journal of Geophysical Research, v. 94, p. 4561-4578.
- Gordon, T.M., Hunt, P.A., Bailes, A.H. and Syme, E.C., 1990, U-Pb zircon ages from the Flin Flon and Kiseynew belts, Manitoba: Chronology of crust formation at an Early Proterozoic accretionary margin: in Lewry, J.F. and Stauffer, M.R., eds., The Early Proterozoic Trans-Hudson Orogen of North America: Geological Association of Canada, Special Paper 37, p. 177-199.
- Harper, G.D., 1999, Structural styles of hydrothermal discharge in ophiolite/sea-floor systems: Reviews in Economic Geology, 8, p. 53-73.
- Harrison, J.M., 1949, Geology and mineral deposits of the File-Tramping Lakes area, Manitoba: Geological Survey of Canada, Memoir 250, 92 p.
- Heaman, L.M., Kamo, S.L., Ashton, K.E., Reilly, B.A., Slimmon, W.L. and Thomas, D.J., 1992, U-Pb geochronological investigations in the Trans-Hudson Orogen, Saskatchewan: in Summary of Investigations 1992, Saskatchewan Geological Survey, Saskatchewan Energy and Mines, Miscellaneous Report 92-4, p. 120-123.
- Hodges, D.J. and Manojvic, P.M., 1993, Application of litho geochemistry to exploration for deep VMS deposits in high grade metamorphic rocks, Snow Lake, Manitoba: Journal of Geochemical Exploration, 48, p. 201-224.
- Hoffman, P. F., 1988, United plates of America, the birth of a craton: Early Proterozoic assembly and growth of Laurentia: Annual Review of Earth and Planetary Science Letters, v. 16, p. 543603.
- Holk, G. J., 1997, Stable isotope studies of silicification at Snow Lake, The Use of Regional-Scale Alteration Zones and Subvolcanic Intrusions in the Exploration for Volcanic-Associated Massive Silfide Deposits, p. 393-400.
- Holland, H.D., Feakes, C.R. and Zbinden, E.A., 1989, The Flin Flon paleosol and the composition of the atmosphere 1.8 BYBP: American Journal of Science, v. 289, p. 362-389.
- Kennedy, G.C. 1950, A portion of the system silica-water: Economic Geology, 45, p. 629-653.
- Koo, J. and Mossman, D. J., 1975, Origin of metamorphism of the Flin Flon stratabound Cu-Zn sulphide deposit, Saskatchewan and Manitoba, Economic Geology, v. 70, p. 48-62.
- Krause, J., and Williams, P.F., 1998, Relationships between foliation development, porphyroblast growth and large-scale folding in a metaturbidite suite, Snow Lake, Manitoba, Journal of Structural Geology, v. 20, p. 61-76.
- Krause, J. and Williams, P.F., 1999, Structural development of the Snow Lake allochthon and its role in the evolution of the southeastern Trans-Hudson Orogen in Manitoba, central Canada: Canadian Journal of Earth Sciences, v. 36. no. 11, p. 1881-1899.
- Kremer, P. D. and Simard, R. L., 2007, Geology of the Hook Lake Block, Flin Flon area, Manitoba (part of NTS 63K12): in Report of Activities 2007, Manitoba Science, Technology, Energy and Mines, Manitoba Geological Survey, p. 21-32.
- Lafrance, B., Gibson, H.L., Pehrsson, S., Schetselaar, E., DeWolfe, Y. M., and Lewis, D., Submitted, Structural reconstruction of the Flin Flon volcanogenic massive sulfide mining district, Saskatchewan and Manitoba, Canada. Economic Geology Special Issue "Paleoproterozoic Tectonics and Ore Deposits of the Western Trans-Hudson Orogen".
- Lewis, D., Lafrance, B. and MacLachlan, K., 2007, Kinematic evidence for thrust faulting and reactivation within the Flin Flon Mining Camp, Creighton, Saskatchewan: in Summary of Investigations 2007, Saskatchewan Geological Survey, Saskatchewan Ministry of Energy and Resources, Miscellaneous Report 2007-4.2, CD-ROM, Paper A-2, p. 10.

- Lewis, D., Lafrance, B., MacLachlan, K. and Gibson, H., 2006, Structural investigations of Millrock Hill and the Hinge Zone of the Beaver road Anticline, Creighton, Saskatchewan: in Summary of Investigations 2006, Volume 2, Saskatchewan Geological Survey, Saskatchewan Industry Resources, Miscellaneous Report 2006-4.2, CD-ROM, Paper A-10, p. 11.
- Lewry, J. F., and Collerson, K. D., 1990: The Trans-Hudson Orogen: extent, subdivisions and problems: In: Lewry, J. F. and Stauffer M. R. (eds) The Early Proterozoic Trans-Hudson Orogen of North America. Geological Association of Canada, Special Paper 37, p.114.
- Lucas, S.B., Stern, R.A., Syme, E.C., Reilly, B.A., and Thomas, D.J., 1996, Intraoceanic tectonics and the development of continental crust: 1.92-1.84 Ga evolution of the Flin Flon Belt, Canada: Geological Society of America (GSA), Geological Society of America Bulletin, v. 108, no. 5, p. 602-629
- MacLachlan, K., 2006a, Bedrock geology Douglas Lake area, Flin Flon Domain (part of NTS 63K12): Saskatchewan Geological Survey, Saskatchewan Industry and Mines, Summary of Investigations 2007, Volume 2, Miscellaneous Report 2006-4.2, Geological Map, scale 1:3 000.
- MacLachlan, K., 2006b, Bedrock geology Green Lake area, Flin Flon Domain (part of NTS 63K12): Saskatchewan Geological Survey, Saskatchewan Industry and Mines, Summary of Investigations 2007, Volume 2, Miscellaneous Report 2006-4.2, Geological Map, scale 1:3 000.
- MacLachlan, K., 2006c, Stratigraphy, structure, and silicification: new results from mapping in the Flin Flon Mining Camp, Creighton, Saskatchewan: in Summary of Investigations 2006, Volume 2, Saskatchewan Geological Survey, Saskatchewan Industry and Resources, Miscellaneous Report 2006-4.2, p. 25.
- MacLachlan, K. and Devine, C., 2007, Stratigraphic evidence for volcanic architecture in the Flin Flon Mining Camp: implications for mineral exploration: in Summary of Investigations 2007, Saskatchewan Geological Survey, Saskatchewan Ministry of Energy and Resources, Miscellaneous Report 2007-4.2, CD-ROM, Paper A-1, p. 29.
- Malinowski, M., White, D. J., Mwenifumbo, C. J., Salisbury, M., Bellefleur, G., Schmitt, D., Dietiker, B., Schetselaar, E., and Duxbury, A., 2008, Seismic exploration for VMS deposits within the Paleoproterozoic Flin Flon Belt, Trans-Hudson Orogen, Canada: in European Geosciences Union general assembly 2008, Anonymous, Geophysical Research Abstracts, 10
- McPhie, J., Doyle, M. and Allen, R., 1993, Volcanic textures: a guide to the interpretations in volcanic rocks: CODES, Hobart, 198 p.
- Morrison, G.W., 1980, Characteristics and tectonic setting of the shoshonite rock association: Lithos, v. 13, p. 97-108.
- NATMAP Shield Margin Project Working Group, 1998, Geology, NATMAP Shield Margin Project area Flin Flon Belt, Manitoba/Saskatchewan: Geological Survey of Canada, "A" Series Map 1968A, 7 maps, 2 folded sheets + 1 v. (54 p. : col. ill.) scale 1:100 000.
- Percival, J. A., Zwanzig, H. V., and Rayner, N., 2006, New tectonostratigraphic framework for the northeastern Kiseynew Domain, Manitoba (parts of NTS 63O: in Explore in Manitoba; report of activities 2006, Manitoba Geological Survey, p. 74-84
- Pehrsson, S. and the TGI-3 Flin Flon project team, 2009, New models and metalotects for the Trans Hudson orogen; Exploration 2007, Manitoba Mining and Minerals convention, online abstracts.
- Podolsky, T., 1951, Cranberry Portage (east half): Geological Survey of Canada, Paper 51-17, preliminary map with marginal notes: 1:63 360 (1 inch to 1 mile).
- Podolsky, T., 1958, Cranberry Portage (west half): Geological Survey of Canada, Preliminary Map 26-1957, with marginal notes: 1:63 360 (1 inch to 1 mile).
- Price, D. P., 1977, Flin Flon, Snow Lake geology: Canadian Institute of Mining and Metallurgy Field Trip, October 3-6, 1977: Hudson Bay Mining and Smelting Co. Ltd., Flin Flon, Manitoba, 55 p.
- Rayner, N., 2010, New U-Pb zircon ages from the Flin Flon Targeted Geoscience Initiative Project 2006-2009: Flin Flon and Hook Lake blocks, Manitoba and Saskatchewan, Geological Survey of Canada, Current Research (Online) no. 2010-4, 2010: 15 pages, doi:10.4095/261489
- Reilly, B.A., 1990, Bedrock geological mapping: Mystic Lake - West Arm, Schist Lake area (Part of NTS 63K-12): in Summary of Investigations 1990, Saskatchewan Geological Survey, Saskatchewan Energy and Mines, Miscellaneous Report 90-4. p. 25-35.
- Reilly, B.A., 1991, Revision bedrock geological mapping: Mystic Lake - Kaminis Lake area (parts of NTS 63K-12 and 63L-9): in Summary of Investigations 1991, Saskatchewan Geological Survey, Saskatchewan Energy and Mines, Miscellaneous Report 91-4. p. 9-15.
- Reilly, B.A., 1992, Early thrusting and granitoid diapirism in the southern Flin Flon greenstone belt, Saskatchewan: in Geological Association of Canada, Programs with Abstracts, v. 17, p. A95.
- Robert, F., Boullier, A.-M., Firdaus, K., 1995, Gold-quartz veins in metamorphic terranes and their bearing on the role of fluids in faulting. Journal of Geophysical Research, v. 100, No. B7, p. 12861-12879.
- Rosenbauer, J. R. and Bischoff, J.L., 1983, Uptake and transport of heavy metals by heated seawater: A summary of the experimental results, in P. A. Rona, Bostrom, K., Laubier, L., and Smith, K.L., ed., Hydrothermal Processes at Seafloor Spreading Centres, New York, Plenum, p. 177-198.
- Sangster, D. F., 1972, Precambrian volcanogenic massive sulphide deposits in Canada: A review, Geological Survey of Canada, Paper 72-22.
- Schetselaar, E., Pehrsson, S.J., Devine, C., Currie, M., and White, D. 2010. The Flin Flon 3D Knowledge Cube, Geological Survey of Canada Open File Open File 6313, 35 p.
- Schiffman, P. and Smith, B.M., 1988, Petrology and oxygen isotope geochemistry of a fossil seawater hydrothermal system within the Solea Graben, northern Troodos ophiolite, Cyprus: Journal of Geophysical Research, 93, p. 4612-4624.
- Schiffman, P. S., Varga, R.J., and Moores, E.M., 1987, Geometry, conditions, and timing of off-axis hydrothermal metamorphism and ore deposition in the Solea graben: Nature, 325, p. 423-425.
- Seyfried, W. E., Jr., Berndt, M.E. and Seewald, J.S., 1988, Hydrothermal alteration processes at mid-ocean ridges: Constraints from diabase alteration experiments, hot spring fluids and composition of the oceanic crust: Canadian Mineralogist, 26,p. 787-804.
- Seyfried, W.E. and Bischoff, J.L., 1977, Hydrothermal transport of heavy metals by seawater: the role of seawater/basalt ratio: Earth and Planetary Science Letters, 34, p. 71-77.
- Sibson, R.H., Robert, F., Poulsen, K.H., 1988, High-angle reverse faults, fluid-pressure cycling, and mesothermal gold-quartz deposits. Geology, v. 16, p. 551-555.

- Simard, R. L. and Creaser, R. A., 2007, Implications of new geological mapping, geochemistry and Sm-Nd isotope data, Flin Flon area, Manitoba (part of NTS 63K12): in Report of Activities 2007, Manitoba Sciences, Technology, Energy and Mines, Manitoba Geological Survey, p. 7-20.
- Simard, R. L., MacLachlan, K., Gibson, H. L., DeWolfe, Y. M., Devine, C., Kremer, P. D., Lafrance, B., Ames, D. E., Syme, E. C., Bailes, A. H., Bailey, K., Price, D. P., Pehrsson, S., Cole, E. M., Lewis, D. and Galley, A. G., 2010, Geology of the Flin Flon area, Manitoba and Saskatchewan (part of NTS 63K12, 13): Innovation, Energy and Mines, Manitoba Geological Survey, Geoscientific Map MAP 2009-1, colour map, scale 1:10 000.
- Skirrow, R.G., 1987, Silicification in a lower semiconformable alteration zone near the Chisel Lake Zn-Cu massive sulphide deposit, Manitoba: M.Sc. thesis, Carleton University, Ottawa, Ontario, 171 p.
- Skirrow, R.G. and Franklin, J.M., 1994, Silicification and metal leaching in subconcordant alteration zones beneath the Chisel Lake massive sulphide deposit, Snow Lake, Manitoba: *Economic Geology*, 89, p. 31-50.
- Smith, R.L., and Bailey, R.A., 1968, Resurgent cauldrons, *Geological Society of America Memoire*, v. 116, p. 613-662.
- Stauffer, M., 1974, Geology of the Flin Flon area: a new look at the sunless city, *Geoscience Canada*, v. 1, no. 3, p. 30-35.
- Stauffer, M.R., 1990, The Missi formation: an Aphebian molasse deposit in the Reindeer Zone of the Trans-Hudson orogen, Canada: in Lewry, J.F. and Stauffer, M.R., eds.: *The Early Proterozoic Trans-Hudson Orogen of North America: Geological Association of Canada, Special Paper 37*, p. 121-141.
- Stauffer, M. and Mukherjee, A. C., 1971, Superimposed deformation in the Missi metasedimentary rocks near Flin Flon, Manitoba, *Canadian Journal of Earth Science*, v. 12, p. 2021-2035.
- Stauffer, M. R., Mukherjee, A. C. and Koo, J., 1975, The Amisk Group: an Aphebian(?) island arc deposit, *Canadian Journal of Earth Science*, v. 12, p. 2021-2035.
- Stern, R. A., Machado, N., Syme, E. C., Lucas, S. B. and David, J., 1999, Chronology of crustal growth and recycling in the Paleoproterozoic Amisk collage (Flin Flon Belt), Trans-Hudson Orogen, Canada, *Canadian Journal of Earth Sciences*, v. 36, p. 1827-1807.
- Stern, R.A. and Lucas, S.B., 1994, U-Pb zircon constraints on the early tectonic history of the Flin Flon accretionary collage, Saskatchewan: in *Radiogenic Age and Isotopic Studies: Report 8*, Geological Survey of Canada, Paper 94-F, p. 75-86.
- Stern, R.A., Lucas, S.B., Syme, E.C., Bailes, A.H., Thomas, D.J., LeClair, A.D. and Hulbert, L., 1993, Geochronological studies in the Flin Flon Domain, Manitoba-Saskatchewan, NATMAP Shield Margin Project area: results for 1992-1993: in *Radiogenic Age and Isotopic Studies, Report 7*, Geological Survey of Canada, Paper 93-2, p. 59-70.
- Stern, R.A., Syme, E.C., Bailes, A.H. and Lucas, S.B., 1995a, Paleoproterozoic (1.86-1.90 Ga) arc volcanism in the Flin Flon belt, Trans-Hudson Orogen, Canada: *Contributions to Mineralogy and Petrology*, v. 119, p. 117-141.
- Stern, R.A., Syme, E.C. and Lucas, S.B., 1995b, Geochemistry of 1.9 Ga MORB- and OIB-like basalts from the Amisk collage, Flin Flon belt, Canada: Evidence for an intra-oceanic origin: *Geochimica et Cosmochimica Acta*, v. 59, p. 3131-3154.
- Stockwell, C.H., 1960, Flin Flon-Mandy area, Manitoba and Saskatchewan: Geological Survey of Canada, Map 1078A, scale 1:12 000.
- Surka, M., 2001, Metal mobility during silicification of the 1.89 Ga Welch Lake primitive arc basalts, Snow Lake arc assemblages, Snow Lake, Manitoba: B.Sc. thesis, University of Manitoba, 102 p.
- Swinden, H. S., 1996, The application of volcanic geochemistry to the metallogeny of volcanic-hosted sulphide deposits in central Newfoundland, in D. A. Wyman, ed., *Trace Element Geochemistry of Volcanic Rocks: Applications for Massive Sulphide Exploration, Short Course Notes*, Geological Association of Canada, p. 239-279.
- Syme, E.C., 1987, Athapapuskow Lake Project: in Manitoba Energy and Mines, Minerals Division, Report of Field Activities, 1987, p. 30-39.
- Syme, E.C., 1988, Athapapuskow Lake Project: in Manitoba Energy and Mines, Minerals Division, Report of Field Activities, 1988, p. 20-34.
- Syme, E.C., 1991, Elbow Lake project - Part A: supracrustal rocks and structural setting, in Manitoba Energy and Mines, Minerals Division, Report of Activities, 1991, p. 14-27.
- Syme, E.C., 1992, Elbow Lake project - Part A: supracrustal rocks and structural setting: in Manitoba Energy and Mines, Minerals Division, Report of Activities, 1992, p. 32-46.
- Syme, E.C., 1993, Cranberry - Simonhouse reconnaissance: in Manitoba Energy and Mines, Minerals Division, Report of Activities, 1993, p. 61-66.
- Syme, E.C., 1994, Supracrustal rocks of the Iskwasum Lake area (63K/10W): in Manitoba Energy and Mines, Minerals Division, Report of Activities, 1994, p. 47-56.
- Syme, E.C., 1995, 1.9 Ga arc and ocean floor assemblages and their bounding structures in the central Flin Flon belt: in Trans-Hudson Orogen Transect, LITHOPROBE Report No. 48, p. 261-272.
- Syme, E.C. and Bailes, A.H., 1993, Stratigraphic and tectonic setting of volcanogenic massive sulfide deposits, Flin Flon, Manitoba: *Economic Geology*, v. 88, p. 566-589.
- Syme, E.C., Bailes, A.H. and Lucas, S.B., 1995, Geology of the Reed Lake area (parts of NTS 3K/9 and 10): in Report of Activities 1995, Manitoba Energy and Mines, Geological Services, p. 42-60.
- Syme, E.C., Bailes, A.H., Lucas, S.B., 1996, Tectonic assembly of the Paleoproterozoic Flin Flon belt and setting of VMS deposits: Geological Association of Canada: Mineralogical Association of Canada, Geological Association of Canada: Mineralogical Association of Canada: Joint Annual Meeting, Winnipeg, MB, Field Trip Guidebook B1, 131 p.
- Syme, E. C., Bailes, A. H., Stern, R. A. and Lucas, S. B., 1996, Geochemical characteristics of 1.9 Ga tectonostratigraphic assemblages and tectonic setting of massive sulphide deposits in the Paleoproterozoic Flin Flon Belt, Canada: in *Trace element geochemistry of volcanic rocks : applications for massive sulphide exploration*, A. H. Bailes (ed.), Geological Association of Canada, vol. 12, p. 279-327.
- Syme, E. C. and Forester, R. W., 1977, Petrogenesis of the Boundary Intrusions in the Flin Flon area of Saskatchewan and Manitoba, *Canadian Journal of Earth Sciences*, v. 14, p. 444-455.
- Syme, E.C., Lucas, S.B., Bailes, A.H., and Stern, R.A., 1999, Contrasting arc and MORB-like assemblages in the Paleoproterozoic Flin Flon Belt, Manitoba, and the role of intra-arc extension in localizing volcanic-hosted massive sulphide deposits, *Canadian Journal of Earth Sciences*, v. 36, no. 11, p. 1767-1788.

- Taylor, B.E., and Timbal, A., 1998, Regional Stable Isotope Studies in the Snow Lake Area: 1998 CAMIRO 94e07 Annual Rept., 271-279: in Database for CAMIRO Project 94E07: interrelationships between subvolcanic intrusions, large-scale alteration zones and VMS deposits, Ontario, Manitoba, Quebec and Sweden (Galley, A., Bailes, A., Hannington, M., Holk, G., Katsube, J., Paquette, F., Paradis, S., Santaguida, F., and Taylor, B. (compiled by B. Hillary), 2002, Geological Survey of Canada, Open File 4431, 1-CD-ROM.
- Tardif, N. P., 2003, Hanging wall alteration above the Paleoproterozoic, Callinan and 777 volcanogenic massive sulphide deposits, Flin Flon, Manitoba, Canada: M.Sc. thesis, Laurentian University, Sudbury, 100 p.
- Thomas, D.J., 1989, Geology of the Douglas Lake-Phantom Lake area (Part of NTS 63K-12 and -13): in Summary of Investigations 1989, Saskatchewan Geological Survey, Saskatchewan Energy and Mines, Miscellaneous Report 89-4, p. 44-54.
- Thomas, D.J., 1990, New perspectives on the Amisk Group and regional metallogeny, Douglas Lake - Phantom Lake area, northern Saskatchewan: in Summary of Investigations 1990, Saskatchewan Geological Survey: Saskatchewan Energy and Mines, Miscellaneous Report 90-4, p. 13-20.
- Thomas, D.J. 1991, Revision bedrock geological mapping: Bootleg Lake - Birch Lake area (parts of 63K-12 and 63L-9): in Summary of Investigations 1991, Saskatchewan Geological Survey: Saskatchewan Energy and Mines, Miscellaneous Report 91-4, p. 2-8.
- Thomas, D. J., 1992, Highlights of investigations around the Flin Flon mine: reassessment of structural history: in Summary of investigations 1992, Saskatchewan Geological Survey, Saskatchewan Energy and Mines, Miscellaneous Report 92-4, p. 3-13.
- Thomas, D.J. 1993, Geological highlights of the Hamell Lake area, Flin Flon-Amisk Lake region (parts of NTS 63K-13, 63L-16): in Summary of Investigations 1993, Saskatchewan Geological Survey, Miscellaneous Report 93-4, p. 3-11.
- Thomas, D. J., 1994, Stratigraphic and structural complexities of the Flin Flon mine sequence: in Summary of investigations 1994, Saskatchewan Geological Survey, Saskatchewan Energy and Mines, Miscellaneous Report 94-4, p. 3-10.
- Wallace, R.C., 1984, Mining and Mineral Prospects in Northern Manitoba Northern Manitoba Bulletin published by Authority of Government of Manitoba
- Wentworth, C.K., 1922, A scale of grade and clast terms for elastic sediments. *Journal of Geology*, v.30, p. 377-392.
- White, J. D. L., McPhie, J. and Skilling, I., 2000, Peperite: a useful genetic term, *Bulletin of volcanology*, v. 62, p. 65-66.
- White, J.D.L., and Houghton, B.F., 2006. Primary volcanoclastic rocks. *Geology*, v.34, p. 677-680.
- Zaleski, E. Froese, E. and Gordon, T.M., 1991, Metamorphic petrology of Fe-Zn Mg-Al alteration zones at the Linda volcanogenic massive sulphide deposit, Snow Lake, Manitoba: *Canadian Mineralogist*, v. 29, p. 995-1017.

PUBLICATIONS IN THIS SERIES:

**Tectonic Evolution and Sedimentary Record of the Ottawa-Bonnechere Graben:
Examining the Precambrian and Phanerozoic History of Magmatic Activity,
Faulting and Sedimentation**

W. Bleeker, G.R. Dix, A. Davidson, and A. LeCheminant
Guidebook to Field Trip 1A

The Defining Tectonic Elements of Ganderia in New Brunswick

*C.R. van Staal, S.M. Barr, L.R. Fyffe, S.C. Johnson, A.F. Park,
C.E. White, and R.A. Wilson*
Guidebook to Field Trip 1B

**The Blake River Group of the Abitibi Greenstone Belt and
Its Unique VMS and Gold-Rich VMS Endowment**

*P. Mercier-Langevin, J. Goutier, P-S. Ross, V. McNicoll, T. Monecke, C. Dion,
B. Dubé, P. Thurston, V. Bécu, H. Gibson, M. Hannington, and A. Galley*
Guidebook to Field Trip 2B

**The Volcanological and Structural Evolution of the
Paleoproterozoic Flin Flon and Snow Lake Mining Districts**

*H. Gibson, S. Pehrsson, B. Lafrance, M. DeWolfe, R. Syme, A. Bailes,
K. Gilmore, C. Devine, R-L. Simard, K. MacLachlan, and B. Pearson*
Guidebook to Field Trip 3B

**Carbonatites, Alkalic Rocks and Astroblems in the Outaouais:
New Data and Conclusions**

D.D. Hogarth
Guidebook to Field Trip 4B

Geological Highlights of the National Capital Region

A. Donaldson and B. Halfkenny
Guidebook to Field Trip 5B

Geological Setting of the Mountain Pass REE Deposit, California

P. Dockweiler and S. Castor
Guidebook to Field Trip 7B